F. HOFFMANN-LA ROCHE LTD

INVESTIGATOR'S BROCHURE

RO7499790

GAVRETO® (pralsetinib)

Version 10

April 2025

Investigator Brochure Company Approval Date: See electronic signature on the last page of this document.

SUMMARY OF SIGNIFICANT CHANGES IN UPDATED INVESTIGATOR'S BROCHURE

RO7499790

GAVRETO® (pralsetinib)

Version 10

April 2025

Replacing Version 9, April 2024

The main changes (summarized below) in this update of the Investigator's Brochure are as follows:

Section	Changes from Previous Version of the Investigator's Brochure
Section 1.2	Summary of physical, chemical, and pharmaceutical properties and clinical formulation updated.
Section 1.4.1	Clinical pharmacology data updated for Studies BO42863 and GP43163.
Section 1.4.2	Clinical efficacy data updated for Studies BO42863 and ML42439.
Section 1.4.3	Clinical safety data updated for Studies BO42863 and ML42439.
Section 2.4	Updated status of the Studies BO41932, ML41591, ML42439, BO42863 and BO42864.
Section 5.1	Updated status of the Studies BO41932, ML41591, ML42439, BO42863 and BO42864.
Section 5.2	Updated pharmacokinetic data for Studies BO42863 and GP43163.
Section 5.4	Updated efficacy data for Studies BO42863 and ML42439.
Section 5.5	Updated safety data for Study BO42863 and ML42439.
Section 5.6	Updated marketing experience for Gavreto.
Section 6.3	Updated warnings and precautions for severe infections.
Section 6.4	Added severe infections details to identified risks table.
Section 6.4.1	Table displaying SAR reactions to pralsetinib updated with the most recent data
Section 6.5	Section was updated to remove severe infection details.
Appendices	Updated where necessary to reflect changed status of studies.

Additional minor changes have been made throughout the document to improve clarity and consistency.

TABLE OF CONTENTS

LIST OF TABLES

LIST OF FIGURES

LIST OF APPENDICES

GLOSSARY OF ABBREVIATIONS

$5\text{-}HT_{2A}$	5-hydroxytryptamine 2A receptor
ADME	absorption, distribution, metabolism, and excretion
ADR	adverse drug reaction
AE	adverse event
ALT	alanine aminotransferase
AST	aspartate aminotransferase
AUC	area under the plasma concentration versus time curve
$AUC_{0\text{-}24}$	area under the plasma concentration versus time curve from 0 to 24 hours
$AUC_{0\text{-}last}$	area under the concentration-time curve from time 0 to the last measurable concentration above the lower limit of quantification
$AUC_{(0\text{-}t)}$	area under the plasma concentration versus time curve from 0 to the last measurable concentration
$AUC_{0\text{-}t,\ ss}$	area under the plasma concentration versus time curve from time zero to steady-state
$AUC_{0\text{-}\infty}$	area under the plasma concentration versus time curve from time 0 to infinity
BCRP	breast cancer resistance protein
BDC	bile-duct cannulated
BID	twice daily
BOIN	Bayesian optimal interval
BSEP	bile salt efflux pump
C1D1	Cycle 1, Day 1
C1D15	Cycle 1, Day 15
CCDC6	coiled-coil domain containing 6
CCOD	clinical cutoff date
CL	Clearance
CL/F	apparent oral clearance
CL_{plasma}	plasma clearance
C_{max}	maximum plasma concentration
C_{min}	minimum plasma concentration
CRC	colorectal cancer
CR	complete response
CUP	Compassionate Use Program
CYP	cytochrome P450
DDI	drug-drug interaction

DOR	duration of response
DLT	dose-limiting toxicity
ECG	Electrocardiogram
eGFR	estimated glomerular filtration rate
ELISA	enzyme-linked immunosorbent assay
F	Bioavailability
FDA	Food and Drug Administration
FGFR	fibroblast growth factor receptor
GCP	Good Clinical Practice
GDNF	Glial cell line derived neurotrophic factors
GFRα	GDNF family receptor alpha
GLDH	gamma-glutamyl transferase
GLP	Good Laboratory Practice
GMR	geometric mean ratio
GSH	Glutathione
hERG	human ether-à-go-go related gene
HNSTD	highest nonseverely toxic dose
HPLC	high-performance liquid chromatography
HPMC	hydroxypropyl methylcellulose
HR	heart rate
IBD	international birth date
IC_{50}	half-maximal inhibitory concentration
ICH	International Council for Harmonisation
ILD	interstitial lung disease
IND	Investigational New Drug Application
IV	intravenous(ly)
JAK	Janus kinase
K_d	dissociation constant
KDR	kinase insert domain receptor
K_I	concentration required to achieve half-maximal inactivation
KIF5B	kinesin family member 5B
K_{inact}	maximal inactivation rate constant
KM	Kaplan-Meier
KTR	absorption transit rate constant
MAD	Mutual Acceptance of Data
MATE	multidrug and toxin extrusion protein
MDCK	Madin-Darby canine kidney type II cells
MDR1	multidrug-resistant-1 gene

MS/MS	tandem mass spectrometry
MTC	medullary thyroid cancer
MTD	maximum tolerated dose
NOAEL	no-observed-adverse-effect level
NR	not reached
NSCLC	non-small cell lung cancer
OAT	oganic anion transporter
OCT	organic cation transporter
ORR	overall response rate
OS	overall survival
PAAP	Pre-approval Access Program
PBPK	physiologically-based pharmacokinetic
PD	pharmacodynamic(s)
PDX	patient-derived xenograft
PFS	progression-free survival
P-gp	P-glycoprotein
PK	pharmacokinetic(s)
PO	Oral
PR	partial response
PT	Preferred Term
PTC	papillary thyroid cancer
QD	once daily
QTcB	QT corrected for heart rate by Bazett’s formula
RET	rearranged during transfection
SARs	serious adverse reactions
SAE	serious adverse event
SOC	standard of care
STD_{10}	severely toxic dose in 10% of animals
$t_{1/2}$	elimination half-life
TGI	tumor growth inhibition
TKI	tyrosine kinase inhibitor
TLS	tumor lysis syndrome
TK	toxicokinetic(s)
T_{max}	time to maximum plasma concentration
TRA	total radioactivity
TRKC	tropomyosin receptor kinase C
UGT	uridine 5'-diphospho-glucuronosyltransferase
ULN	upper limit of normal

U.S.	United States
V_{dss}	volume of distribution at steady-state
V_z/F	apparent volume of distribution
VEGFR	vascular endothelial growth factor receptor
WT	wild-type

1. SUMMARY

1.1 SCIENTIFIC RATIONALE

Rearranged during transfection (RET) is a receptor tyrosine kinase expressed in several neural, neuroendocrine, and genitourinary tissue types that normally requires ligand and co-receptor binding for activation (Mulligan 2014). Aberrant activation of RET is a critical driver of tumor growth and proliferation across a broad number of solid tumors (Mulligan 2014).

As the prevalence of tumor genomic sequencing has increased, the importance of RET alterations in human cancers provides a strong rationale for the development of therapeutics targeting RET.

Pralsetinib (previously known as BLU-667) is a potent and selective oral inhibitor of RET fusion proteins and oncogenic RET mutant. Since July 2020, pralsetinib was being co-developed as an anticancer therapeutic by Genentech/Roche (hereafter referred to as "Roche") in collaboration with Blueprint Medicines Corporation (hereafter referred to as "Blueprint Medicines"), as well as CStone Pharmaceuticals (Suzhou) Co. Ltd. in Greater China and Chugai Pharmaceutical Co. Ltd. in Japan (hereafter referred to as "Chugai"). Effective February 22, 2024, all rights to pralsetinib previously granted to Roche and Chugai were returned to Blueprint Medicines and the collaboration between parties has been terminated.

1.2 PHYSICAL, CHEMICAL, AND PHARMACEUTICAL PROPERTIES AND CLINICAL FORMULATION

Pralsetinib drug substance is isolated in crystalline form. The molecule is slightly hygroscopic, and has a melting point of 206^{0}C (determined by differential scanning calorimetry). Pralsetinib is provided as an orally administered hard capsule. The immediate release capsules are supplied as 100 mg dose strength in size 0 light blue opaque hydroxypropyl methylcellulose (HPMC) capsules.

The pralsetinib capsules are supplied in high-density polyethylene bottles (with desiccant). The drug product should be stored at room temperature in their original container, according to the package label. Refer to the label or certificate of analysis for the expiry date.

The polymer stabilized spray dried dispersion of the drug substance is blended with compendial excipients during manufacturing. The drug product is manufactured and formulated following current Good Manufacturing Practices.

1.3 NONCLINICAL INFORMATION

1.3.1 Nonclinical Pharmacology

Pralsetinib has demonstrated potent inhibition of RET kinase activity at the biochemical and cellular level. In biochemical assays, pralsetinib inhibits both wild-type (WT) and

oncogenic RET (mutants and fusions) with a half-maximal inhibitory concentration (IC_{50}) of enzyme activity in the sub-nanomolar range (0.33 nM to 0.45 nM). Pralsetinib has demonstrated inhibitory activity in cellular assays where the RET oncogene, either as a RET fusion protein or a RET mutant, drives RET autophosphorylation, RET substrate phosphorylation, and downstream pathway activity that leads to cellular proliferation with IC_{50}s in the low nanomolar range (3 – 22 nM) (Suzuki et al. 2013; Subbiah et al. 2020; Carlomagno et al. 1995; Cooley et al. 1995; BPM-0016 and BPM-0017; Appendix 1). Pralsetinib shows high selectivity for RET over a large panel of other kinases, including kinases known to be inhibited by multikinase inhibitors, including the kinase insert domain receptor (KDR, also known as vascular endothelial growth factor receptor [VEGFR]2) and the fibroblast growth factor receptor (FGFR)1, with 81-fold and 26-fold biochemical selectivity, respectively (BPM-0015; Appendix 1), and 14- and 40-fold cellular selectivity (BPM-0018; Appendix 1).

Pralsetinib demonstrated dose-dependent anti-tumor activity across a diverse set of RET-driven tumor models including the KIF5B-RET non-small cell lung cancer (NSCLC), CCDC6-RET (WT and V804M), the NCOA4-RET colorectal cancer patient-derived xenograft (PDX) tumor model, the TT medullary thyroid cancer (MTC) xenograft tumor model that harbors the RET C634W mutant, and an engineered Ba/F3-KIF5B-RET (V804L) allograft model. Microdialysis data from rat showed a partition coefficient for unbound brain-to-plasma concentrations for pralsetinib of ~0.14, which indicated a potential for brain penetration. Consistent with this observation, pralsetinib demonstrated anti-tumor activity in an intracranial tumor model when dosed at 10 or 30 mg/kg twice daily, resulting in 40% and 100% tumor regressions at the end of study, respectively (see Section 4.1.2.2). Pralsetinib was well tolerated at all doses in tumor-bearing animals and exhibited dose-dependent modulation of oncogenic RET activity in all in vivo models tested, including those insensitive to the multikinase inhibitor cabozantinib.

1.3.2 Pharmacokinetics and Drug Metabolism in Animals

In vitro permeability for pralsetinib was evaluated in C2BBe1 cells (a clone of Caco-2 cell lines), Madin Darby canine kidney (MDCK), multidrug resistance 1 gene (MDR1)-MDCK cells, and breast cancer resistance protein (BCRP). Pralsetinib showed moderate permeability in C2BBe1 cells and is a dual substrate of efflux transporters P-glycoprotein (P-gp) and BCRP. Despite the potential efflux transport at the gut membrane via P-gp and BCRP, the oral bioavailability (F) of pralsetinib dosed as a solution was high (~100%) in rats, dogs, and monkeys.

In vivo, prasetinib showed low plasma clearance (CL_{plasma}) with moderate volume of distribution at steady-state (V_{dss}) in the three species evaluated- rats, dogs, and monkeys corresponding to ~26%, 6.4%, and 15% of the hepatic blood flow, respectively.

Pralsetinib was found to be highly protein bound, with the unbound fraction estimated at $<$ 5% in mice, rats, dogs, monkeys and humans. Pralsetinib also showed limited preferential distribution into red blood cells.

Pralsetinib underwent low to moderate metabolism in liver microsomes and cryopreserved hepatocytes from mice, rats, dogs, monkeys, and humans. All metabolites detected in humans were also present in either rats and/or monkeys. The proposed metabolism pathway in hepatocytes includes oxidation/hydroxylation of the pralsetinib pyrazolpyridine ring system (M549a and M449c), oxidation of cyclohexyl moiety (M549c), direct N-glucuronidation (M709), and glutathione (GSH) conjugate formation with and without defluorination.

Following an oral administration of [^{14}C]-pralsetinib in rats, hydroxylation/oxidation (M549a,b, M563), glucuronidation (M709a,b,c), and GSH conjugation (M836, M838) were detected in vivo, consistent with in vitro metabolic profile.

Hepato-biliary excretion was a major route of elimination of pralsetinib in a mass balance study in rats. Only 1.5% of the dose after PO administration to rats was recovered in urine, suggesting a minor role of urinary excretion in elimination of pralsetinib.

In vitro, pralsetinib is mainly metabolized by cytochrome P450 (CYP) 3A4 (with a minor contribution by CYP1A2 and CYP2D6) and UGT1A4. In addition, pralsetinib is a direct inhibitor of CYP2C8, CYP2C9, and CYP3A4/5 (testosterone 6β-hydroxylation) and a time–dependent inhibitor of CYP3A4/5 enzyme. Pralsetinib also induced CYP1A2, CYP2B6, CYP2C8, CYP2C9, and CYP3A4 mRNA expression, while induction of enzyme activity was noted only for CYP2C8, CYP2C9, and CYP3A4.

In vitro, pralsetinib is a substrate of P-gp and BCRP. Pralsetinib inhibited the transport activities of human P-gp, BCRP, bile salt efflux pump (BSEP), organic anion transporter (OAT) P1B1, OATP1B3, OAT1, OAT3, multidrug and toxin extrusion protein (MATE) 1, and MATE2-K.

1.3.3 Toxicology and Safety Pharmacology

Safety pharmacology screening efforts against a panel of 55 transmembrane or soluble receptors, ion channels and monoamine transporters, and the hERG channel supported a favorable profile for pralsetinib. The hERG channel results, combined with the lack of effect on ECG observed in the GLP-compliant 28-day and 13-week repeated-dose toxicology studies in monkeys, suggest a low potential for pralsetinib prolonging the QT interval in patients. In vivo safety pharmacology studies using radiotelemetry-implanted rats revealed that pralsetinib can increase blood pressure; this effect is attributed to VEGFR inhibition.

Pralsetinib has been evaluated in a comprehensive toxicology program that included GLP and International Council for Harmonisation (ICH) S9 compliant repeat-dose toxicity studies up to 13 weeks in Sprague-Dawley rats and cynomolgus monkeys, a battery of in vitro and in vivo genotoxicity studies, a 26-week carcinogenicity study in transgenic (Tg.rasH2) mice, fertility and early embryonic development and embryo-fetal developmental toxicity studies in rats, and in vitro phototoxicity studies. The rat and

monkey are pharmacologically responsive to pralsetinib and all human metabolites detected in vitro were also detected with rats and/or monkeys. Key common toxicities noted in both rat and monkeys included hematological abnormalities (reduced bone marrow and lymphoid organ cellularity, reduced red blood cells, reduced reticulocytes) and effects on bony tissues (physeal dysplasia), soft tissues (hemorrhage/mineralization), and gastrointestinal tract (erosion and ulceration). Reproductive and development toxicities observed with pralsetinib treatment in rats included degeneration/atrophy in the testis in males and degeneration of the corpus luteum in the ovary of the females and postimplantation losses and visceral and skeletal fetal malformations after administration to pregnant rats. Pralsetinib had no adverse effects on male and female reproductive performance in rats. With the exception of teratogenenicity, which was consistent with on-target RET inhibition, the majority of the pralsetinib-related toxicologic effects were attributed to off-target kinase inhibition (Janus kinase [JAK] 2, VEGF and/or FGFR). Pralsetinib was not mutagenic in in vitro assays or in an in vivo micronucleus study in rats, nor did pralsetinib demonstrate any phototoxic potential in vitro. Pralsetinib was not carcinogenic in male or female transgenic (Tg.rasH2) mice. Most pralsetinib-related effects in the 28-day repeated-dose toxicology studies showed evidence of reversibility after the 14-day recovery period, and most are considered to be monitorable. After 13 weeks of dosing, the no-observed-adverse-effect level (NOAEL) in both species is 10 mg/kg/day (60 mg/m^2/day in rats and 120 mg/m^2/day in monkeys).

1.4 CLINICAL INFORMATION

To date, 15 clinical studies have been initiated with pralsetinib, of which 7 Phase I studies in healthy volunteers have been completed and 8 studies in patients with RET-altered solid tumors are ongoing/completed. See Section 2.4 for an overview of the pralsetinib clinical development program and Appendix 4 for study details.

1.4.1 Clinical Pharmacology

The pharmacokinetics (PK) of pralsetinib have been evaluated in one completed clinical study in patients (BO42863) and seven completed clinical pharmacology studies in healthy volunteers (BP42858, BP42859, BP42860, BP42861, BP42862, GP43162 and GP43163). A summary of results is provided below:

Study BO42863: Phase I/II Study in Patients RET-altered Cancers

At a 400 mg dose, the pralsetinib concentration-time profiles for RET fusion-positive NSCLC, Thyroid (MTC, PTC, ANPTC, Poorly Differentiated Thyroid Cancer, Poorly Differentiated Carcinoma), RET-fusion positive other than NSCLC and thyroid cancer (Tumor-Agnostic), Group 6, and Group 7 patients following single oral dose administration, showed rapid absorption into the systemic circulation (median T_{max} of 4 hours for NSCLC patients and 2 hours for thyroid patients) followed by an apparent monophasic elimination, with a comparable PK profile to that observed in healthy

volunteer studies. The mean elimination half-life ($t_{1/2}$) of pralsetinib on C1D1 at 400 mg was 13 hours for NSCLC patients and 15 hours for Thyroid Cancer patients, supporting once daily dosing. Approximately 2-fold accumulation was observed at steady state following once daily dosing for both NSCLC and thyroid patients, consistent with the frequency of dosing and the half-life of pralsetinib. Dose proportionality for pralsetinib could not be concluded in patients over the full dose range (60 to 600 mg) or over a limited dose range (200 to 400 mg) due to the low number of patients receiving doses other than 400 mg QD. However, in healthy subjects, dose proportionality was seen across the range of 200 to 400 mg after single dose administration of pralsetinib.

The steady-state exposures of pralsetinib following 400 mg QD dosing are generally comparable between different groups in this study. Although the steady state exposures in NSCLC patients following 400 mg QD dosing were slightly higher (34% higher for C_{max} and 43% higher for AUC_{0-24}) compared to thyroid patients, all guidance regarding dose adjustments related to DDI, hepatic impairment, administration with food, etc. remain the same for these indications, given that the risk-benefit of pralsetinib was appropriate for both the indications at 400 mg QD. PK data from other indications should be interpreted with caution, as the small sample size ($n=5$ for tumor agnostic, $n=3$ for Group 6 and $n=4$ for Group 7) limits the accuracy and reliability of these findings.

Study BP42858: Food Effect Study
The oral bioavailability of 200 mg of pralsetinib was increased when given under fed (standardized high-fat meal) conditions. Compared with fasted conditions, systemic exposure, maximum plasma concentration (C_{max}) and the area under the plasma concentration versus time curve from time 0 extrapolated to infinity ($AUC_{0-\infty}$), increased by 104% and 122%, respectively.

Study BP42859: Bioequivalence Study
Based on the lack of bioequivalence between tablets and capsules, the tablet formulation was not developed further.

Study BP42860: Mass Balance Study
Excretion in feces was the predominant route of elimination of drug-related material and excretion in urine was the minor route of elimination. In feces and urine, unchanged pralsetinib accounted for majority of the drug-related radioactivity of administered dose. Metabolites from oxidation and glucuronidation were detected in small to trace amounts. Overall, the metabolism of pralsetinib in humans was qualitatively similar to nonclinical toxicology species (rat and monkey), with no unique human metabolites observed.

Study BP42861: Effects of Itraconazole and Rifampin on Pharmacokinetics of Pralsetinib
Co-administration of pralsetinib with itraconazole, a combined P-gp and strong CYP3A4 inhibitor, resulted in a clinically relevant increase in systemic exposure (C_{max} increased

by ~84% and the area under the plasma concentration versus time curve [AUC] increased by ~250%) to pralsetinib, while co-administration of pralsetinib with rifampin, a strong CYP3A4 inducer, resulted in a clinically relevant decrease in systemic exposure (C_{max} decreased by ~30% and AUC decreased by ~68%) to pralsetinib.

Study BP42862: Effect of Esomeprazole on Pharmacokinetics of Pralsetinib
Coadministration of esomeprazole, a proton pump inhibitor, with pralsetinib resulted in only a modest decrease in systemic exposure (C_{max} decreased by ~25% and AUC decreased by ~15%) when compared to administration of pralsetinib alone. The median time to reach maximum plasma concentration (T_{max}) of pralsetinib increased slightly with coadministration of pralsetinib with esomeprazole.

Study GP43162: **Effect of Cyclosporine on Pharmacokinetics of Pralsetinib**
Systemic exposure of pralsetinib increased when pralsetinib was coadministered with a single dose of cyclosporine, a P-gp inhibitor, compared to when pralsetinib was administered alone (C_{max} increased by 48% and AUC increased by 81%). The half-life was similar regardless of cyclosporine administration.

Study GP43163: **Effect of Hepatic Impairment on Pharmacokinetics of Pralsetinib**

This study was conducted in patients with moderate and severe hepatic impairment, and a heatlhy control group with normal hepatic function. C_{max} and AUCs in subjects with moderate hepatic impairment were similar to subjects with normal hepatic function (GMRs: 98.6% for C_{max} and 112% for $AUC_{0-\infty}$). In subjects with severe hepatic impairment, the C_{max} was lower but the AUC was similar to subjects with normal hepatic function (GMRs: 67.9% for C_{max} and 85.8% for $AUC_{0-\infty}$). Overall, the results from this study suggested that moderate and severe hepatic impairment did not have a clinically meaningful impact on the exposure of pralsetinib to warrant a dose adjustment in these patients.

1.4.2 Efficacy

1.4.2.1 Study BO42863: ARROW Study

The antitumor activity of pralsetinib has been evaluated in Study BO42863 in patients with RET fusion-positive NSCLC, RET-mutant MTC, RET fusion-positive thyroid cancer and other RET fusion-positive tumors. Key efficacy results for patients treated with a starting dose of 400 mg once daily (QD) are summarized below:

- Overall response rate (ORR):
  - RET fusion-positive NSCLC: 70.3% (95% CI: 64.3, 75.8), including 18 complete responses (CR) and 164 partial responses (PR) out of 259 evaluable patients
  - RET-mutant MTC: 68.2% (95% CI: 59.5, 76.0)
  - RET fusion-positive thyroid cancer: 85.2% (95% CI: 66.3, 95.8)
  - Other RET fusion-positive tumors: 46.4% (95% CI: 27.5, 66.1) including 3 CR and 10 PR out of 28 evaluable patients

- Median duration of response (DOR):
  - RET fusion-positive NSCLC: 19.1 months (95% CI: 14.5, 27.9), with a DOR rate at 12 months of 59.5%
  - RET-mutant MTC: 39.6 months (95% CI: 29.4, not reached [NR])
  - RET fusion-positive thyroid cancer: NR (95% CI: 12.9, NR)
- Median progression-free survival (PFS):
  - RET fusion-positive NSCLC: 13.1 months (95% CI: 11.4, 16.8), with Kaplan-Meier (KM) estimates of PFS rates of 74.4% 95% CI: 69.1, 79.6) at 6 months, 54.7% (95% CI: 48.7, 60.8) at 12 months, 43.1% (95% CI: 37.0, 49.2) at 18 months, and 37.7% (95% CI: 31.7, 43.7) at 24 months
  - RET-mutant MTC: 37.2 months (95% CI: 27.5, 55.5), with an estimated PFS rate of 89.4% at 6 months, 84.9% at 9 months, 80.4% at 12 months, 74.2% (95% CI: 66.8, 81.6) at 18 months, 65.5 (95% CI: 57.3, 73.6) at 24 months and 43.4 (95% CI: 34.5, 52.2) at 48 months
  - RET fusion-positive thyroid cancer: NR, with an estimated PFS rate of 80.6% (95% CI: 66.7, 94.6) at 6 months and 9 months, 70.8% (95% CI: 54.8, 86.9) at 12 months, 60.5% (95% CI: 43.1, 78.0) at 18 months, 56.7% (95% CI: 38.9, 74.6) at 24 months, and 52.7% (95% CI: 34.4, 71.0) at 30 months and 36 months
- Median overall survival (OS):
  - RET fusion-positive NSCLC: 44.3 months (95% CI: 30.9, 53.1), with KM estimates for the OS rate of 77.8% at 12 months and 63.1% at 24 months
  - RET-mutant MTC: KM estimates for median OS were not reached; the estimated OS rate was 90.7% (95% CI: 85.9, 95.5) at 12 months, 86.9% (95% CI: 81.3, 92.6) at 18 months and 83.9 (95% CI: 77.7, 90.1) at 24 months
  - RET fusion-positive thyroid cancer: KM estimates for median OS was not reached; the estimated OS rate was 87.1% (95% CI: 75.3, 98.9) at 6 months and 9 months, 80.4% (95% CI: 66.3, 94.5) at 12 months and 69.9% (95% CI: 53.4, 86.4) at 18 months, 66.4% (95% CI: 49.4, 83.5) at 24 months and 62.5% (95% CI: 44.8, 80.2) at 30 months and 36 months

For further details on the efficacy results of Study BO42863, see Section 5.4.1.

1.4.2.2 Study ML42439: MyTACTIC Study (Arm O)

Key efficacy results from Study ML42439 (Arm O) are summarized below:

- One out of 3 patients (33.3%) achieved a confirmed objective response (95% CI: 0.8, 90.6). This patient (33.3%) achieved a PR. One patient (33.3%) had SD as their confirmed best overall response.
- The median DOR was not estimable.
- Two out of 3 patients achieved disease control (DCR of 66.7%, 95% CI: 9.4, 99.2).

- The median PFS was 7.10 months (95% CI: 1.84, not estimable) and the PFS rate at 3 months was 66.67% (95% CI: 13.32, 100.00).

For further details on the efficacy results of Study ML42439 (Arm O), see Section 5.4.1.

1.4.3 Safety

1.4.3.1 Study BO42863: ARROW Study

Key safety results from Study BO42863 (LPLV: 21 March 2024) are summarized below:

- Safety was generally consistent across safety populations, regardless of indication and dose.
- Within the safety analysis (all patients who started treatment at 400 mg QD; n = 540), all patients experienced an adverse event (AE).
- Grade ≥ 3 AEs and treatment-related Grade ≥ 3 AEs were reported in 86.1% and 64.4% of patients, respectively.
- Serious adverse events (SAEs) and treatment-related SAEs were reported in 70.6% and 24.6% of patients, respectively.
- A total of 105 patients (19.4%) died due to an AE, of whom 8 patients (1.5%) died due to a related AE.
- Although a high proportion of patients had their treatment interrupted due to an AE (75.4%), or had their dose reduced due to an AE (52.4%) during the course of the study, only a modest proportion of patients discontinued study treatment due to an AE (24.1%). Considering the investigator-assessed treatment related AEs that led to study drug discontinuation, the proportion was even lower (9.6%) and demonstrates the acceptable tolerability in patients treated at 400mg.

For further details on the safety results of Study BO42863, see Section 5.5.1.

1.4.3.2 Study ML42439: MyTACTIC Study (Arm O)

Key safety results from Study ML42439 (Arm O) are summarized below:

- All patients (3/3, 100%) in Arm O experienced at least one AE during the study. The three most frequent AEs by PT were anaemia (3 patients, 100%), diarrhoea, and pyrexia (2 patients, 66.7% each).
- All patients (3/3, 100%) in Arm O experienced at least one AE that was considered by the investigator as related to study treatment (pralsetinib). The most frequent related AE by PT was diarrhoea (2 patients, 66.7%).
- All patients (3/3, 100%) in Arm O experienced AEs of Grade 3–5 as highest severity, including 1 patient (33.3%) who experienced a Grade 5 AE. There were no patients with Grade 4 AEs in Arm O of the study. The most frequently reported Grade 3 AE by PT (≥ 2 patients) was anaemia (3 patients, 100%). All other Grade 3 and Grade 5 AEs occurred in single patients.
- One out of 3 patients (33.3%) in Arm O died due to an AE. The patient experienced a Grade 5 AE of brain oedema that was not considered by the investigator as related to study treatment.

- Two patients (66.7%) in Arm O experienced at least one SAE during the study. All reported SAEs by PT occurred in single patients. There were no reported SAEs that were considered by the investigator as related to study treatment.
- There were 2 patients (66.7%) in Arm O who experienced at least one AE leading to withdrawal of treatment during the study. The reported AEs leading to withdrawal of treatment by PT were anaemia, brain oedema, and cognitive disorder (1 patient, 33.3% each).
- All patients (3/3, 100%) in Arm O experienced at least one AE leading to dose modification or interruption of the study treatment during the study. The most frequently reported AE leading to dose modification or interruption of the study treatment by PT ($\geq$2 patients) was diarrhoea (2 patients, 66.7%).

For further details on the safety results of Study ML42439 (Arm O), see Section 5.4.1.

2. INTRODUCTION

2.1 BACKGROUND ON RET KINASE

RET is a receptor tyrosine kinase expressed in several neural, neuroendocrine, and genitourinary tissues types that normally requires ligand and co-receptor binding for activation (Mulligan 2014). Along with Glial cell line derived neurotrophic factors (GDNF) and GDNF family receptor alpha (GFRα), RET is required for the development, maturation, and maintenance of several neural, neuroendocrine, and genitourinary tissue types.

2.2 CURRENT THERAPIES AND UNMET MEDICAL NEED

Increasing evidence implicates aberrant activation of RET as a critical driver of tumor growth and proliferation across a broad number of solid tumors (Mulligan 2014). As reviewed in Drilon et al. 2018, oncogenic activation of RET can occur by 2 primary mechanisms. Both mechanisms of oncogenic activation result in constitutively active, ligand-independent RET kinase activity and activation of downstream signaling pathways. First, chromosomal rearrangements can produce hybrid proteins that fuse the RET kinase domain with a partner protein that often contains a dimerization domain (Kohno et al. 2012; Lipson et al. 2012; Takeuchi et al. 2012; Romei et al. 2016). Second, mutations can directly or indirectly activate the kinase (Donis-Keller et al. 1993; Mulligan et al. 1993; Hofstra et al. 1994). Both mechanisms of oncogenic activation result in constitutively active, ligand-independent RET kinase activity and activation of downstream signaling pathways (Drilon et al. 2018).

As the prevalence of tumor genomic sequencing has increased, it has become apparent that oncogenic RET alterations occur in a variety of solid tumors. Activating RET mutations have been observed at high frequency (90%) of advanced MTC as well as a variety of other solid tumors, including ovarian, colorectal, and breast cancer (Kato et al. 2017; Romei et al. 2018).

RET fusions as a result of chromosomal rearrangement have been found in tumors NSCLC, papillary thyroid cancer (PTC), colon, breast, pancreatic, ovary, salivary carcinomas, and inflammatory myofibroblastic tumors, and suggest that RET fusions may be oncogenic in many tumor types (Santoro et al. 1992; ATA Guidelines Taskforce et al. 2009; Ballerini et al. 2012; Kohno et al. 2012; Lipson et al. 2012; Medico et al. 2015; Stransky et al. 2014; Takeuchi et al. 2012; Antonescu et al. 2015; Wang et al. 2016; Kang et al. 2017).

2.3 SCIENTIFIC RATIONALE

Pralsetinib (RO7499790; trade name GAVRETO™; formerly referred to as BLU-667, BLU123244, or X581238) is a potent and selective inhibitor of RET kinase and oncogenic RET mutants. Pralsetinib was designed as a highly potent and selective inhibitor of oncogenic RET fusion and mutant proteins. RET fusions are oncogenic drivers in 1–2% of NSCLC, 10–20% of PTC and at lower prevalence, below 1% across multiple other tumor types. RET mutations have been shown to be oncogenic in MTC with a prevalence of up to 60% in the sporadic and above 90% in the hereditary form of MTC. Pralsetinib inhibits the ligand independent constitutive activation of the RET tyrosine kinase activity and therefore prevents downstream oncogenic cell signalling. Pralsetinib demonstrates robust antitumor activity in several RET-driven in vitro and in vivo mouse models, and tolerability at pharmacologically active doses in nonclinical toxicology studies in rats and monkeys. Together, these data provide strong rationale for exploring the clinical utility of pralsetinib in advanced cancer patients with RET alterations (RET fusions, activating mutations, and some resistance mutations). Overall, the available nonclinical data demonstrate an acceptable benefit-risk profile for the clinical testing of pralsetinib.

2.4 OVERVIEW OF CLINICAL DEVELOPMENT

Studies in the clinical development program of pralsetinib include:

- Five completed clinical studies/cohorts evaluating safety, efficacy, and PK of pralsetinib in adult patients with solid tumors with RET alterations including gene fusions:BO41932 (cohort K), ML41591 (RET cohort), ML42439, BO42863 and BO42864 (LPLV: 27 January 2025; CSR under preparation).
- Three ongoing clinical pharmacology studies:
    - Patients with RET-altered solid tumors (JO43175 and JO43701)
    - Patients with advanced or metastatic solid tumors (GP43164)
- Seven dedicated clinical pharmacology studies (completed) to determine the absorption, metabolism, disposition, and PK of pralsetinib in humans, and to explore the effects of extrinsic factors (food, drug-drug interactions [DDIs]) on PK parameters, to compare the relative bioavailability of different pralsetinib formulations, or to assess the impact of hepatic impairment on pralsetinib PK (BP42858, BP42859, BP42860, BP42861, BP42862, GP43162, and GP43163). All

were conducted in healthy adult subjects except GP43163 which was conducted in patients with hepatic impairment and healthy volunteers.

Key design features of these studies are summarized in Appendix 4. For further details, please refer to the respective study protocols.

A Pre-approval Access Program and individual Investigational New Drug Applications (INDs), including 449 patients with unresectable or metastatic NSCLC, MTC or a cancer of an unknown type were treated with pralsetinib under the Compassionate Use Program (CUP) and expanded access program (EAP) as of 3 March 2024.

3. PHYSICAL, CHEMICAL, AND PHARMACEUTICAL PROPERTIES AND CLINICAL FORMULATION

3.1 PHYSICAL AND CHEMICAL PROPERTIES

Pralsetinib drug substance is isolated in crystalline form. The molecule is slightly hygroscopic, and has a melting point of 206°C (determined by differential scanning calorimetry). The solubility of pralsetinib is presented in Table 1.

Table 1 Physical and Chemical Properties

Conditions	Media	Solubility (mg/mL)
Solubility in aqueous solution at 25ºC	50 mM USP buffer, pH 4	0.07
	50 mM USP buffer, pH 7	0.06
	50 mM USP buffer, pH 10	0.04
Solubility at 37ºC in biorelevant media	Water	0.06
	0.1 N HCl	1.61
	SGF	0.77
	FaSSIF	0.05
	FeSSIF	0.07

FaSSIF = fasted state simulated intestinal fluid; FeSSIF = fed state simulated intestinal fluid; HCl = hydrochloric acid; SGF = simulated gastric fluid; USP = United States Pharmacopeia.

USP solubility definitions: < 0.1 mg/mL: practically insoluble; 0.1–1 mg/mL: very slightly soluble; 1–10 mg/mL: slightly soluble; 10–33 mg/mL: sparingly soluble; 33–100 mg/mL: soluble; 100–1000 mg/mL: freely soluble.

3.2 CLINICAL FORMULATION

Pralsetinib drug product is supplied for oral administration as immediate release HPMC hard capsules. The polymer stabilized spray dried dispersion of the drug substance is blended with compendial excipients during manufacturing. The drug product is manufactured and formulated following current Good Manufacturing Practices.

The immediate release capsules are supplied in 100 mg dose strength in size 0 light blue opaque HPMC capsules. The excipients and their respective pharmacopeial reference are presented in Table 2.

Table 2 Excipients in the Pralsetinib Capsules

Excipient	Pharmacopeial Reference
Hydroxypropyl methylcellulose (HPMC)	USP, Ph. Eur
Microcrystalline cellulose (MCC)	USP, Ph. Eur
Pregelatinized starch	USP, Ph. Eur
Sodium bicarbonate	USP, Ph. Eur
Citric acid	USP, Ph. Eur
Magnesium stearate	USP, Ph. Eur

HPMC = hydroxypropyl methylcellulose; MCC = Microcrystalline cellulose; Ph. Eur = Pharmocopeia European; USP = United States Pharmacopeia.

Pralsetinib should be administered as specified in the clinical protocols. Pralsetinib should be administered with a glass of water (at least 8 ounces or 250 mL) in a fasted state, with no food intake from 2 hours before until 1 hour after study drug administration. Patients should be instructed to swallow study drug whole and to not chew the study drug. Pralsetinib study drug should be stored in the container provided and not above 25°C (59°F).

4. NONCLINICAL STUDIES

4.1 NONCLINICAL PHARMACOLOGY

4.1.1 Introduction

A summary of all nonclinical pharmacology and safety pharmacology studies can be found in Appendix 1.

4.1.2 Primary Pharmacodynamics

4.1.2.1 In Vitro Studies

4.1.2.1.1 Inhibition of WT RET and Oncogenic RET Mutants and Fusions in Vitro

Pralsetinib (formerly called X581238, BLU123244, or BLU-667) was designed as a potent and selective inhibitor of oncogenic RET mutant and fusion proteins. In vitro, pralsetinib inhibited WT RET (IC_{50} = 0.43 nM), and the disease-driving RET V804L (IC_{50} = 0.33 nM), RET V804M (IC_{50} = 0.38 nM), RET M918T (IC_{50} = 0.40 nM), and CCDC6-RET mutant kinases (IC_{50} = 0.45 nM). Pralsetinib was at least 10-fold more potent on RET in biochemical assays than the multikinase inhibitors cabozantinib and vandetanib. In addition, these multikinase inhibitors and others in clinical testing in RET-altered patients were vulnerable to substitutions at the MTC-associated V804 position (BPM-0015; Appendix 1).

Selectivity of pralsetinib on RET versus other human kinases was characterized by profiling binding across a panel of over 450 human kinases and disease-relevant kinase mutants (BLU005-03-s/BLU005-04-p; Appendix 1). Pralsetinib had a high degree of selectivity for RET and RET kinase mutants over other kinases tested, with a greater than 100-fold biochemical selectivity for RET versus 95% of the kinome tested in binding assays. Furthermore, only JAK1, JAK2, and tropomyosin receptor kinase C (TRKC) demonstrated dissociation constant (K_d) values within 10–fold of RET, further demonstrating the potency and selectivity of pralsetinib.

To differentiate pralsetinib from multikinase inhibitors with biochemical activity against RET, the activity of pralsetinib against recombinant KDR (also known as VEGFR2) and FGFR1 was tested, as inhibition of these kinases is associated with clinical toxicities in humans. Pralsetinib was 81-fold and 26-fold more potent on WT RET than KDR/VEGFR2 and FGFR1, respectively. In contrast, the multikinase inhibitors-cabozantinib, vandetanib, and regorafenib exhibited approximately equal or increased potency on KDR versus WT RET (BPM-0015; Appendix 1).

In cellular systems, the activity of pralsetinib was measured by inhibition of RET mutant or RET fusion autophosphorylation, RET-dependent signaling, and by inhibition of RET dependent cell proliferation in both Ba/F3 models engineered to express KIF5B-RET and cancer cell lines endogenously expressing activated RET fusions or mutants, such as the LC2/ad cells, a non-engineered NSCLC cell line that expressed a CCDC6-RET fusion (Suzuki et al. 2013; Springuel et al. 2015; Subbiah et al. 2020; BPM-0017; Appendix 1). Similar effects were seen with pralsetinib in multiple RET-driven cell lines. In all RET-driven cell lines tested, pralsetinib inhibited RET activity and RET-driven proliferation more potently than the multikinase inhibitors cabozantinib and vandetanib (BPM-0016; BPM-0017; Appendix 1). In contrast, pralsetinib poorly inhibited proliferation in parental Ba/F3 cells that do not express a KIF5B-RET fusion (BPM-0016; Appendix 1), demonstrating that pralsetinib is selective for cell lines dependent on oncogenic RET.

4.1.2.2 In Vivo Studies

4.1.2.2.1 Inhibition of Oncogenic RET Activity in Vivo

Pralsetinib demonstrated robust antitumor activity in several RET-driven in vivo models, including a KIF5B-RET NSCLC PDX model (1110-003; Appendix 1), the TT metastatic thyroid cancer (MTC) xenograft driven by a RET C634W mutation (CPB-P16-5645; Appendix 1), the KIF5B-RET (V804L) fusion protein in an engineered Ba/F3-KIF5B-RET (V804L) allograft tumor model (CPB-P15-5515; Appendix 1), and in colorectal cancer PDX models bearing either the CCDC6-RET (WT) fusion (E0400-U1608; Appendix 1), the CCDC6-RET (V804M) fusion (E0400-U1523; Appendix 1), or NCOA4-RET fusion (E0400-U1806; Appendix 1), respectively. The RET V804M and V804L mutants have been observed in rare cases of MTC and are predicted to be insensitive to cabozantinib and vandetanib in vitro and in vivo (Carlomagno et al. 2004; Carlomagno et al. 2004; Bentzien et al. 2013; BPM-0016; Appendix 1). Oral administration of 3 mg/kg, 10 mg/kg,

30 mg/kg twice daily (BID), or 60 mg/kg QD pralsetinib resulted in dose-dependent antitumor efficacy, with > 90% tumor growth inhibition (TGI) at 10 mg/kg and tumor stasis and regressions observed at 30 mg/kg BID and 60 mg/kg QD in all models tested.

Pralsetinib demonstrated antitumor activity in intracranial tumors using the Ba/F3-KIF5B-RET-luc brain orthotopic inoculation model with 10 mg/kg and 30 mg/kg BID doses resulting in improved animal survival (CPB-P18-21802; Appendix 1). These data were confirmed in an intracranially inoculated colorectal cancer (CRC) model bearing the CCDC6-RET fusion, with 10 mg/kg and 30 mg/kg doses resulting in a statistically significant improvement in median survival with 6/10 and 0/10 animals showing intracranial tumors at end of study (day 96) (E0400-U1804; Appendix 1; Figure 1).

Across all studies, all doses of pralsetinib were well tolerated throughout the dosing periods, whereas the non-selective inhibitor cabozantinib (60 mg/kg QD) was poorly tolerated, requiring cessation of treatment and euthanasia of animals after 2 weeks of treatment due to declining heath.

Figure 1 Survival Curves of Mice in the Different Treatment Groups in a CCDC6-RET Colorectal Cancer Xenograft Model via Intracranial Inoculation

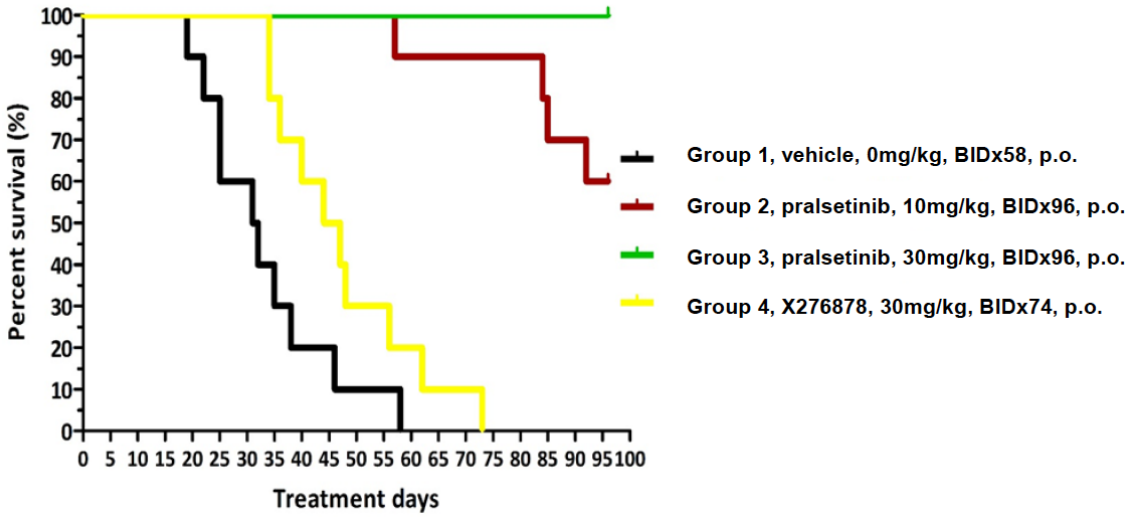

BID = twice daily; CCDC6 = coiled-coil domain containing 6; RET = rearranged during transfection.

Mice was intracranially injected with CCDC6-RET fusion colorectal cancer xenograft tumor cells and randomized into 10 mice per group, and dosed orally as indicated with 10 or 30 mg/kg BID of pralsetinib, or 30 mg/kg BID of a tool compound X276878. The animals were checked daily for tumor formation. $p < 0.001$ for Vehicle vs. either pralsetinib at 10 mg/kg or 30 mg/kg.

Source: E0400-U1804; Appendix 1.

Pralsetinib demonstrated robust pharmacodynamics in both the Ba/F3-KIF5B-RET or Ba/F3-KIF5B-RET (V804L) tumor models with a corresponding decrease in RET kinase activity in tumors as pralsetinib plasma levels increased (BPM-0020; Appendix 1). Robust antitumor efficacy was associated with doses of pralsetinib demonstrating

approximately 90% RET kinase inhibition. The mouse plasma concentration required for 90% inhibition of RET phosphorylation across all experiments was calculated using a 4-parameter non-linear regression curve fitting and was determined to be 769 ng/mL (BPM-0020; Appendix 1). This pralsetinib minimum plasma concentration (C_{min}) of 769 ng/mL (1442 nM) in mouse plasma associated with 90% RET inhibition was determined to be equivalent to 212 ng/mL in human, after adjustment for plasma protein binding species differences (CPB-P16-10980; Appendix 1). The partition coefficient for unbound brain to unbound plasma for pralsetinib was ~0.14, or 14% brain penetration rate. After adjusting for the brain penetration rate, the plasma concentration of pralsetinib associated with 90% RET inhibition in the human brain is equivalent to 1514 ng/mL.

4.1.3 Safety Pharmacology

Refer to Section 4.3.8.

4.1.4 Pharmacodynamic Drug Interactions

No studies have been performed.

4.2 PHARMACOKINETICS AND DRUG METABOLISM IN ANIMALS

4.2.1 Introduction

The PK, absorption, distribution, metabolism, and excretion profiles of pralsetinib were characterized in vitro and in vivo in nonclinical species studies and in vitro in human cells studies.

A summary of all PK and absorption, distribution, metabolism, and excretion (ADME) studies can be found in Appendix 2.

4.2.2 Methods of Analysis

Plasma samples obtained from Good Laboratory Practice (GLP) toxicology studies were analyzed for concentrations of pralsetinib using high-performance liquid chromatography (HPLC)/tandem mass spectrometry (MS/MS) methods with multiple reaction monitoring.

4.2.3 Absorption/Pharmacokinetic/Toxicokinetic Parameters

In vitro permeability for pralsetinib was evaluated in C2BBe1 cells, MDCK, MDR1-MDCK cells, and BCRP. Pralsetinib showed moderate permeability in C2BBe1 cells and is a dual substrate of efflux transporters P-gp and BCRP (CBP- P15-10082-CACO2, CPB-P15-10141; Appendix 2).

4.2.3.1 Single-Dose Pharmacokinetics

The plasma PK properties of pralsetinib upon single dosing in nonclinical species are summarized in Table 3. CL_{plasma} upon bolus IV administration of pralsetinib was low in rats, dogs, and monkeys (corresponding to ~26%, 6.4%, and 15% of the hepatic blood flow, respectively.

The apparent V_{dss} were low to moderate in the 3 species investigated (rats, dogs, and monkeys) and either equal to or up to 4-fold higher than the volumes of total body water.

The oral bioavailability of pralsetinib dosed as a solution was high (~100%) in rats, dogs, and monkeys.

Table 3 Cross Species Comparison of Single-Dose Pharmacokinetics of Pralsetinib

PK Parameter	Rat	Dog	Monkey
CL_{plasma} (mL/min/kg)	14.6 ± 1.6	2.0 ± 0.3	6.5 ± 3.0
V_{dss} (L/kg)	3.3 ± 0.4	0.5 ± 0.1	1.7 ± 0.2
$T_{1/2}$ (h)	3.5	3.5 ± 0.2	3.7 ± 1.2
Oral F (%)	> 100	100	100

CL_{plasma} = plasma clearance; F = bioavailability; PK = pharmacokinetics; $T_{1/2}$ = apparent elimination half-life; V_{dss} = apparent volume of distribution at steady-state.

4.2.3.2 Repeated-Dose -Toxicokinetics

In an exploratory 7-day repeated-dose toxicology study in rats (WIL-124551; Appendix 2), Day 0 exposures (AUC_{0-24} and C_{max}) increased over-proportionally with increasing doses from 15 mg/kg to 200 mg/kg. After 7-days of daily dosing, pralsetinib accumulated in plasma ~3 and 1.7-fold at the 15 mg/kg and 50 mg/kg doses, respectively.

In a 7-day repeated-dose toxicology study in monkeys (WIL-124572; Appendix 2), both C_{max} and AUC_{0-24} increased in a nearly dose-proportional manner with increasing doses, from 10 mg/kg to 150 mg/kg/day on Day 0 and from 10 mg/kg to 30 mg/kg/day on Day 6. No apparent accumulation of pralsetinib in plasma was observed.

In a developmental toxicity study in pregnant female rats that were administered pralsetinib for 12 days from Gestation Days 6 to 17 (Report 00124766; Appendix 2), the increase in maternal exposure, in terms of AUC_{0-24} and C_{max}, was greater than dose-proportional over the dosing range on both evaluation days (Gestation Days 6 and 17). Accumulation ratios were 2.5, 1.4, 1.4, and 1.4 at 5 mg/kg/day, 10 mg/kg/day, 20 mg/kg/day, and 30 mg/kg/day, respectively.

The toxicokinetics (TK) of pralsetinib was also investigated in rats and monkeys in GLP-compliant 28-day repeated-dose toxicology studies (WIL-124570 and WIL-124571, respectively; Appendix 2). In the 28-day GLP-compliant study in rats, the exposure at the end of the study increased in an over-proportional manner to dose in male rats and slightly less than dose-proportional in female rats over the range of 10 mg/kg to 30 mg/kg. Exposure to pralsetinib attained in the 7-day study in male rats was comparable to that attained in the 28-day study. Accumulation of pralsetinib in rat

plasma in the 28-day GLP-compliant study was minor with overall accumulation ratios < 2-fold (1.6- to 1.8-fold for males and 1.0- to 1.6-fold for females).

In the GLP-compliant 28-day repeated-dose toxicology study in monkeys, the exposure at the end of the study increased in a dose-proportional to slightly greater than dose-proportional manner in males and females from 2.5 mg/kg to 7.5 mg/kg. There was no notable difference in exposure between male and female monkeys on both evaluation days.

The TK of pralsetinib was also investigated in rats and monkeys in GLP-compliant 13-week repeated-dose toxicology studies (00124770 and 00124768, respectively; Appendix 2). In the 13-week GLP-compliant toxicology study in rats, the peak concentrations of pralsetinib were observed from 1 to 8 hours postdose across all dose levels and evaluation days, with the majority of peak concentrations being observed at 2 hours postdose in males and females. Following T_{max}, pralsetinib concentrations decreased slightly through 24 hours postdose. There was no notable difference (< 2-fold) in pralsetinib exposure, in terms of $AUC_{(0-t)}$ and C_{max} between male and female rats; however, there was a trend towards increasing exposure in females. Pralsetinib exposure, in terms of the area under the plasma concentration versus time curve from 0 to the last measurable concentration ($AUC_{(0-t)}$) and C_{max}, increased with increasing dose in a greater than dose-proportional manner from 5 mg/kg/day to 20 mg/kg/day in males and females on Day 1 and Day 91.

There was notable accumulation of pralsetinib following repeat dosing. Accumulation ratios were 2.36, 2.64, and 2.43 in males and 2.72, 3.27, and 2.32 in females at the 5 mg/kg/day, 10 mg/kg/day, and 20 mg/kg/day dose levels, respectively. There were no measurable pralsetinib concentrations at 2 hours postdose in the vehicle control group or at predose on Day 1 in the pralsetinib treatment groups.

In the 13-week GLP-compliant toxicology study in monkey, the majority of peak concentrations of pralsetinib were observed at 1 or 2 hours postdose across all animals and dose levels on Day 1 and Day 91. Following T_{max}, pralsetinib concentrations decreased through 24 hours postdose. There was no notable difference (< 2-fold) in pralsetinib exposure between male and female monkeys. Pralsetinib exposure, in terms of $AUC_{(0-t)}$ and C_{max}, increased with increasing dose in an approximately dose-proportional manner in male and female monkeys from 2 mg/kg/day to 10 mg/kg/day on Day 1 and Day 91 after taking into account the variability of $AUC_{(0-t)}$ and C_{max}.

Pralsetinib exposure, in terms of $AUC_{(0-t)}$, was similar on Day 91 when compared to Day 1 suggesting no accumulation of pralsetinib following repeat dosing. There were no measurable pralsetinib concentrations in the vehicle control group or at predose on Day 1 in the pralsetinib treatment groups.

4.2.4 Distribution

In plasma from mice, rats, and humans, pralsetinib was highly bound to proteins with the fraction unbound estimated at $<5\%$ (Report 1905093; Appendix 2).

In the in vitro studies in nonclinical species and humans, pralsetinib distribution was greater in plasma compared to blood (CPB-P15-10118; Appendix 2). Blood-to-plasma ratios ranged from 0.49 to 0.64. The blood-to-plasma ratio in humans was 0.49. However, in vivo, pralsetinib did not show preferential partitioning into red blood cells across species including humans. An in vivo distribution study in rats administered a single PO dose of [^{14}C]-pralsetinib was conducted (BLU-R5482AM1; Appendix 2). The mean blood-to-plasma ratio was 0.76, confirming limited preferential partitioning of pralsetinib into red blood cells.

Upon single oral dose of [^{14}C]-pralsetinib to nonpigmented male Sprague Dawley rats, the whole blood:plasma area under the concentration-time curve from time zero to the last measurable concentration above the lower limit of quantification ($AUC_{0\text{-last}}$) ratio was <1.0, but >0.5, suggesting limited preferential partitioning of [^{14}C]-pralsetinib equivalents into blood cells following oral dose administration (Report 00124834; Appendix 2). Tissue: plasma $AUC_{0\text{-last}}$ ratios for the majority of tissues were ≥ 1.0, indicating [^{14}C]-pralsetinib–derived radioactivity was widely distributed to the majority of tissues analyzed, with tissue:plasma $AUC_{0\text{-last}}$ ratios ranging from as high as 32 for the liver to as low as 0.5 for uveal tract. In pigmented male Long Evans rats, at t_{max}, [^{14}C]-pralsetinib–derived radioactivity was highest in the uveal tract pigmented skin with concentrations in the remaining tissues ranging from not calculable (eye) to 6470 ng equiv./g (adipose). The concentration of [^{14}C]-pralsetinib–derived radioactivity in the uveal tract of the male pigmented Long Evans rats appeared to be eliminated more slowly and was ~20-fold higher than in the male nonpigmented Sprague Dawley rat uveal tract , suggesting that the radioactivity derived from a single oral (gavage) dose of [^{14}C]-pralsetinib at 30 mg/kg and a target radioactivity of 100 μCi/kg had an affinity to this melanin-containing tissue.

A single oral (gavage) dose of [^{14}C]-pralsetinib to male monkeys resulted in whole blood and plasma exposure to [^{14}C]-pralsetinib equivalents (Report 00124835; Appendix 2).. The individual whole blood-to-plasma $AUC_{0\text{-last}}$ ratios following a single oral (gavage) dose of [^{14}C]-pralsetinib ranged from 0.816 to 0.842, with a mean ratio of 0.825. The <1.0, but >0.5 whole blood: plasma $AUC_{0\text{-last}}$ ratios suggest limited preferential partitioning of [^{14}C]-pralsetinib equivalents into blood cells following oral (gavage) dose administration.

The brain distribution study in rats with surgically implemented microdialysis probes showed that free brain concentrations of pralsetinib can be measured up to 24 hours after a single oral administration. The partition coefficient for unbound brain to unbound plasma was ~0.14, suggesting that pralsetinib was distributed into the brain (Report Key 1598; Appendix 2).

4.2.5 Metabolism

An in vitro study was conducted to elucidate the likely routes of metabolism of pralsetinib in mouse, rat, dog, monkey, and human liver microsomes and cryopreserved hepatocytes (Report BLU-R9667; Appendix 2). Pralsetinib underwent low to moderate metabolism in liver microsomes and cryopreserved hepatocytes from mice, rats, dogs, monkeys, and humans under the conditions utilized in this study. The in vitro metabolic pathways of pralsetinib included oxidation, defluorination, glucuronidation, and GSH conjugation. Metabolite M709 generated from direct glucuronide of pralsetinib appeared as the major metabolite observed in human hepatocytes. No unique human-specific metabolite of pralsetinib was found in this study. All metabolites detected in humans were present in either rats and/or monkeys.

4.2.6 Excretion

An excretion study was conducted to investigate the mass balance and routes of excretion in intact and bile-duct cannulated (BDC) rats following either a single PO or IV dose (BLU-R5482AM1; Appendix 2). [^{14}C]-pralsetinib-related radioactivity was rapidly excreted following both routes of administration.

Hepato-biliary excretion was a major route of elimination of pralsetinib. Urinary elimination represented only a minor excretion route for pralsetinib (1.5% of the dose after PO and 5.4% of the dose after IV dosing).

Excretion studies in milk in animals have not been conducted.

4.2.7 Pharmacokinetic Drug Interactions

In vitro data indicate that the Phase 1 metabolism of pralsetinib is mainly catalyzed by CYP3A4, with minor contribution of CYP1A2 and CYP2D6. Phase 2 metabolism is mediated by uridine 5'diphosphoglucuronosyltransferase (UGT) 1A4.

In vitro, pralsetinib is a direct inhibitor of CYP2C8, CYP2C9, and CYP3A4/5 (testosterone 6β-hydroxylation) (Report 1812081; Appendix 2). Pralsetinib also demonstrated time-dependent inhibition of CYP3A4/5 in vitro with a maximal inactivation rate constant (k_{inact}) and concentration required to achieve half-maximal inactivation (K_I) of 0.24 min^{-1} and 154 μM respectively for midazolam 1'-hydroxylation and a k_{inact} and K_I of 0.12 min^{-1} and 77 μM respectively for testosterone 6β-hydroxylation.

Treatment of human hepatocyte cultures with pralsetinib (0.03 μM to 10 μM) resulted in concentration-dependent induction of CYP1A2, CYP2B6, CYP2C8, CYP2C9, and CYP3A4 mRNA expression in at least 1 of the 3 lots tested, while induction of enzyme activity was noted for CYP2C8, CYP2C9, and CYP3A4 in at least 1 of the 3 lots tested (Report 1811301, Report 1910112; Appendix 2).

In vitro, pralsetinib is a substrate of P-gp and BCRP (Report 19BLUPP1R1; Appendix 2).

In vitro, pralsetinib inhibited the transport activities of human P-gp, BCRP, BSEP, OATP1B1, OATP1B3, OAT1, OAT3, MATE1, and MATE2-K. The in vitro IC_{50} values for inhibition of P-gp (C2BBe1 cells), OATP1B3, MATE1, MATE2-K, BCRP (C2BBe1 cells), OATP1B1, BCRP (BCRP-MDCK cells), P-gp (MDR1-MDCK cells), OAT1, OAT3, and BSEP were 0.344 μM, 0.680 μM, 0.796 μM, 0.999 μM, 2.49 μM, 3.59 μM, 4.62 μM, 9.86 μM, $<$10 μM, 17.7 μM, and 20.7 μM, respectively (lowest to highest) (Report 19BLUPP1R1; Appendix 2). Pralsetinib may have the potential for PK drug interactions with substrates of P-gp, BCRP, OATP1B1, OATP1B3, OAT1, OAT3, MATE1, and MATE2-K transporters.

4.3 TOXICOLOGY AND SAFETY PHARMACOLOGY

4.3.1 Introduction

Pralsetinib has been evaluated in a comprehensive toxicology program that included GLP and ICH S9 compliant repeat-dose toxicity studies up to 13 weeks in Sprague Dawley rats and cynomolgus monkeys, a battery of in vitro and in vivo genotoxicity studies, a 26-week carcinogenicity study in transgenic (Tg.rasH2) mice, embryo-fetal developmental toxicity and fertility and early embryonic development studies in rats, and in vitro phototoxicity studies. A 28-day study in wild type CByB6F1/Tg(HRAS)2Jic mice was conducted with pralsetinib to support the 26-week mouse carcinogenicity study. In addition, pralsetinib was evaluated for cardiovascular effects in the GLP-compliant 28-day and 13-week repeated dose toxicology studies of pralsetinib in Cynomolgus monkeys and in radiotelemetry-implanted Sprague Dawley rats in non-GLP safety pharmacology studies. In silico evaluation and bacterial mutagenicity assays were conducted to identify potential genotoxic impurities and in vivo GLP-compliant impurity qualification studies were conducted in Sprague Dawley rats.

Both rat and monkey are pharmacologically responsive to pralsetinib. All human metabolites detected in vitro were also detected with rats and/or monkeys. The rat and monkey contain identical or highly homologous amino acids surrounding the pralsetinib binding site when compared against human RET (BPM-0021; Appendix 3). Taken together, the rat and monkey are suitable species for nonclinical safety evaluation of pralsetinib. Although the Beagle dog was evaluated in non-GLP single-dose and 7-day toxicity and TK studies, it was precluded from evaluation in subsequent GLP repeated-dose toxicology studies because of a species-specific sensitivity to p38 MAPK signaling pathway inhibition (Morris et al. 2010).

Repeat dose-toxicology studies (Table 4) with pralsetinib evaluated tolerability, the potential to adversely affect key organ systems, recovery of the affected systems (28-day studies only), the severely toxic dose eliciting $\geq$10% lethality (STD_{10}) in the rat (28-day study), HNSTD in the monkey (28-day study), and the NOAEL in both species (13-week studies). Dose-related systemic exposures (AUC and C_{max}) for pralsetinib were established in both rat and monkey repeat-dose toxicology studies.

A summary of toxicology studies can be found in Appendix 3.

Table 4 Overview of Repeat-Dose Toxicity Studies with RO7499790

Species/ Reference	Treatment Duration	GLP Status	Dose (mg/kg/day)	NOAEL
Rat (Male) [WIL-124551]	7 days	non-GLP	0, 15, 50, 200	15
Rat (Female) [WIL-124592]	7 days	non-GLP	15, 50	50
Rat [WIL-124570]	28 days	GLP	0, 10, 20, 30, 75	30 (STD_{10})
Rat [00124770]	13 weeks	GLP	0, 5, 10, 20	10
Mouse[a] [20-2057]	28 days	GLP	0, 10, 30, 100	30 (MTD)
Monkey [WIL-124572]	7 days	non-GLP	0, 10, 30, 150/75[b]	10
Monkey [WIL-124571]	28 days	GLP	0, 5/2.5[a], 15/7.5[b], 40	7.5 (HNSTD)
Monkey [00124768]	13 weeks	GLP	0, 5, 10, 20	10

STD_{10} = severely toxic dose in 10% of animals; MTD = maximum tolerated dose; NOAEL = no-observed-adverse-effect level; HNSTD = high non-severely toxic dose.

[a] Conducted to support carcinogenicity assessment in this species only (Section 4.3.5).

[b] Dose reduced during study.

Note: See Appendix 3 for additional detail on each study

The pivotal toxicology and safety pharmacology studies intended to support human clinical trials were conducted in accordance with United States (U.S.) Food and Drug Administration (FDA) GLP regulations (21 CFR Part 58) and were conducted in a country that is a member of the OECD Mutual Acceptance of Data (MAD) program. Additional supportive toxicological, pharmacological, and pharmacokinetic studies were carried out as scientifically carefully conducted non-GLP studies.

4.3.2 Single-Dose Toxicity

Single oral dose toxicity studies were conducted in rats and monkeys. In a non–GLP-compliant study in Sprague Dawley rats (WIL-124550; Appendix 3), no clinical signs were noted in rats at doses up to the highest dose of 300 mg/kg. In a non-GLP-compliant study in Cynomolgus monkeys (WIL-124569; Appendix 3), 1 animal in the highest dose group (300 mg/kg) was found dead prior to the 48-hour post-dosing observation. At necropsy there were multiple dark red areas noted along the surface of the small and large intestines, which were confirmed microscopically to be mucosal epithelium erosion and ulceration associated with inflammation and hemorrhage. These findings are attributed to VEGFR inhibition.

4.3.3 Repeat-Dose Toxicity

Repeat-dose oral toxicity studies up to 13-weeks in duration were conducted in rats and monkeys and included an assessment of recovery from pralsetinib-related effects in the 28-day studies (Table 4). Pralsetinib was administered QD by oral gavage in all studies.

The main toxicities of pralsetinib observed in rat and/or monkeys included hematological abnormalities, effects on bony tissues, reproductive/developmental toxicities, metabolic perturbation, and effects on cardiovascular and gastrointestinal systems, as discussed below. With the exception of embryofetal toxicities discussed in Section 4.3.6, which were attributed to on-target RET inhibition, the majority of the pralsetinib-related toxicologic effects were attributed to off-target kinase inhibition (i.e., JAK2, VEGFR, and FGFR). The severely toxic effects in the rat were primarily the result of inanition, hematologic abnormalities, vascular perturbations, and metabolic alterations. The severely toxic effect in monkeys was attributed to bacterial sepsis secondary to VEGFR-inhibition mediated gastrointestinal barrier dysfunction (erosion/ulceration).

4.3.3.1 Effects on Hematologic and Lymphoid Systems

Hematological abnormalities (reduced bone marrow cellularity, reduced hemoglobin, reduced reticulocytes), and lymphoid effects (reduced lymphoid cellularity and decreased lymphocyte counts) were noted in rat and/or monkey at doses $\geq$ 5 mg/kg. Reduced bone marrow cellularity was considered adverse in rat at doses $\geq$ 20 mg/kg. These effects were dose-dependent and reversible. The primary cellular effects on the bone marrow and erythron parameters were attributed to off-target JAK2 inhibition due to the reliance upon JAK2 for erythropoietin signaling (Parganas et al. 1998; Broxmeyer 2013; Springuel et al. 2015). The decreased cellularity of lymphoid organs corresponding with changes in the leukon, notably decreased lymphocytes with increased neutrophils and monocytes, was attributed to stress response rather than to pralsetinib-related off-target effects (Everds et al. 2013).

4.3.3.2 Effects on Bone

Effects on bone (physeal dysplasia) in both rats and monkeys and incisor tooth degeneration in rats were observed at doses $\geq$ 10 mg/kg in rat and at 15/7.5 mg/kg in monkeys (28-day study only). Physeal dysplasia is a lesion often encountered secondary to impairment of VEGF-dependent angiogenesis, while incisor degeneration has been previously described after VEGF and FGFR tyrosine kinase inhibition (Patyna et al. 2008; Chen and Cleck 2009; Fletcher et al. 2010). In general, the physes of humans close at puberty and thus are not susceptible to drug-related physeal dysorganization observed in rodents, which have a persistent open physis (Frazier 2017; Hall et al. 2016). Similarly, the incisor teeth in rodents grow continuously making the translatability of incisor degeneration to humans unclear.

4.3.3.3 Metabolic Effects

Elevation of circulating phosphorus concentration with corresponding mineralization in soft tissues was present in the rat. The mineralization was minimal and non-adverse at

doses between 5–20 mg/kg, but was adverse at 30 mg/kg. Mineralization was primarily present in the glandular stomach, and was also observed to a lesser extent within the heart, kidneys, ovaries and spinal cord. These findings are attributed to off-target inhibition of FGFR due to its physiologic role of suppressing 1,25-dihydroxy-vitamin D3-mediated phosphate absorption from the gut (Brown et al. 2005; Yanochko et al. 2013). Similar findings were not observed in monkeys.

4.3.3.4 Gastrointestinal Effects

Gastrointestinal effects were observed in monkeys at doses exceeding the maximum tolerated dose (MTD; 15 and 40 mg/kg/day), including bacterial sepsis secondary to gastrointestinal inflammation, which was often erosive or ulcerative and associated with hemorrhage. These effects are consistent with inhibition of VEGF, as altered gut barrier is a known sequela of VEGF pathway inhibition in nonclinical toxicity species and in humans (Chen and Cleck 2009).

4.3.3.5 Effects on the Heart

Necrosis and hemorrhage in the heart was observed in rat and monkey preterm decedents at non-tolerated doses (75 mg/kg/day and ≥ 15 mg/kg/day, respectively). In monkeys, necrosis and hemorrhage were multiorganic and was attributed to sepsis with intralesional bacteria in lymph nodes, spleen, heart, and kidneys, see Section 4.3.3.4. These hemorrhagic effects are considered to be secondary to VEGFR inhibition (Patyna et al. 2008; Chen and Cleck 2009; Fletcher et al. 2010).

4.3.3.6 Other Effects

Pralsetinib administration was associated with dose-dependent and reversible increases of the serum ALT, AST, gamma-glutamyl transferase (GLDH) in rats at doses ≥ 10 mg/kg. However, there were no correlating gross or histologic findings.

4.3.4 Genotoxicity

Pralsetinib was negative for mutagenic activity in a GLP-compliant 5-strain Ames bacterial reverse mutation assay, with and without metabolic activation (rat liver S9). Furthermore, pralsetinib did not induce micronuclei in vitro in TK6 cells with and without metabolic activation or in vivo in Sprague Dawley rats that were administered oral doses of pralsetinib of up to 300 mg/kg/day for 2 consecutive days. Based on these results, pralsetinib is considered to be non-genotoxic.

4.3.5 Carcinogenicity

There was no evidence of pralsetinib-related pre-neoplastic or neoplastic lesions in the completed repeat-dose toxicity studies in rats and monkeys. A GLP-compliant 26-week carcinogenicity study with pralsetinib was conducted in hemizygous CByB6F1/Tg rasH2 (Tg.rasH2) mice (Study 21-1108, Appendix 3). Dose levels for the 26-week study were selected based on a 28-day study in WT CByB6F1/Tg(HRAS)2Jic mice (Study 20-2057; Appendix 3) in which target organs were bone marrow, spleen, thymus, and testis/epididymis (similar to those observed in rats, as described in Section 4.3.3).

Pralsetinib was not carcinogenic and had no impact on survival in male or female Tg.rasH2 mice at daily oral doses up to 30 mg/kg/day (approximately 4.5-times the exposure at the maximum recommended human dose based on AUC). At ≥10 mg/kg/day, pralsetinib-related non-neoplastic findings in Study 21-1108 consisted of testicular degeneration/atrophy accompanied by decreased sperm in the epididymides that correlated with small testes and epididymides. Decreased cellularity in the bone marrow and thymus occurred in females at≥10 mg/kg/day and in males at 30 mg/kg/day. At 30 mg/kg/day, there was decreased splenic cellularity in males and females. At the high dose of 30 mg/kg/day, the mean C_{max} and AUC values for males and females were 19,500 ng/mL and 164,000 ng•h/mL, respectively, after 26 weeks of treatment.

4.3.6 Reproductive and Developmental Toxicity

Consistent with the ICH S9 guideline, studies on postnatal development and effects in juvenile animals were not conducted. No information is available on the safety or efficacy of pralsetinib in lactating females.

No adverse effects were identified in reproductive tissues in the GLP-compliant 28-day repeat-dose toxicology studies in Sprague Dawley rats and and 28-day and 13-week repeat-dose toxicology studies Cynomolgus monkeys. In the GLP-compliant 13-week repeated-dose toxicology study in rats (00124770; Appendix 3), adverse effects on reproductive tissues were noted at the highest dose of 20 mg/kg/day, including degeneration/atrophy in the testis in males and degeneration of the corpus luteum in the ovary of the females. The adverse effects on the ovaries in females were attributed to VEGFR inhibition, since corpus luteum development is dependent upon proliferation of blood vessels within the theca interna, and reduced ovarian weight and decreased number of corpora lutea have been observed in rats given a VEGF inhibitor (Parganas et al. 1998; Morris et al. 2010; Nishino et al. 2017).

In a GLP-compliant repeated-dose fertility and early embryonic development toxicology study in male and female Sprague Dawley rats (Report 00124841; Appendix 3), pralsetinib was given from premating to conception and from conception to implantation. There was no impact on female estrous cyclicity or male sperm parameters and no effects on overall male or female reproductive performance (i.e., no decrease in the mean number of implantations). As a result, the NOAEL for fertility and male and female reproductive toxicity was 20 mg/kg/day, the highest dosage level evaluated. In this same study, the NOAEL for early embryonic toxicity was 10 mg/kg/day due to early post-implantation loss (92.47%) and lower number of viable embryos at 20 mg/kg/day observed on Gestation Day 7, however post-implantation loss occurred at doses as low as 5 mg/kg (approximately 0.35 times the human AUC exposure at the clinical dose of 400 mg based on toxicokinetic data from the 13-week rat toxicology study). This early embryonic toxicity finding is consistent with observations from the GLP-compliant embryofetal development toxicology study in pregnant female Sprague Dawley rats

described below. To further evaluate the potential for pralsetinib exposure in males to contribute to the early embryonic loss observed in the male and female combined fertility study, a second fertility and early embryonic development study was conducted in which male rats administered pralsetinib were mated with untreated female rats (Study 21-0310; Appendix 3). In this study, intrauterine survival of the embryos (mean litter proportions of postimplantation loss and mean numbers and litter proportions of viable embryos) was unaffected by pralsetinib administration to males at the 20 mg/kg dose level (approximately 1.4 times the human exposure (AUC) at the clinical dose of 400 mg based on toxicokinetic data collected in this study). In addition, no pralsetinib-related effects on male reproductive performance (mating, fertility, and pregnancy indices) were observed in this study.

In a GLP-compliant embryofetal toxicology study covering pralsetinib administration from Gestation Days 6 to 17 (Report 00124766; Appendix 3), pralsetinib was tolerated in pregnant Sprague Dawley rats up to the highest tested dose of 30 mg/kg/day (the NOAEL for maternal toxicity). However, a NOAEL for embryofetal development could not be determined based on adverse effects on intrauterine survival and/or fetal morphology at all dose levels. Postimplantation losses of 100% were observed at doses $\geq$ 20 mg/kg/day (approximately 1.8-fold of human AUC exposure at the clinical dose of 400 mg) and post-implantation loss also occurred at the 10 mg/kg dose level (approximately 0.6-fold human AUC exposure at 400 mg). At 5 and 10 mg/kg/day (approximately 0.2- and 0.6-fold human AUC exposure at 400 mg), multiple visceral (kidney and ureter abnormalities) and skeletal (rib, costal cartilage, and vertebral anomalies) malformations were observed. The renal malformations were attributed to on-target inhibition of RET signaling, as RET has a well-conserved role in the embryologic development of the kidney and enteric nervous system. Loss of function RET mutations during early development are associated with congenital abnormalities of the kidney and urinary tract as well as congenital aganglionosis (Hirschsprung's disease), while mice homozygous for a mutation in the RET gene display renal agenesis or severe dysgenesis (Schuchardt et al. 1994; Manié et al. 2001; Costantini and Shakya 2006; Patyna et al. 2008).

4.3.7 Local Tolerance

Local tolerance of pralsetinib in the gastrointestinal tract of rats and Cynomolgus monkeys was characterised in the GLP-compliant 28-day toxicology studies (Study WIL-124570 and WIL-124571; Appendix 3). In rats, there was evidence of soft tissue mineralization within the glandular stomach mucosa attributed to FGFR inhibition-mediated hyperphosphatemia at the STD_{10} (30 mg/kg/day), but no evidence of pralsetinib-related oropharyngeal/esophageal injury up to the non-tolerated dose (75 mg/kg/day). In monkeys, there was no evidence of gastrointestinal disturbances at the HNSTD (7.5 mg/kg/day). However, at non-tolerated doses of 15 and 40 mg/kg/day, deaths were seen secondary to septicemia resulting from gastrointestinal epithelial erosion and ulceration attributed to VEGFR inhibition. There was no evidence of

pralsetinib-related oropharyngeal/esophageal injury in monkeys up to and including the non-tolerated doses.

4.3.8 Safety Pharmacology

Pralsetinib was evaluated for effects on hERG-channel activity and inhibitory potential against a broad class of pharmacologically active receptors, enzymes, and ion channels in vitro. Pralsetinib was also evaluated for the potential to elicit adverse effects on the cardiovascular system in safety pharmacology (in vivo) studies.

The pharmacologic specificity of pralsetinib was assessed against a panel of receptors, transporters, and enzymes (Report 100023499/100023915; Appendix 3). There was $>50\%$ inhibition by pralsetinib against 5-HT_{2A} and sodium ion (Na^+) channel site 2, with biochemical IC_{50} values of 3600 nM against 5-HT_{2A} and 3400 nM against Na^+ channel site 2. The clinical significance of these interactions is unknown. Adverse and/or severely toxic events noted in the 28-day and 13-week GLP-compliant toxicity studies in Sprague Dawley rats and Cynomolgus monkeys were attributed to off-target kinase inhibition and not to inhibition of 5-HT_{2A} or Na^+ channel site 2.

The IC_{50} for the inhibitory effect of pralsetinib on hERG potassium current was 5.18 μM (Hill coefficient = 0.92), suggesting a low potential for prolonging the QT interval (CPB-25-15-010A-0169; Appendix 3). This is consistent with findings from the GLP-compliant 28-day and 13-week repeated dose toxicology studies of pralsetinib in Cynomolgus monkeys in which no pralsetinib-related changes to ECG waveform morphology, heart rate, or PR, QRS, RR, QT, or QTcB interval duration were observed at the highest doses administered in each study (7.5 mg/kg and 10 mg/kg or 90 mg/m^2 and 120 mg/m^2, respectively).

In radiotelemetry-implanted male Sprague Dawley rats, a single oral dose of 25 mg/kg, 50 mg/kg, or 200 mg/kg pralsetinib resulted in higher systolic, diastolic, and mean blood pressure, with a concomitant decrease in heart rate. Lower body temperature was also observed at 200 mg/kg. No clinical observations were observed at any dose level. No changes in cardiovascular function or body temperature were observed at a single dose of 10 mg/kg pralsetinib; therefore, the no-observed-effect level was 10 mg/kg (60 mg/m^2). The increase in blood pressure in rats is attributed to VEGFR inhibition. The potential for pralsetinib to increase blood pressure in monkeys was not monitored.

4.3.9 Other Toxicity Studies

4.3.9.1 Qualification of Impurities, Intermediates, and Excipients

No potential mutagenic impurities of pralsetinib were identified based on in silico evaluation and/or bacterial mutagenicity assays. Three potentially genotoxic impurities of pralsetinib drug substance were tested in the GLP-compliant bacterial reverse mutation assay and were determined to be nonmutagenic. In vivo GLP-compliant impurity qualification studies were conducted in Sprague Dawley rats on the main

impurities found to be above the ICH Q3A/ICH Q3B qualification thresholds (Reports WIL-124665 and WIL-124746; Appendix 3). No toxicities specific to these impurities were identified and specification limits for the drug substance were set based on the impurity levels present in these studies and in the GLP-compliant 28-day toxicology study in rats.

Only common compendial excipients are used in the commercial drug product (refer to Section 3.2), therefore no excipient qualification is warranted.

4.3.9.2 Phototoxicity

Pralsetinib was classified as non-phototoxic in a GLP-compliant in vitro phototoxicity evaluation in 3T3 fibroblasts using the neutral red uptake assay (Report 20143108; Appendix 3).

4.3.10 Toxicokinetics

A summary of pralsetinib mortality and exposures on Day 27 in the 28-day GLP-compliant toxicology studies in rats at the STD_{10} and in monkeys at the HNSTD and on Day 91 in the 13-week GLP-compliant toxicology studies at the NOAEL are presented in Table 5. There were no new severely toxic findings, nor was there an increase in the severity of known adverse findings in the 13-week studies. Exposure at these doses is compared with the clinical exposure at 400 mg QD in patients RET fusion-positive NSCLC (Section 5.2.1.1). NSCLC exposures were used for this comparison as this patient population had the highest exposure.

Table 5 Summary of Pralsetinib Mortality and Exposures in the 28-day and 13-week studies in Rats and Monkeys

Species/ Study	Dose (mg/kg/ day)	Sex	Death	AUC_{0-24} (ng*h/mL)	C_{max} (ng/mL)	Exposure Ratio[d]	
						AUC	C_{max}
Rat WIL-124570	30 (STD_{10})	M	2/24[a]	125,000	7,180	2.8	2.5
		F	2/24[b]	101,000	9,120	2.3	3.2
Rat 00124700	10 (NOAEL)	M	0/10	33,300	2360	0.8	0.8
		F	0/10	42,300	2580	1.0	0.9
Monkey WIL-124571	7.5[c] (HNSTD)	M	0/5	28,400	3,190	0.6	1.1
		F	0/5	25,800	3,320	0.6	1.2
Monkey 00124768	10 (NOAEL)	M	0/4	43,200	2790	1.0	1.0
		F	0/4	31,900	2850	0.7	1.0

AUC = area under the plasma concentration versus time curve; AUC_{0-24} = AUC from 0 to 24 hours; C_{max} = maximum plasma concentration; F = female; HNSTD = highest nonseverely toxic dose; M = male; NOAEL = no observed adverse effect level; STD_{10} = severely toxic dose in 10% of animals.

[a] Animal 5727 was euthanized in extremis on Day 15; animal 5655 was found dead on Day 19.

[b] Euthanized due to gavage error.

[c] Because of the morbidity/mortality at 15 and 40 mg/kg/day, given a 2-day dosing holiday prior to the dosage level being lowered from 15 mg/kg/day to 7.5 mg/kg/day beginning on Day 6 (males) or Day 7 (females).

[d] Based on human steady-state exposure at 400 mg QD in NSCLC patients: the geometric mean (%CV) C_{max} = 2830 ng/mL (52.5%); the geometric mean (%CV) $AUC_{0-\tau,ss}$ = 43900 h•ng/mL (60.2%), see Section 5.2.1.1.

Note: See Appendix 3 for additional detail on each study.

As described in Section 4.3.3, the primary toxicological effects of pralsetinib observed in the GLP-compliant 28-day and 13-week repeated-dose toxicity studies in rats and monkeys were attributed to the pharmacologic effects of inhibiting VEGFR, FGFR, and JAK2. The exposure thresholds for pharmacologic effects thought to be caused by inhibiting these targets in rats and monkeys based on the 28-day repeat-dose toxicity studies are presented in Table 6.

Table 6 Pharmacologic Effects and Toxicokinetics (on Day 27) of Pralsetinib in Rats and Monkeys in GLP-Compliant 28-day Studies

Species	Threshold Dose / AUC_{0-24} for Off-Target Kinase Effects					
	VEGFR		FGFR		JAK2	
	Dose	AUC_{0-24}	Dose	AUC_{0-24}	Dose	AUC_{0-24}
Rat[a]	10 mg/kg (60 mg/m^2)	31,300 ng*h/mL	20 mg/kg (120 mg/m^2)	73,200 ng*h/mL	10 mg/kg (60 mg/m^2)	31,300 ng*h/mL
Monkey[a]	7.5 mg/kg (90 mg/m^2)	27,100 ng*h/mL	*No Effect Observed*		7.5 mg/kg (90 mg/m^2)	27,100 ng*h/mL

AUC = area under the plasma concentration versus time curve; AUC_{0-24} = AUC from 0 to 24 hours; FGFR = fibroblast growth factor receptor; JAK = Janus kinase; VEGFR = vascular endothelial growth factor receptor.

[a] Mean male and female.

4.4 NONCLINICAL PHARMACOLOGY, PHARMACOKINETICS AND TOXICOLOGY INTEGRATED ANALYSIS

Pralsetinib is a highly potent and selective inhibitor of WT and oncogenic RET fusion and mutant proteins, including the disease-driving KIF5B-RET, CCDC6-RET and NCOA4-RET fusion kinase, the RET M918T and C634W mutant kinases and, notably, the RET V804L/M (gatekeeper) mutants. These features have been characterized in vitro and in vivo. Illustrating pralsetinib's potency, there was dose-dependent tumor growth inhibition in several RET-driven tumor animal models. These animal models included: 1) a KIF5B-RET-driven PDX NSCLC model, 2) a Ba/F3-KIF5B-RET-luc brain orthotopic

inoculation model, 3) a RET C634W mutant-driven MTC xenograft model, 4) a CCDC6-RET-expressing colorectal cancer PDX model, and 5) an intracranial inoculation RET fusion colorectal cancer xenograft model. Antitumor efficacy in these models correlated well with systemic drug exposure and PD modulation of tumor biomarkers, including direct inhibition of RET activity. In vitro selectivity studies demonstrated a high degree of selectivity for RET over 450 kinases. Follow-up assays confirmed the selectivity of pralsetinib for RET over KDR (also known as VEGFR2), FGFR1, and JAK2. Additional safety pharmacology screening efforts against a panel of 55 transmembrane or soluble receptors, ion channels and monoamine transporters, and the hERG channel supported a favorable profile for pralsetinib. The hERG channel results, combined with the lack of effect on ECG observed in the GLP-compliant 28-day and 13-week repeated-dose toxicology studies in monkeys, suggest a low potential for pralsetinib prolonging the QT interval in patients. In vivo safety pharmacology studies using radiotelemetry-implanted rats revealed that pralsetinib can increase blood pressure; this effect is attributed to VEGFR inhibition.

No PD interaction studies were performed. Pralsetinib is selective for RET and therefore, coadministration with products that have the same pharmacological target is unlikely. Pralsetinib is well absorbed from the gastrointestinal tract in humans, as suggested by the high oral bioavailability (100%) in nonclinical species. Despite the findings from MDR1-MDCK and C2BBe1 assays, efflux transport in gut is not expected to limit the oral bioavailability of pralsetinib in humans. This could be due to autoinhibition of P-gp- or BCRP-mediated transport, since pralsetinib is both inhibitor and substrate of P-gp and BCRP. This correlated with an appropriate dose–exposure relationship in the GLP-compliant 13-week repeated-dose toxicology studies in rats and monkeys.

Pralsetinib was highly protein bound ($\geq$95%) in mouse, rat, dog, monkey, and human plasma. In vitro, pralsetinib was minimally associated with red blood cells in all nonclinical species, as well as in humans, suggesting that plasma is an appropriate matrix for measuring systemic exposure of pralsetinib. Pralsetinib distributed widely to majority of tissues in rats, including the brain. There was a high unbound concentration of pralsetinib in the striatal interstitial fluid of rats, suggesting a potential for high brain penetration of pralsetinib. The unbound concentration of pralsetinib in the striatal interstitial fluid at the therapeutic doses in humans is predicted to be high enough to inhibit RET protein expressed by metastatic NSCLC cells in the brain.

Pralsetinib showed a potential affinity to melanin-containing tissues such as the skin and the uveal tract. However, there were no specific toxic effects of pralsetinib in these tissues in the GLP-compliant 13-week repeated-dose toxicology studies in rats and monkeys. The metabolite profile of pralsetinib was generally comparable across mouse, rat, dog, monkey, and human. In vivo, all human metabolites were produced in either rats and/or monkeys. In vitro, pralsetinib metabolism in human primary hepatocytes and liver microsomes is mainly mediated by CYP3A4 (Phase 1) and UGT1A4 (Phase 2).

The proposed metabolic pathway in vitro and in vivo resulted from oxidation/hydroxylation of the pralsetinib pyrazolpyridine ring system (M549a and M449c), oxidation of cyclohexyl moiety (M549c), direct N-glucuronidation (M709), and GSH conjugation with or without defluorination. Metabolite M709 generated from direct N-glucuronidation of pralsetinib appeared as the major metabolite observed in human primary hepatocytes.

In nonclinical species, excretion of pralsetinib occurred mainly as the unchanged parent compound via the hepatobiliary route with a minor role by an active intestinal epithelial excretion. Given the results, urinary excretion is not predicted to be a major elimination pathway in humans. Excretion studies in milk of lactating animals have not been conducted. It is not known if pralsetinib and/or its metabolites are excreted in human milk. Therefore, patients treated with pralsetinib should not nurse.

The potential for pralsetinib to be a victim or perpetrator of PK drug-drug interaction were evaluated in vitro. As pralsetinib metabolism is mainly mediated by CYP3A4, on comitant treatment with drugs that are inhibitors or inducers of CYP3A4 may alter pralsetinib plasma concentrations.

In vitro, pralsetinib is an inhibitor of CYP2C8, CYP2C9, and CYP3A4/5 (testosterone 6β-hydroxylation) with K_I values of 9.6 μM, 4.1μM, and 24 μM, respectively. Pralsetinib also demonstrated time-dependent inhibition of CYP3A4/5 (testosterone 6β-hydroxylation) in vitro with a K_{inact} and K_I of 0.24 min^{-1} and 154 μM, respectively. Therefore, pralsetinib has a potential to increase the plasma exposures of concomitant medications that are substrates of CYP2C8, CYP2C9, or CYP3A4. Pralsetinib did not show inhibition of CYP1A2, CYP2B6, CYP2C19, or CYP2D6 at clinically relevant concentrations. As such, PK drug-drug interactions with substrates of these enzymes is unlikely. Pralsetinib induced the mRNA expression of CYP1A2, CYP2B6, CYP2C8, CYP2C9, and CYP3A4 in vitro. Pralsetinib is a weak inducer of CYP1A2, but may cause clinically significant induction of CYP2B6 and CYP3A4 activity. No relevant induction was seen with CYP2C19, but pralsetinib may cause induction of CYP2C8 or CYP2C9. Therefore, pralsetinib has a potential to increase or decrease the plasma exposures of concomitant medications that are substrates of CYP2B6, CYP2C8, CYP2C9, or CYP3A4/5. The net effect of concurrent induction and inhibition of these enzymes is unknown.

Pralsetinib is a dual P-gp/BCRP substrate, but is not a substrate of OAT1, OAT3, OATP1B1, OATP1B3, organic cation transporter (OCT) 1, OCT2, BSEP, MATE1, or MATE2K. Therefore, P-gp inhibitors may decrease the gastrointestinal secretion of pralsetinib and potentially increase its plasma concentration.

In vitro studies indicate that at clinically relevant concentrations, pralsetinib is an inhibitor of P-gp, BCRP, BSEP, OATP1B1, OATP1B3, OAT1, OAT3, MATE1, and MATE2K, but not of OCT1 or OCT2. In vitro IC50 values for inhibition of P-gp (C2BBe1 cells),

OATP1B3, MATE1, MATE2K, BCRP (C2BBe1 cells), OATP1B1, BCRP (BCRP-MDCK cells), P-gp (MDR1-MDCK cells), OAT1, OAT3, and BSEP were 0.344 μM, 0.680 μM, 0.796 μM, 0.999 μM, 2.49 μM, 3.59 μM, 4.62 μM, 9.86 μM, < 10 μM, 17.7 μM, and 20.7 μM, respectively. Therefore, pralsetinib may change the PK of drugs that are substrates for these transporters.

A comprehensive nonclinical toxicology program consistent with ICH guideline S9 assessed the potential of pralsetinib for genotoxicity, phototoxicity, embryofetal-development toxicity, and fertility and early embryonic toxicity as well as the effects of acute and chronic repeated administration (QD) in pharmacologically responsive rats and monkeys. In Sprague Dawley rat and Cynomolgus monkey single-dose and repeated-dose toxicology studies, there was no clear evidence of toxicity associated with RET inhibition; all toxicological effects in these studies were attributed to off-target (kinase) pharmacology, including VEGFR, FGFR, and/or JAK2 inhibition. Key common toxicities noted in both Sprague Dawley rats and Cynomolgus monkeys included hematological abnormalities (reduced bone marrow and lymphoid organ cellularity, reduced red blood cells, reduced reticulocytes) and effects on bony tissues (physeal dysplasia), soft tissues (hemorrhage/mineralization) and gastrointestinal tract (erosion and ulceration). Effects on the bone marrow and erthyron parameters were attributed to JAK2 inhibition (Broxmeyer 2013; Broxmeyer 2013; Springuel et al. 2015), while effects on lymphoid organs were considered secondary to stress (Everds et al. 2013; Everds et al. 2013). Effects on bone, soft tissues, and gastrointestinal tract were attributed to impaired angiogenesis secondary to VEGFR inhibition (Patyna et al. 2008; Chen and Cleck 2009; Fletcher et al. 2010). Toxicities only observed in rats included myocardial hemorrhage, incisor tooth degeneration, and degeneration of the corpus luteum in the ovary (all secondary to VEGFR inhibition), as well as electrolyte and metabolic effects (increases in blood phosphorus with corresponding mineralization in the stomach secondary to FGFR inhibition) and degeneration in the testes. Toxicities that were only observed in monkeys included gastrointestinal effects including mucosal ulcerations and hemorrhage (consistent with inhibition of VEGFR) with subsequent fatal secondary bacterial sepsis.

Most pralsetinib-related effects in the 28-day repeated-dose toxicology studies showed evidence of reversibility after the 14-day recovery period, and most are considered to be monitorable. There were no new severely toxic findings, nor was there an increase in the severity of known adverse findings in the 13-week studies. After 13 weeks of dosing, the NOAEL in both species is 10 mg/kg/day (60 mg/m^2/day in rats and 120 mg/m^2/day in monkeys).

Visceral and skeletal fetal malformations, including kidney and ureter abnormalities, were observed in the GLP-compliant embryofetal-development toxicity study in pregnant Sprague Dawley rats at dosage levels of 5 mg/kg/day and 10 mg/kg/day (30 mg/m^2/day and 60 mg/m^2/day, respectively) and were attributed to on-target RET inhibition. RET is an essential component of a signaling pathway required for renal organogenesis

(Schuchardt et al. 1994; Costantini and Shakya 2006). Postimplantation loss was also observed in this study and the fertility and early embryonic toxicity study in Sprague Dawley rats, an effect that has been observed with other anti-VEGF compounds due to their antiangiogenic effects (Patyna et al. 2008). The potential risk of these findings for the human fetus is unknown. There are no studies in pregnant women. Based on nonclinical findings, pralsetinib should not be used during pregnancy.

In addition, pralsetinib was negative for mutagenic and genotoxic activity in a GLP-compliant Ames bacterial reverse mutation assay, in a GLP-compliant in vitro micronucleus assay, and in a GLP-compliant in vivo micronucleus assay in Sprague Dawley rats. Pralsetinib was not carcinogenic in a GLP-compliant 26-week study in male and female Tg.rasH2 mice at oral doses up to 30 mg/kg/day (approximately 4.5-times the exposure at the maximum recommended human dose based on AUC). Pralsetinib was classified as nonphototoxic based on a GLP-compliant in vitro phototoxicity evaluation in 3T3 fibroblasts.

Overall, the nonclinical pharmacology, PK, and safety profile indicates that pralsetinib can treat patients with RET-fusion positive solid tumors, has an appropriate PK profile for QD dosing, and has an acceptable nonclinical safety profile. Therefore, the nonclinical data support the use of pralsetinib for the treatment of patients with RET-fusion positive solid tumors.

5. EFFECTS IN HUMANS

5.1 INTRODUCTION

To date, 15 clinical studies have been initiated with pralsetinib (Appendix 4). Seven Phase I studies in healthy volunteers have been completed (BP42858, BP42859, BP42860, BP42861, BP42862, GP43162 and GP43163). Three studies in patients with RET-altered tumors are ongoing (JO43175, JO43701 and GP43164) and five studies have been completed (BO41932 [Cohort K], ML41591 [RET cohort only, other cohorts are ongoing], ML42439, BO42863 and BO42864). Studies BO42864 and BO41932 have reached LPLV on 27 Jan 2025 and 6 Feb 2025, respectively, and their CSRs are under preparation.

Studies with clinically relevant data discussed in this IB include: BO42863, BO42864, ML42439, BP42858, BP42859, BP42860, BP42861, BP42862, GP43162, GP43163, and BO41932.

In addition, patients have been treated with pralsetinib as part of a pre-approval access program (PAAP), including some who were treated in combination with osimertinib. Safety data for patients treated under the PAAP are summarized in Section 5.5.5. All clinical studies have been conducted in compliance with Good Clinical Practice (GCP) and international ethical and scientific quality standards for designing, conducting, recording, and reporting trials that involve human subjects.

5.2 CLINICAL PHARMACOKINETICS

5.2.1 Pharmacokinetics

The single dose (Cycle 1 Day 1; C1D1) and steady-state (Cycle 1 Day 15; C1D15) PK of pralsetinib have been evaluated in Study BO42863 (ARROW) in patients with RET fusion-positive NSCLC (N＝298; Group 1, 2, 8 and dose escalation) [CCOD: 4 March 2022], in patients with thyroid cancer (N=226; Group 3, 4, 5, 6, 7, 9 and dose escalation), in tumor agnostic patients (N=28; Group 5 and dose escalation group), patients with RET-altered (fusion or mutation) solid tumors treated with a prior selective RET inhibitor (N=22; Group 6) and RET-mutated patient populations other than MTC (N=14; Group 7) [CCOD: 20 May 2024]. The PK population (N) for this study consists of all patients who received at least one dose of pralsetinib (60-600 mg QD and 100/100, 200/100 mg BID) and from whom at least one post dose PK sample was collected.

5.2.1.1 Study BO42863: Arrow (RET fusion-positive NSCLC patients)

The mean pralsetinib plasma concentration over time profiles for each dose level following oral QD administration on C1D1 (single dose) and C1D15 (steady-state) for NSCLC patients from dose escalation and expansion are shown in Figure 2. The PK parameters from samples collected and analyzed as of the 4 March 2022 data cut in NSCLC are presented in Table 7 and Table 8. Following administration of single oral dose of pralsetinib 400 mg, pralsetinib was rapidly absorbed, with a median T_{max} of approximately 4 hours postdose. The mean elimination half-life ($t_{1/2}$) of 13.4 hours (400 mg dose) following a single dose supported QD dosing regimen for pralsetinib. Approximately 2-fold accumulation was observed at steady state following once daily dosing, consistent with the frequency of dosing and the half-life of pralsetinib. With 400 mg once daily dosing under fasting conditions, the steady state geometric mean [% coefficient of variation (CV%)] of maximum observed plasma concentration (C_{max}) and area under the concentration-time curve ($AUC_{0\text{-}24h}$) of pralsetinib in patients with thyroid cancer were 2840 (50.7%) ng/mL and 40100 (59.5%) h•ng/mL, respectively. Dose proportionality for pralsetinib could not be concluded over the full dose range (60 to 600 mg) or over a limited dose range (200 to 400 mg) due to the low number of patients receiving doses other than 400 mg QD. In healthy subjects, dose proportionality was seen across the range of 200 to 400 mg after single dose administration of pralsetinib.

Figure 2 Mean (±SD) Plasma Concentration-Time Profiles of pralsetinib on C1D1 (Single Dose) and C1D15 (Steady-State) Following Once Daily Dosing in RET fusion-positive NSCLC patients

a) Single Dose

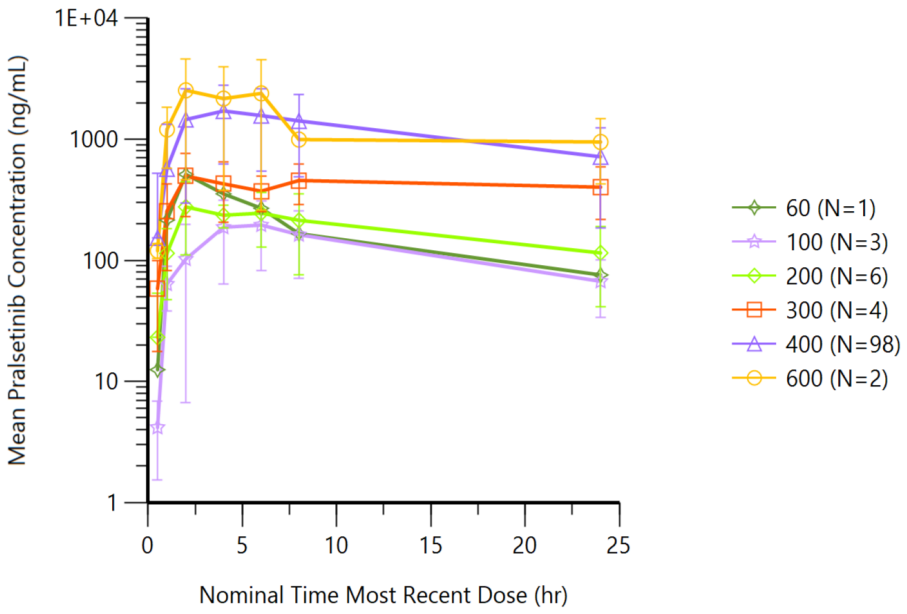

b) Steady State

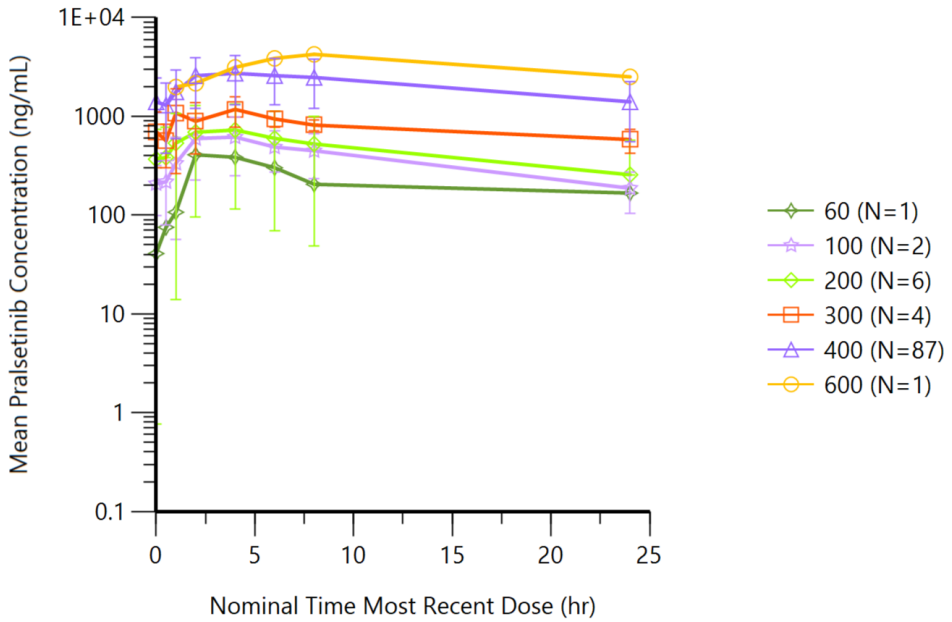

Table 7 Summary of Pralsetinib Plasma PK Parameters on C1D1 (Single Dose) and on C1D15 (Steady State) Following Multiple Once Daily Doses in RET fusion-positive NSCLC Patients

	Dose (mg)	C_{max} (ng/mL)	T_{max} (hr)	T_{last} (hr)	$AUC_{0\text{-}last}$ (hr*ng/mL)	$AUC_{0\text{-}24}$ (hr*ng/mL)	$AUC_{0\text{-}\infty}$ (hr*ng/mL)	AUC_{ext} (%)	C_{24} (ng/mL)	CL/F (L)	V/F (L/day)	$t_{1/2}$ (hr)	Accumulation Ratio C_{max} Ratio	Accumulation Ratio $AUC_{0\text{-}24}$ Ratio
Single Dose (C1D1)	60	513; 1	2.00 (2.00-2.00); 1	24.1 (24.1-24.1); 1	4170; 1	4160; 1	5240; 1	20.6; 1	75.70; 1	11.40; 1	163.0; 1	9.87; 1	-	-
	100	197 (72.8); 3	4.00 (2.00-6.00); 3	24.0 (22.7-24.1); 3	2510 (61.1); 3	2150 (79.7); 2	4160; 1	15.20; 1	62.13 (49.8); 3	24.0; 1	281; 1	16.0 (123); 2	-	-
	200	316 (49.5); 6	3.05 (2.00-8.00); 6	24.3 (23.8-25.7); 6	3970 (42.7); 6	3430 (27.3); 5	3190; 1	10.20; 1	95.70 (79); 6	62.8; 1	632; 1	15.0 (73.7); 4	-	-
	300	634 (17.2); 4	1.95 (1.70-7.90); 4	23.8 (20.4-24.0); 4	9290 (18.0); 4	9120 (20.1); 2	10700; 1	26.1; 1	351 (80); 3	28.0; 1	493; 1	12.2; 1	-	-
	400	1680 (69.4); 98	4.00 (1.90-23.7); 98	23.9 (2.40-24.8); 98	21800 (69.2); 97	20400 (64.2); 70	29900 (56.8); 30	20.2 (38.2); 30	540 (75.4); 92	13.4 (56.8); 30	187 (59.1); 30	13.4 (44.1); 57	-	-
	600	2070 (118); 2	2.00 (2.00-2.00); 2	23.7 (23.4-24.0); 2	33500 (95.3); 2	33800 (96.8); 2	83600; 1	29.1; 1	873 (64); 2	7.18; 1	132; 1	12.8; 1	-	-
Steady State (C1D15)	60	408; 1	2.00 (2.00-2.00); 1	24.4 (24.4-24.4); 1	5350; 1	5280; 1	ND	ND	167	-	-	-	0.80; 1	1.27; 1
	100	560 (70.1); 2	4.00 (4.00-4.00); 2	24.0 (23.6-24.3); 2	8110 (55.5); 2	8110 (56.9); 2	ND	ND	177 (48.8); 2	12.3 (56.8); 2	230 (62.9); 2	12.9 (4.92); 2	1.96 (49.4); 2	3.35; 1

	Dose (mg)	C_{max} (ng/mL)	T_{max} (hr)	T_{last} (hr)	$AUC_{0\text{-}last}$ (hr*ng/mL)	$AUC_{0\text{-}24}$ (hr*ng/mL)	$AUC_{0\text{-}\infty}$ (hr*ng/mL)	AUC_{ext} (%)	C_{24} (ng/mL)	CL/F (L)	V/F (L/day)	$t_{1/2}$ (hr)	Accumulation Ratio C_{max} Ratio	Accumulation Ratio $AUC_{0\text{-}24}$ Ratio
	200	605 (77.3); 6	3.95 (2.00-4.10); 6	24.0 (8.00-24.5); 6	6840 (109); 5	6820 (109); 5	ND	ND	154 (152); 5	27.9 (134); 4	572 (79.8); 4	14.2 (34.7); 4	1.92 (100.1); 6	2..39 (121.5); 4
	300	1170 (36.6); 4	3.05 (1.00-4.00); 4	16.2 (7.90-24.8); 4	17300 (18.1); 2	17100 (13.9); 3	ND	ND	571 (28); 2	18.8 (10.9); 2	285 (240); 2	10.5 (201); 2	1.85 (38.5); 4	1.85; 1
	400	2840 (50.7); 87	4.00 (1.00-8.10); 87	23.8 (7.80-26.5); 87	42800 (55.7); 81	40100 (59.5); 50	ND	ND	1150 (69); 82	9.91 (58.9); 47	255 (78.7); 47	17.9 (58.8); 47	1.69 (63); 87	1.96 (76.8); 87
	600	4240; 1	8.00 (8.00-8.00); 1	24.2 (24.2-24.2); 1	77900; 1	ND	ND	ND	2510; 1	ND	ND	ND	3.96; 1	-

AUC = area under the plasma concentration versus time curve; $AUC_{0\text{-}24}$ = AUC from 0 to 24 hours; $AUC_{0\text{-}\infty}$ = AUC from 0 to ∞; AUC_{last} = area under the plasma concentration versus time curve from time zero to time of last measurable concentration above the lower limit of quantitation; C_{24} = maximum concentration at 24hr postdose; CxDx = Cycle x, Day x; CL/F = apparent oral clearance; C_{max} = maximum plasma concentration; ND = Not Derived; $t_{1/2}$ = terminal elimination half-life; T_{max} = time to maximal concentration; V/F = apparent volume of distribution.

Descriptive statistics are presented as Geometric mean (geo CV%); n for all parameters except T_{max} where it is presented as median (min-max); n. Note: PK parameters were reported in 3 significant digits only where patients had sufficient PK samples collected.

Accumulation ratio was determined by dividing the C1D15 (steady-state) parameter value by the C1D1 (single dose) parameter value.

Table 8 Summary of Pralsetinib Plasma PK Parameters on C1D1 (Single Dose) and on C1D15 (Steady State) Following Multiple Twice Daily Doses in RET Fusion-Positive NSCLC Patients

	Dose (mg)	C_{max} (ng/mL)	T_{max} (hr)	T_{last} (hr)	$AUC_{0\text{-}last}$ (hr*ng/mL)	$AUC_{0\text{-}12}$ (hr*ng/mL)	Accumulation Ratio C_{max} Ratio	Accumulation Ratio $AUC_{0\text{-}12}$ Ratio
Single Dose (C1D1)	100/100	192 (73); 2	4.05 (2.1-6); 2	7 (6-8); 2	909 (75.3); 2	755; 1	-	-
Steady State (C1D15)	100/100	783 (44.8); 2	0.550 (0.500-0.600); 2	7.95 (7.90-8.00); 2	5500 (43.7); 2	7840 (38.5); 2	4.08	13.50

$AUC_{0\text{-}12}$ = AUC from 0 to 12 hours; AUC_{last} = area under the plasma concentration versus time curve from time zero to time of last measurable concentration above the lower limit of quantitation; CxDx = Cycle x, Day x; C_{max} = maximum plasma concentration; ND = Not Derived; T_{max} = time to maximal concentration.

Descriptive statistics are presented as Geometric mean (geo CV%); n for all parameters except T_{max} where it is presented as median (min-max); n.

Note: PK parameters were reported only where patients had sufficient PK samples collected.

Accumulation ratio was determined by dividing the C1D15 (steady-state) parameter value by the C1D1 (single dose) parameter value.

5.2.1.2 Study BO42863: Arrow (All Thyroid Patients)

A total of 226 thyroid cancer patients (195 MTC patients [33 from Dose Escalation, 71 from Group 3, 50 from Group 4, 7 from Group 6 and 34 from Group 9]) and 31 other thyroid cancer patients (26 papillary thyroid cancer [PTC; Group 7, 5 and dose escalation], 3 with ANPTC [Group 5], 1 poorly differentiated thyroid cancer [Group 5], and 1 poorly differentiated carcinoma [Group 5]), irrespective of their RET status, met the analysis inclusion criteria and were included in the PK population dataset. Out of 195 MTC patients, 170 patients had RET mutations while 25 did not have any RET alterations. Out of 31 PTC patients, 30 were RET fusion-positive thyroid patients and 1 patient did not have any RET alterations. No statistically significant PK difference was observed between the RET-altered patients and those with no RET alterations, hence the PK analysis is based on the data from all the patients with thyroid cancer (MTC, PTC, ANPTC, poorly differentiated thyroid cancer, or poorly differentiated carcinoma) enrolled in this study, irrespective of their RET status.

Mean (±StdDev) plasma concentration-time profiles for all thyroid patients who took once daily dose of pralsetinib on C1D1 (Single Dose) and C1D15 (Steady-State) are shown in Figure 3. Following a single dose, quantifiable concentrations of pralsetinib were present across all dose levels at 24 hours post-dose. Additionally, an apparent monophasic elimination profile was evident across the dose levels.

Figure 3 Mean (±StdDev) Plasma Concentration-Time Profiles of Pralsetinib on C1D1 (Single Dose) and C1D15 (Steady-State) Following Once Daily Dosing for All Thyroid Patients

a) Single Dose

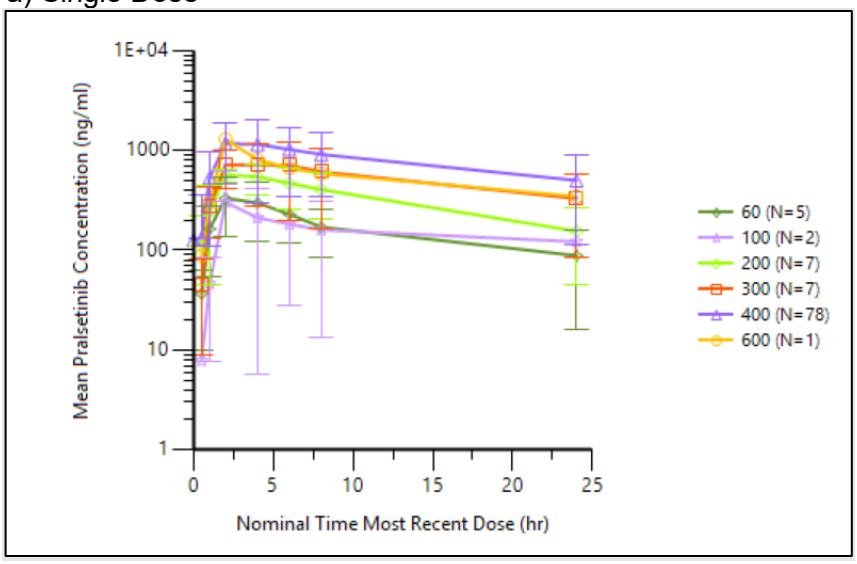

b) Steady-State

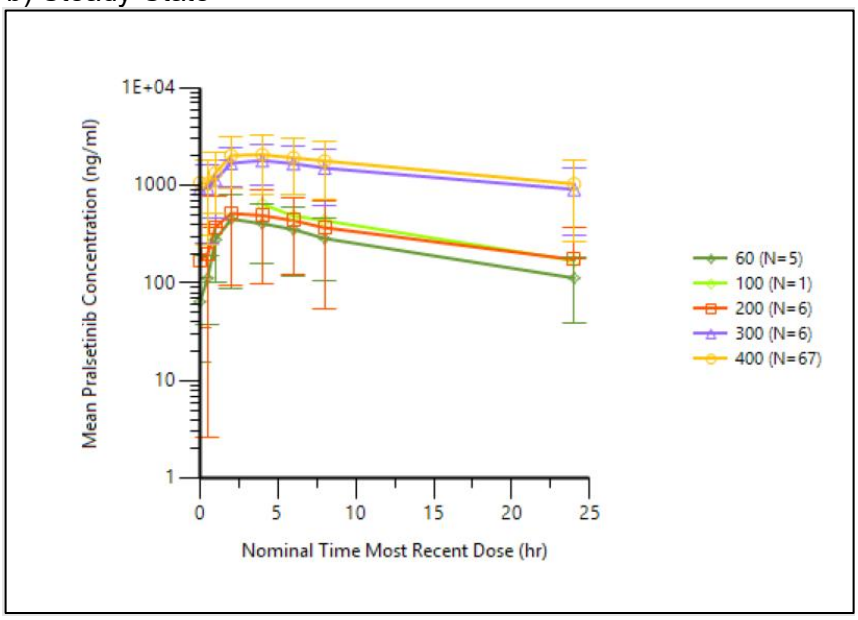

The summary of PK parameters of pralsetinib for all thyroid patients at 60–600 mg QD and BID (100/100, 200/100 mg) dosing on C1D1 and C1D15 are displayed in Table 9 and Table 10.

The description of the PK results is limited to the QD dose groups, as the data are limited for BID dose groups.

Following administration of single oral doses of pralsetinib ranging from 60–600 mg, pralsetinib was rapidly absorbed, with a median T_{max} around 2 hours post-dose, which was followed by an apparent monophasic elimination profile across the dose levels. The mean $t_{1/2}$ of 16.4 hours (400 mg dose) following a single dose supported QD dosing regimen for pralsetinib. Approximately 2-fold accumulation was observed at steady-state following once daily dosing, consistent with the frequency of dosing and the half-life of pralsetinib. With 400 mg once daily dosing under fasting conditions, the steady state geometric mean [% coefficient of variation (CV%)] of maximum observed plasma concentration (C_{max}) and area under the concentration-time curve ($AUC_{0\text{-}24h}$) of pralsetinib in patients with thyroid cancer were 2120 (54.1%) ng/mL and 28000 (68%) h•ng/mL, respectively.

Table 9 Summary of Pralsetinib Plasma PK Parameters on C1D1 (Single Dose) and on C1D15 (Steady-State) Following Multiple Once Daily Doses for All Thyroid Patients

	Dose (mg)	C_{max} (ng/mL)	T_{max} (hr)	T_{last} (hr)	AUC_{0-last} (hr*ng/ mL)	AUC_{0-24} (hr*ng/ mL)	$AUC_{0-\infty}$ (hr*ng/ mL)	AUC_{ext} (%)	C_{24} (ng/mL)	CL/F (L)	V/F (L/day)	$t_{1/2}$ (hr)	Accumulation Ratio C_{max} Ratio	Accumulation Ratio AUC_{0-24} Ratio
Single Dose (C1D1)	60	308 (53.6); 5	2.10 (2.00-4.00); 5	24.0 (23.1-24.4); 5	3400 (57.9); 5	3410 (58.2); 5	3290 (47.6); 3	17.9 (16.2); 3	68.8 (95.2); 5	18.2 (47.6); 3	248 (42.1); 3	11.1 (34.3); 4	–	–
	100	200 (240); 2	2.00; 2	16.0 (7.90-24.0); 2	5270; 1	2490 (144); 2	ND	ND	122; 1	ND	ND	14.4; 1	–	–
	200	633 (20.3); 7	2.00 (1.00-6.00); 7	23.6 (21.9-24.8); 7	6930 (38.8); 7	6400 (32.5); 6	6850 (25.8); 4	15.2 (35.6); 4	128 (73.8); 7	29.2 (25.7); 4	365 (21.0); 4	11.3 (51.4); 6	–	–
	300	721 (69.6); 7	2.00 (1.90-6.00); 7	23.9 (7.90-24.0); 7	10000 (74.5); 6	8370 (55.2); 6	15600 (8.18); 2	22.4 (21.0); 2	271 (77.5); 6	19.3 (8.08); 2	291 (4.86); 2	17.3 (66.6); 4	–	–
	400	1190 (61.3); 78	2.10 (1.00-8.00); 78	23.8 (2.00-24.9); 78	15900 (64.4); 70	14100 (55.4); 58	16100 (43.7); 23	17.4 (52.5); 23	352 (138); 71	24.8 (43.7); 23	334 (43.0); 23	14.8 (65.5); 50	–	–
	600	1300; 1	2.00; 1	23.8; 1	12900; 1	12900; 1	ND	ND	347; 1	ND	ND	19.7; 1	–	–
Steady-State (C1D15)	60	422 (64.8); 5	2.00 (2.00-4.10); 5	24.0 (23.9-24.2); 5	5010 (58.6); 5	5000 (58.6); 5	ND	ND	83.6 (137); 5	12.3 (69.0); 4	185 (162); 4	10.5 (121); 4	1.37 (17.5); 5	1.47 (13.4); 5
	100	643; 1	3.90;1	27.8; 1	9810; 1	9110; 1	ND	ND	170; 1	11.0; 1	228; 1	14.4; 1	8.53; 1	7.69; 1
	200	455 (71.3); 6	2.05 (1.10-4.10); 6	24.1 (8.00-26.6); 6	5690 (108); 5	5610 (103); 5	ND	ND	116 (127); 5	35.7 (103); 5	697 (66.3); 5	13.5 (29.3); 5	0.71 (77.7); 6	0.73 (128); 5

Dose (mg)	C_{max} (ng/mL)	T_{max} (hr)	T_{last} (hr)	AUC_{0-last} (hr*ng/ mL)	AUC_{0-24} (hr*ng/ mL)	$AUC_{0-\infty}$ (hr*ng/ mL)	AUC_{ext} (%)	C_{24} (ng/mL)	CL/F (L)	V/F (L/day)	$t_{1/2}$ (hr)	Accumulation Ratio C_{max} Ratio	Accumulation Ratio AUC_{0-24} Ratio
300	1780 (41.9); 6	3.05 (2.00-6.00); 6	23.9 (22.2-24.7); 6	27500 (53.6); 6	23600 (35.1); 5	ND	ND	786 (62.9); 6	12.8 (40.7); 4	324 (80.5); 4	17.5 (44.3); 4	1.87 (48.0); 5	2.25 (27); 4
400	2120 (54.1); 67	4.00 (0-8.00); 67	24.0 (2.00-25.7); 67	30800 (63.8); 59	28000 (68.0); 43	ND	ND	849 (105); 66	15.4 (63.9); 38	356 (47.5); 38	16.0 (54.3); 38	1.85 (59.3); 67	2.18 (58.7); 33

AUC = area under the plasma concentration versus time curve; AUC_{0-24} = AUC from 0 to 24 hours; $AUC_{0-\infty}$ = AUC from 0 to ∞; AUC_{last} = area under the plasma concentration versus time curve from time zero to time of last measurable concentration above the lower limit of quantitation; C_{24} = maximum concentration at 24hr postdose; CxDx = Cycle x, Day x; CL/F = apparent oral clearance; C_{max} = maximum plasma concentration; ND = Not Derived; $t_{1/2}$ = terminal elimination half-life; T_{max} = time to maximal concentration; V/F = apparent volume of distribution.

Descriptive statistics are presented as Geometric mean (geo CV%); n for all parameters except T_{max} where it is presented as median (min-max); n. Note: PK parameters were reported in 3 significant digits only where patients had sufficient PK samples collected.

One patient with MTC had a dose reduction from 400 mg to 300 mg on day 6, therefore this patient has been included in the steady-state 300 mg dose group and not in the 400 mg dose group.

Accumulation ratio was determined by dividing the C1D15 (steady-state) parameter value by the C1D1 (single dose) parameter value.

Table 10 Summary of Pralsetinib Plasma PK Parameters on C1D1 (Single Dose) and on C1D15 (Steady-State) Following Multiple Twice Daily Doses for All Thyroid Patients

	Dose (mg)	C_{max} (ng/mL)	T_{max} (hr)	T_{last} (hr)	$AUC_{0\text{-}last}$ (hr*ng/mL)	$AUC_{0\text{-}12}$ (hr*ng/mL)	Accumulation Ratio C_{max} Ratio	Accumulation Ratio $AUC_{0\text{-}12}$ Ratio
Single Dose (C1D1)	100/100	311 (141); 3	4.00 (2.00-8.00); 3	7.90 (7.80-8.00); 3	1540 (100); 3	2690; 1	–	–
	200/100	455 (27.5); 2	2.05 (2.00-2.10); 2	8.00; 2	2530 (22.2); 2	3430 (19.7); 2	–	–
Steady-State (C1D15)	100/100	1230 (38.9); 2	5 (3.9-6.1); 2	7.9 (7.8-8); 2	8150 (43); 2	ND	4.49 (147); 2	–
	200/100	787 (141); 2	2; 2	8; 2	4500 (126); 2	ND	1.73 (217); 2	–

$AUC_{0\text{-}12}$ = AUC from 0 to 12 hours; AUC_{last} = area under the plasma concentration versus time curve from time zero to time of last measurable concentration above the lower limit of quantitation; CxDx = Cycle x, Day x; C_{max} = maximum plasma concentration; ND = Not Derived; T_{max} = time to maximal concentration.

Descriptive statistics are presented as Geometric mean (geo CV%); n for all parameters except T_{max} where it is presented as median (min-max); n.

Note: PK parameters were reported only where patients had sufficient PK samples collected.

Accumulation ratio was determined by dividing the C1D15 (steady-state) parameter value by the C1D1 (single dose) parameter value.

5.2.1.3 Study BO42863: ARROW (All Tumor Agnostic Patients)

The summary of PK parameters of pralsetinib for the Tumor-Agnostic patient population [Group 5 and Dose Escalation group] at 400 mg QD (N=5) and BID (200/100 mg; N=1) dosing on C1D1 and C1D15 are displayed in Table 11.

Following administration of single oral doses of pralsetinib at 400 mg, pralsetinib was rapidly absorbed, with a median time to achieve maximum plasma concentration (T_{max}) around 4 hours post-dose, which was followed by an apparent monophasic elimination profile across the dose levels. The mean elimination half-life ($t_{1/2}$) of 18.4 hours (400 mg dose) following a single dose supported QD dosing regimen for pralsetinib. Approximately 2-fold accumulation was observed at steady state following once-daily dosing, consistent with the frequency of dosing and the half-life of pralsetinib.

Table 11 Summary of Pralsetinib Plasma PK Parameters on C1D1 (Single Dose) and on C1D15 (Steady State) Following Multiple Once and Twice Daily Doses for in Tumor-Agnostic Patients

	Dose (mg)	Cmax (ng/mL)	T_{max} (hr)	T_{last} (hr)	AUC_{0-last} (hr*ng/mL)	AUC_{0-24} (hr*ng/mL)	$AUC_{0-\infty}$ (hr*ng/mL)	AUC_{ext} (%)	C_{24} (ng/mL)	CL/F (L)	V/F (L/day)	$t_{1/2}$ (hr)	Accumulation Ratio	
													C_{max} Ratio	AUC_{0-24} Ratio
Single Dose (C1D1)	400	1380 (65.4); 5	3.90 (2.0-6.0); 5	12.2 (64.1); 5	11100 (90.3); 5	17400 (152); 2	31400 (347); 2	37.2 (82.3); 2	519 (197); 5	12.7 (347); 2	338 (91.1); 2	18.4 (98.8); 2		
	200/100	1400; 1	11.9; 1	11.9; 1	12800; 1	ND	ND	ND	ND	ND	ND	ND		
Steady State (C1D15)	400	2200 (36.7); 5	5.00 (2.0-8.0); 5	15.3 (66.5); 5	19100 (126); 5	33900 (27.4); 3	ND	ND	797 (42.8); 5	7.49 (64.4); 2	178 (16.5); 2	16.5 (44.6); 2	1.59 (33.6); 5	1.89 (82.2); 2
	200/100	1970; 1	2.00; 1	11.5; 1	18100; 1	33100; 1	ND	ND	934; 1	4.44; 1	145; 1	22.6; 1	1.41; 1	

Descriptive statistics are presented as Geometric mean (geo CV%); n for all parameters except T_{max} where it is presented as median (min-max); n.
Note: PK parameters were reported only where patients had sufficient PK samples collected. C24 was derived using nominal time.

PK parameters were reported in 3 significant digits

ND= Not Derived.

Accumulation ratio was determined by dividing the C1D15 (steady state) parameter value by the C1D1 (single dose) parameter value.

5.2.1.4 Study BO42863: Arrow (Other Indications)

5.2.1.4.1 Group 6 Pharmacokinetic Parameters

The summary of PK parameters of pralsetinib for the measurable patient populations with any solid tumor with a RET alteration (fusion or mutation) treated with a prior selective RET inhibitor (Group 6) treated at 400 mg QD and BID (100/100 mg) dosing on C1D1 and C1D15 are displayed in Table 12.

Based on the limited data, following administration of single oral doses of pralsetinib at 400 mg, pralsetinib was rapidly absorbed, with a median time to achieve maximum plasma concentration (T_{max}) around 4 hours post-dose, which was followed by an apparent monophasic elimination profile across the dose levels. After multiple repeated QD dosing, the T_{max} was similar with a median around 4 hours. Slight accumulation (~20%) was observed at steady state following once-daily dosing.

Table 12 Summary of Pralsetinib Plasma PK Parameters on C1D1 (Single Dose) and on C1D15 (Steady State) Following Multiple Once and Twice Daily Doses for Group 6

	Dose (mg)	C_{max} (ng/mL)	T_{max} (hr)	T_{last} (hr)	$AUC_{0\text{-}last}$ (hr*ng/mL)	$AUC_{0\text{-}24}$ (hr*ng/mL)	$AUC_{0\text{-}\infty}$ (hr*ng/mL)	AUC_{ext} (%)	C_{24} (ng/mL)	CL/F (L)	V/F (L/day)	$t_{1/2}$ (hr)	Accumulation Ratio	
													C_{max} Ratio	$AUC_{0\text{-}24}$ Ratio
Single Dose (C1D1)	400	2450 (164); 3	4.0 (4.0-6.0); 3	16.4 (68.9); 3	27100 (179); 3	103000; 1	200000; 1	48.6; 1	1020 (225); 3	2.00; 1	59.9; 1	20.8; 1		
	100/ 100*	490; 1	0.30; 1	7.80; 1	2170; 1	ND	4690, 1	53.8, 1	ND	42.7, 1	532,	8.65; 1		
Steady State (C1D15)	400	3440 (93.9); 3	4.00 (2.00-6.00); 3	16.6 (71.4); 3	40900 (257); 3	91100 (46.8); 2	ND	ND	1400 (207); 2	2.92; 1	109; 1	25.8; 1	1.40 (37.7); 3	1.21; 1
	100/ 100*	2040; 1	4.00; 1	7.80; 1	10300; 1	ND	ND	ND	856; 1	ND	ND	ND		

Descriptive statistics are presented as Geometric mean (geo CV%); n for all parameters except T_{max} where it is presented as median (min-max); n.
Note: PK parameters were reported only where patients had sufficient PK samples collected. C24 was derived using nominal time.

PK parameters were reported in 3 significant digits

ND= Not Derived.

*N=1

Accumulation ratio was determined by dividing the C1D15 (steady state) parameter value by the C1D1 (single dose) parameter value.

5.2.1.4.2 Group 7 Pharmacokinetic Parameters

The summary of PK parameters of pralsetinib for the measurable RET-mutated patient populations other than MTC (Group 7) treated at 400 mg QD and 600 mg QD dosing on C1D1 and C1D15 are displayed in Table 13.

Following administration of single oral doses of pralsetinib at 400 mg, pralsetinib was rapidly absorbed, with a median time to achieve maximum plasma concentration (T_{max}) around 2 hours post-dose, which was followed by an apparent monophasic elimination profile across the dose levels. After multiple repeated QD dosing, the T_{max} was similar with a median around 3 hours. The mean elimination half-life ($t_{1/2}$) of 11 hours (400 mg dose) following a single dose supported QD dosing regimen for pralsetinib. Approximately 2-fold accumulation was observed at steady state following once-daily dosing.

Table 13 Summary of Pralsetinib Plasma PK Parameters on C1D1 (Single Dose) and on C1D15 (Steady State) Following Multiple Once for Group 7

	Dose (mg)	C_{max} (ng/mL)	T_{max} (hr)	T_{last} (hr)	$AUC_{0\text{-}last}$ (hr*ng/mL)	$AUC_{0\text{-}24}$ (hr*ng/mL)	$AUC_{0\text{-}\infty}$ (hr*ng/mL)	AUC_{ext} (%)	C_{24} (ng/mL)	CL/F (L)	V/F (L/day)	$t_{1/2}$ (hr)	Accumulation Ratio	
													C_{max} Ratio	$AUC_{0\text{-}24}$ Ratio
Single Dose (C1D1)	400	1770 (87.2); 4	2.05 (2-8); 4	10.6 (59.1); 4	10300 (98.5); 4	18400 (69.8); 3	24800 (43.3); 3	44.1 (64.3); 3	415 (140); 3	16.1 (43.3); 3	255 (115); 3	11.0 (55.8); 3		
	600*	1990; 1	2.00; 1	23.9; 1	24800; 1	24900; 1	67900; 1	63.4; 1	829; 1	8.83; 1	459; 1	36.0; 1		
Steady State (C1D15)	400	2430 (55.3); 4	3.05 (2-6); 4	24.0 (0.4); 4	32000 (90.8); 4	32000 (90.8); 4	ND	ND	1050 (94.0); 4	1.39 (1220); 2	126 (15); 2	63.0 (882); 2	1.37 (33.8); 4	1.62 (53.2); 3
	600*	4420; 1	4.00; 1	24.0; 1	60700; 1	60700; 1	ND	ND	1500; 1	6.76; 1	127; 1	13.0; 1	2.22; 1	2.43; 1

Descriptive statistics are presented as Geometric mean (geo CV%); n for all parameters except T_{max} where it is presented as median (min-max); n.
Note: PK parameters were reported only where patients had sufficient PK samples collected. C24 was derived using nominal time.

PK parameters were reported in 3 significant digits

ND= Not Derived.

*N = 1

Accumulation ratio was determined by dividing the C1D15 (steady state) parameter value by the C1D1 (single dose) parameter value.

5.2.2 Absorption, Bioavailability, Distribution, Metabolism, and Elimination

5.2.2.1 BP42860: Mass Balance Study

Study BP42860 was an open-label study to assess the absorption, metabolism, excretion, and mass balance of [^{14}C]-pralsetinib following a single oral dose in 6 healthy adult male subjects. Following an overnight fast of at least 10 hours, subjects received a single oral dose of ~310 mg pralsetinib administered as 3×100 mg capsules plus 1 capsule containing approximately 10 mg of [^{14}C]–pralsetinib (approximately 100 μCi). Taking into account the measured specific activity, the actual dose administered was approximately 309 mg (~100 μCi) [^{14}C]-pralsetinib. The actual dose was used for all individual PK calculations.

Plasma, urine, and feces samples were collected over at least 216 hours postdose (Day 10) to measure total radioactivity (TRA) and pralsetinib concentrations (plasma samples only). Whole blood samples were collected over 96 hours (Day 5) to measure TRA.

Mean plasma pralsetinib and TRA concentration versus time profiles were similar. Peak mean concentrations were reached by 4 hours postdose at 952 ng/mL and 961 ng eq/mL, respectively, and post peak mean concentrations showed a linear decline over 4 to 5 days.

The PK parameters for pralsetinib and TRA results indicated that most of the radioactivity in systemic circulation represented the parent drug, with a low level of metabolism ($<10\%$). The median T_{max} was approximately 4 hours for pralsetinib and TRA. The geometric mean $AUC_{0\text{-}t}$ values were similar for pralsetinib and TRA in plasma, with individual ratios ranging from 0.60 to 2.01. The mean $t_{1/2}$ was approximately 13 hours for pralsetinib and 20 hours for TRA.

Drug-derived radioactivity was confined mostly in plasma, as evidenced by a blood-to-plasma ratio of 0.6 to 0.7, indicating that pralsetinib and its metabolites do not preferentially distribute to red blood cells.

The mean cumulative excretion of TRA in urine and feces over time as a percentage of the dose is shown in Figure 4. The mean total recovery of the administered radioactivity was 78.6%, of which 6.06% was in urine, and 72.5% was in feces, indicating that excretion in feces was the major elimination pathway for [^{14}C]-pralsetinib in humans. The recovery of TRA across subjects ranged from 76.2% to 80.5%, and most of the radioactivity (74% of the dose) had been recovered by 120 hours postdose.

Figure 4 Cumulative Total Radioactivity Excretion as a Percentage of [^{14}C]-pralsetinib Dose in Urine and Feces Following Administration of a Single Oral Dose of ~310 mg (~100 μCi) [^{14}C]-pralsetinib (Study BP42860)

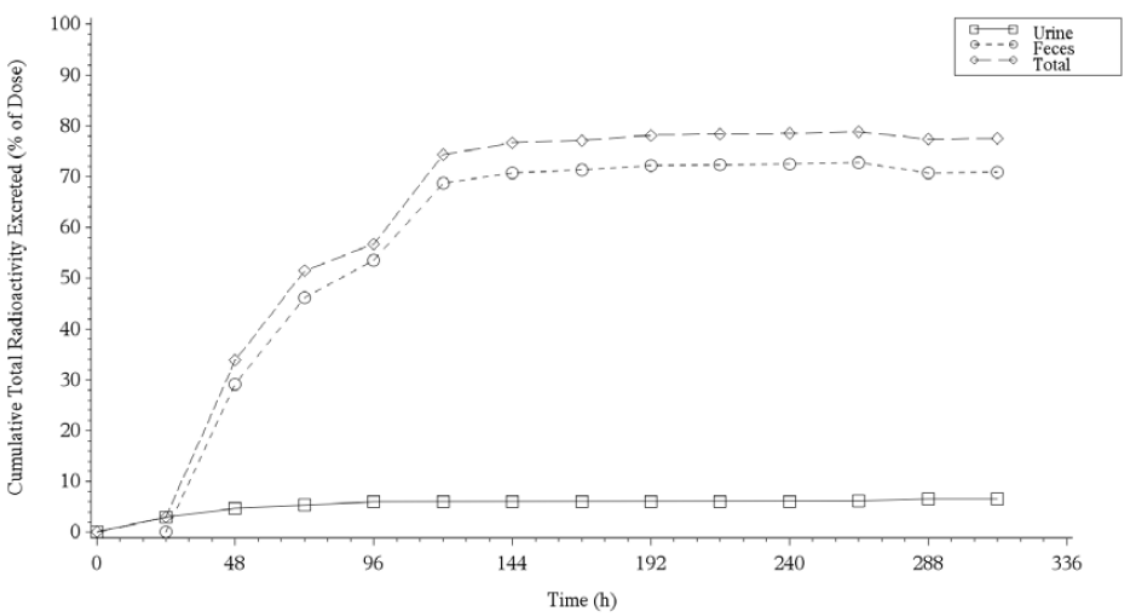

Note: Mean data are shown. One subject was excluded from urine and total data after 72 hours because an estimated 200 mL of urine was lost in a spill.

Pralsetinib underwent limited metabolism following the single oral dose of [^{14}C]-pralsetinib. Unchanged pralsetinib was the predominant radioactive component in plasma, urine, and feces, while its metabolites from oxidation (M531, M453, M549b) and glucuronidation (M709) were detected in small to trace amounts (~ 5%) (Table 14).

In plasma, pralsetinib accounted for 94.9% of the plasma radioactivity. M709 (direct glucuronide) was a minor metabolite and accounted for a mean of 4.18% of the plasma radioactivity; the oxidative metabolites (M453 and M549b) were detected in small to trace amounts and together accounted for <1% of the plasma radioactivity.

In urine, pralsetinib accounted for 91.5% of the urine radioactivity (4.83% of the administered dose). The oxidative metabolite M549b and the glucuronide conjugate M709 were detected in small amounts (each on average <0.3% of the administered dose). Trace amounts of the oxidative metabolite M453 were also detected in urine by MS only.

In feces, pralsetinib accounted for 96.4% of the plasma radioactivity (66.1% of the administered dose). The oxidative metabolites, M531, M549b, and M563b, were detected in small amounts (each on average ≤ 2% of the administered dose).

Table 14 Percentage of Metabolites in Different Matrices Following Single-Dose Oral Administration of ~310 mg (~100 µCi) [14C]-Pralsetinib (Study BP42860)

Metabolite Identifier	Proposed Biotransformation	Mean % Radioactivity in Pooled Matrix (N = 6)		
		Plasma (0–24 h)	Urine (0–72 h) [a]	Feces (0–144 h) [b]
Pralsetinib	Parent drug	94.9	91.5	96.4
M531	Oxidative defluorination	—	—	0.55
M453	Oxidation	0.97	—	—
M549b	Oxidation		3.53	1.87
M563b	Oxidation, dehydrogenation	—	—	1.20
M709	Glucuronidation	4.18	5.03	—

[a] Pooled sample that represented >90% of excreted radioactivity in urine (or about 5% of the administered dose).

[b] Pooled sample that represented >90% of excreted radioactivity in feces (or about 66% of the administered dose).

The proposed biotransformation pathways of pralsetinib in humans are shown in Figure 5. Overall, the metabolism of pralsetinib in humans was qualitatively similar to nonclinical toxicology species (rat and monkey), with no unique human metabolites observed.

Figure 5 Proposed Biotransformation Pathways of Pralsetinib in Humans (Study BP42860)

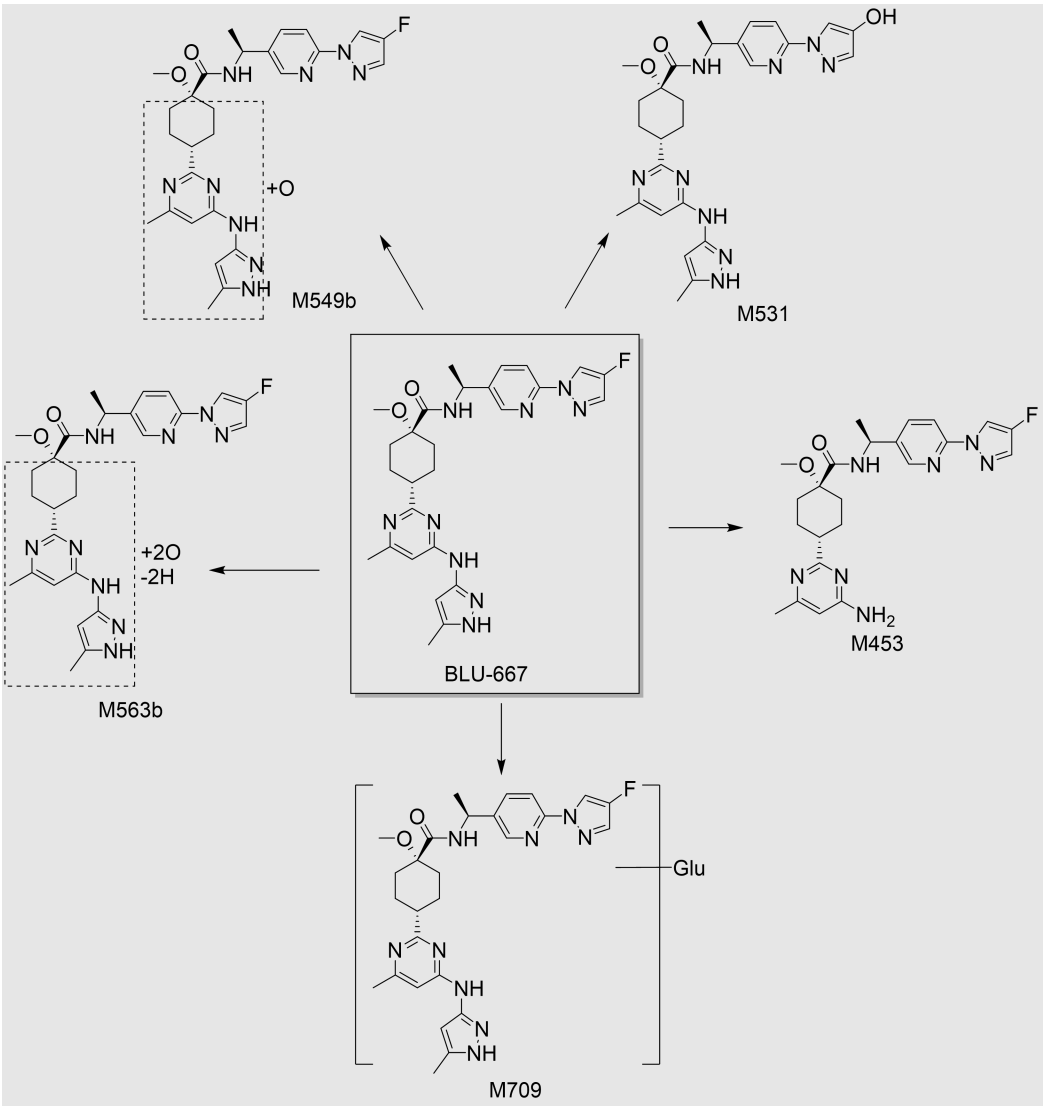

BLU-667 = pralsetinib.

In conclusion, following a single ~310 mg (~100 μCi) oral dose of [^{14}C]-pralsetinib, excretion in feces (72.5%) was the predominant route of elimination of drug-related material and excretion in urine (6.06%) was the minor route of elimination. In feces and urine, unchanged pralsetinib accounted for majority of the drug-related radioactivity (70.9%) of administered dose. Metabolites from oxidation (M531, M453, M549b) and glucuronidation (M709) were detected in small to trace amounts (~5%). Overall, the metabolism of pralsetinib in humans was qualitatively similar to nonclinical toxicology species (rat and monkey), with no unique human metabolites observed.

5.2.2.2 BP42859: Bioequivalence Study

Study BP42859 was an open-label, randomized, 2-period crossover study in 90 healthy adults (27 females and 63 males). The objective was to assess the relative bioavailability and bioequivalence of pralsetinib 100 mg tablets and capsules given as a single 400 mg dose. Treatments were administered under fasted conditions, with a 14-day washout period between treatments. Blood samples for analysis of pralsetinib in plasma were taken at prespecified time points for up to 192 hours after administration.

The oral bioavailability of pralsetinib was increased when given as 4×100 mg tablets, compared with 4×100 mg capsules. The systemic exposure, C_{max} and $AUC_{0-\infty}$, increased by 70.5% and 75.2%, respectively. In addition, administration as the tablet formulation advanced the absorption of pralsetinib, with a statistically significant median T_{max} difference of approximately 1 hour compared with the capsule formulation. Based on the lack of bioequivalence between the tablet and capsule formulations, the tablet formulation was not developed further.

5.2.3 Pharmacokinetics of Metabolites

In the human mass balance study (BP42860), unchanged pralsetinib was the predominant radioactive component in plasma, urine, and feces, while its metabolites from oxidation and glucuronidation were detected in small to trace amounts (~5%).

5.2.4 Pharmacokinetic Interactions

5.2.4.1 BP42858: Food Effect Study

Study BP42858 was an open-label, 2-period crossover study in 20 healthy adults (7 females and 13 males). The objective was to compare the PK of pralsetinib given as a single 200 mg dose when administered with or without a standardized high-fat meal. The following treatments were administered with a 14-day washout period between treatments:

- Test: 200 mg pralsetinib administered as 2×100 mg capsules after a standardized high-fat meal.
- Reference: 200 mg pralsetinib administered as 2×100 mg capsules after an overnight fast of at least 10 hours.

Blood samples for analysis of pralsetinib in plasma were taken at prespecified time points for up to 192 hours after administration. The mean plasma concentrations of pralsetinib were higher under fed conditions than under fasted conditions (Figure 6).

Figure 6 Mean (±Standard Deviation) Plasma Concentration-time Profiles After Administration of 200 mg Pralsetinib Under Fasted and Fed Conditions (Study BP42858)

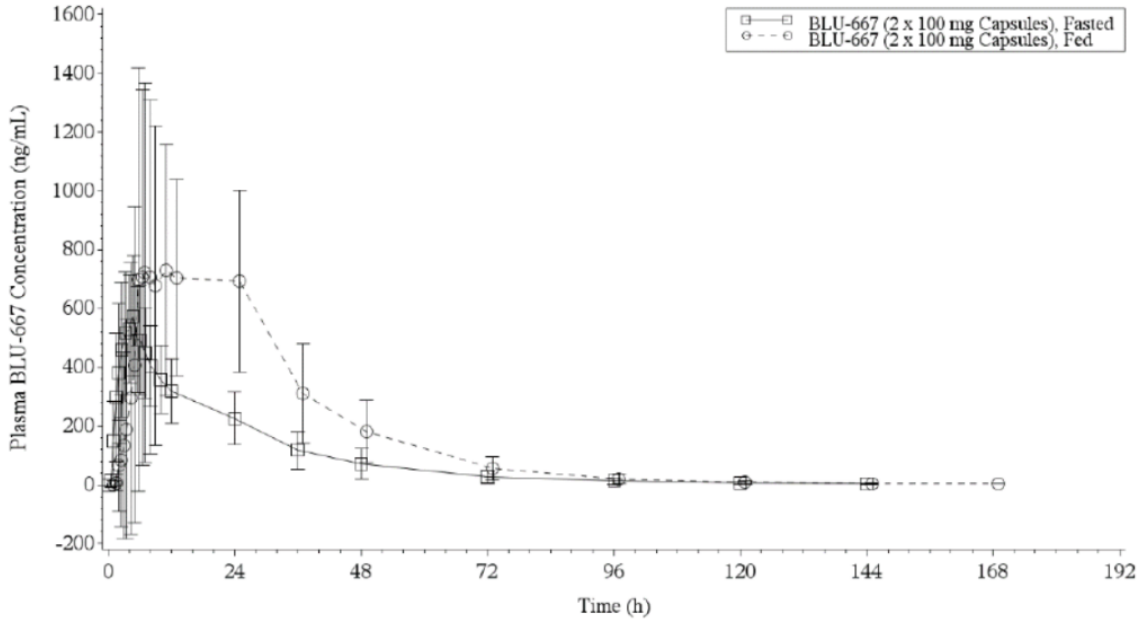

BLU-667 = pralsetinib.
Note: The data for the fed condition are offset to the right to enhance clarity.

Under fed conditions, a delay in T_{max} was observed (median T_{max} = 8.50 hours), compared with fasted conditions (median T_{max} = 4.00 hours) ($p < 0.0001$). Based on geometric mean ratio (GMR) values, a standardized high-fat meal increased C_{max} by 104%, AUC_{0-t} by 124%, and $AUC_{0-\infty}$ by 122%. The 90% CIs of the GMR values for each comparison were not contained within the equivalence limits of 80.00% to 125.00%. The mean $t_{1/2}$ values were similar between the 2 conditions (Table 15)

The interindividual variability (%CV) for C_{max} and AUC parameters were lower under fed (29.1% to 41.9%) than fasted (40.4% to 48.8%) conditions. The intraindividual variability was 42.1% for C_{max}, 23.3% for AUC_{0-t}, and 23.1% for $AUC_{0-\infty}$.

Table 15 Summary and Statistical Comparison of Pralsetinib Pharmacokinetic Parameters After Administration of 200 mg Pralsetinib Under Fasted and Fed Conditions (Study BP42858)

	GeoMean (GeoMean %CV)[a]			
Parameter	2 × 100 mg Pralsetinib, Fed (Test)	2 × 100 mg Pralsetinib, Fasted (Reference)	Geometric Mean Ratio (%)	90% Confidence Interval (Lower–Upper)
N	20	20	—	—
C_{max} (ng/mL)	1181 (33.6)	578.6 (48.8)	204.19	164.59–253.32
T_{max} (h)[b]	8.501 (4.01–24.09)	4.002 (2.00–8.00)	—	—
AUC_{0-24} (h•ng/mL)	13530 (41.9)	7502 (40.4)	—	—
AUC_{0-t} (h•ng/mL)	26590 (29.2)	11880 (46.6)	223.81	197.26–253.94
$AUC_{0-\infty}$ (h•ng/mL)	26680 (29.1)	11990 (46.0)	222.47	196.37–252.02
$\%AUC_{extrap}$ (%)	0.2887 (63.8)	0.7219 (82.4)	—	—
$t_{1/2}$ (h)	13.179 (2.0004)	13.153 (3.2638)	—	—
CL/F (L/h)	7.495 (29.1)	16.67 (46.0)	—	—
V_z/F (L)	140.9 (28.7)	307.7 (39.5)	—	—

AUC_{0-24} = area under the plasma concentration-time curve from time 0 to 24 hours postdose; AUC_{0-t} = area under the plasma concentration-time curve from time 0 to time of last measurable concentration above the lower limit of quantitation; $AUC_{0-\infty}$ = area under the plasma concentration-time curve from time 0 to infinity; $\%AUC_{extrap}$ = percent of $AUC_{0-\infty}$ extrapolated; CL/F = apparent oral clearance; C_{max} = maximum plasma concentration; %CV = percent coefficient of variation; GeoMean = geometric mean; N = number of subjects in pharmacokinetic population; $t_{1/2}$ = apparent terminal elimination half-life; T_{max} = time of maximal plasma concentration; V_z/F = apparent volume of distribution.

[a]Median (minimum-maximum) for T_{max} and arithmetic mean (standard deviation) for $t_{1/2}$.

[b]Median treatment difference: 6.18 h; $p < 0.0001$; Wilcoxon signed-rank test.

In conclusion, the oral bioavailability of pralsetinib was increased when given under fed (standardized high-fat meal) conditions. Compared with fasted conditions, systemic exposure, C_{max} and $AUC_{0-\infty}$, increased by 104% and 122%, respectively. In addition, food delayed the absorption of pralsetinib, with a statistically significant median T_{max} difference of approximately 6 hours between the administration of pralsetinib under fed and fasted conditions.

5.2.4.2 BP42861: Effects of Itraconazole and Rifampin on Pharmacokinetics of Pralsetinib

Study BP42861 was an open-label, 2-part, 2-period, fixed-sequence study in 50 healthy subjects to assess the effect of concomitant administration of itraconazole or rifampin on the PK of a single dose of pralsetinib. Pralsetinib Phase I oxidative metabolism is predominantly mediated by CYP3A4. Therefore, CYP3A inhibitors and/or inducers may

affect the plasma exposure of pralsetinib. Itraconazole is a strong CYP3A and P-gp inhibitor, and rifampin is a strong CYP3A and P-gp inducer.

In each part (Part 1 and Part 2) of the study, 25 subjects (males and females) were enrolled for a total of 50 subjects. The effects of itraconazole (Part 1) and rifampin (Part 2) on pralsetinib were evaluated. The following treatments were administered orally to each subject under fasted conditions, except when itraconazole or rifampin were administered alone, with a washout period of at least 14 days between pralsetinib treatments:

- Period 1 (pralsetinib alone): Single-dose administration of pralsetinib 200 mg (Part 1; 2×100 mg capsules) or 400 mg (Part 2; 4×100 mg capsules) on Day 1.
- Period 2 (Part 1; pralsetinib + itraconazole): Itraconazole 200 mg BID on Day 1 followed by itraconazole 200 mg QD on Days 2 through 14, with single-dose coadministration of pralsetinib 200 mg (2×100 mg capsules) on Day 4.
  Period 2 (Part 2; pralsetinib + rifampin): Rifampin 600 mg QD (two 300 mg capsules) on Days 1 through 16, with single-dose coadministration of pralsetinib 400 mg (4×100 mg capsules) on Day 9.

Blood samples for analysis of pralsetinib in plasma were taken at prespecified time points after administration for up to 192 hours in Period 1 and up to 264 hours in Period 2 (Part 1) or for up to 192 hours in Periods 1 and 2 (Part 2). In addition, in Period 2 of Part 2, morning urine was collected at prespecified time intervals up to Day 17 for assessment of 6β-hydroxycortisol and free cortisol concentrations to evaluate the level of CYP3A4 enzyme induction.

Part 1: Itraconazole Interaction

Coadministration of itraconazole (200 mg twice daily on Day 1 followed by 200 mg once daily for 13 days) with a single 200 mg dose of pralsetinib on Day 4 caused a substantial decrease in total clearance of pralsetinib, thereby resulting in a clinically relevant increase in systemic exposure to pralsetinib. Based on GMRs, coadministration of itraconazole increased C_{max} by 180% and $AUC_{0-\infty}$ by 350%, relative to a 200 mg dose of pralsetinib administered alone. The median T_{max} of pralsetinib was delayed from 2.00 hours when administered alone to 7.12 hours when coadministered with itraconazole. The CL/F of pralsetinib was approximately 72% lower when coadministered with itraconazole. This finding was consistent with the increase in mean $t_{1/2}$ from 16.1 hours for pralsetinib alone to 30.3 hours when coadministered with itraconazole.

Part 2: Rifampin Interaction

Coadministration of rifampin (600 mg QD for 16 days) with a single 400 mg dose of pralsetinib on Day 9 caused a substantial increase in CL/F of pralsetinib, thereby resulting in a clinically relevant decrease in systemic exposure to pralsetinib. Based on GMRs, coadministration of rifampin decreased pralsetinib C_{max} by 30% and $AUC_{0-\infty}$ by 68%, relative to a 400 mg dose of pralsetinib administered alone. The median T_{max} was

similar when pralsetinib was administered alone (1.55 hours) and when coadministered with rifampin (2.00 hours). The CL/F of pralsetinib was approximately 3.1-fold higher when coadministered with rifampin. This finding was consistent with the decrease in mean $t_{1/2}$ from 14.4 hours for pralsetinib alone to 11.1 hours when coadministered with rifampin.

The mean 6β-hydroxycortisol-to-free cortisol ratio at baseline (Day 1) was 5.23, and increased (range: 25.3 to 45.2) with QD dosing of rifampin, commensurate with CYP3A4 induction. The mean percent increase from baseline (Day 1) ranged from 4.53- to 8.83-fold. The concomitant use of strong CYP3A inhibitors with pralsetinib should be avoided.

5.2.4.3 BP42862: Effect of Esomeprazole on Pharmacokinetics of Pralsetinib

Study BP42862 was an open-label, 2-period, fixed-sequence study in 36 healthy subjects to assess the effect of concomitant administration of a proton-pump inhibitor, esomeprazole, on the PK of a single dose of pralsetinib.

The following treatments were administered orally to each subject under fasted conditions, with a washout period of at least 14 days between pralsetinib treatments:

- Period 1 (pralsetinib alone): Single-dose administration of pralsetinib 400 mg (4 × 100 mg capsules) on Day 1.
- Period 2 (pralsetinib + esomeprazole): Esomeprazole 40 mg QD on Days 1 through 6, with single-dose coadministration of pralsetinib 400 mg (4 × 100 mg capsules) administered after esomeprazole on Day 6.

Blood samples for analysis of pralsetinib in plasma were taken at prespecified time points after administration for up to 192 hours in Periods 1 and 2.

Coadministration of esomeprazole with pralsetinib had little effect on the total clearance of pralsetinib, thereby resulting in only a modest decrease in systemic exposure to pralsetinib. Based on GMRs, the decreases were 25% for C_{max}, and 15% for AUC_{0-t} and $AUC_{0-\infty}$ (Table 16). The median T_{max} of pralsetinib increased from 2 hours (range: 1.50 to 12.0 hours) when administered alone to 4 hours (range: 1.50 to 24.0 hours) when coadministered with esomeprazole. The median difference in T_{max} of 0.75 hours between treatment groups was not statistically significant ($p = 0.2029$) and is unlikely to be clinically relevant. The mean $t_{1/2}$ of pralsetinib was comparable between treatments (approximately 16 hours).

The interindividual variability (%CV) for pralsetinib C_{max} and AUC parameters was generally similar in the absence and presence of esomeprazole.

Table 16 Summary of Pralsetinib Pharmacokinetics Following Administration of Pralsetinib 400 mg With and Without Coadministration of Esomeprazole 40 mg QD (Study BP42862)

Parameter	GeoMean (GeoMean %CV)[a] Pralsetinib + Esomeprazole (Test)	Pralsetinib Alone (Reference)	Geometric Mean Ratio (%)[a]	90% Confidence Interval (Lower–Upper)
N	35	36	—	—
C_{max} (ng/mL)	748 (45.9)	1001 (44.7)	74.74	63.93–87.37
T_{max} (h)[b]	4.01 (1.50–24.0)	2.02 (1.50–12.0)	—	—
AUC_{0-24} (h•ng/mL)	11870 (43.1)	15350 (41.4)	—	—
AUC_{0-t} (h•ng/mL)	23310 (48.4)	27490 (46.7)	84.59	74.26–96.39
$AUC_{0-\infty}$ (h•ng/mL)	23450 (48.2)	27600 (46.6)	84.76	74.45–96.49
$\%AUC_{extrap}$ (%)	0.424 (87.7)	0.324 (77.2)	—	—
$t_{1/2}$ (h)	15.5 (5.10)	15.1 (4.30)	—	—
CL/F (L/h)	17.1 (48.2)	14.5 (46.6)	—	—
V_z/F (L)	366 (48.5)	305 (49.2)	—	—

AUC_{0-24} = area under the plasma concentration-time curve from time 0 to 24 hours postdose; AUC_{0-t} = area under the plasma concentration-time curve from time 0 to time of last measurable concentration above the lower limit of quantitation; $AUC_{0-\infty}$ = area under the plasma concentration-time curve from time 0 to infinity; $\%AUC_{extrap}$ = percent of $AUC_{0-\infty}$ extrapolated; CL/F = apparent oral clearance; C_{max} = maximum plasma concentration; %CV = percent coefficient of variation; GeoMean = geometric mean; N = number of subjects in pharmacokinetic population; $t_{1/2}$ = apparent terminal elimination half-life; T_{max} = time of maximal plasma concentration; V_z/F = apparent volume of distribution.

[a] Median (minimum-maximum) for T_{max} and arithmetic mean (standard deviation) for $t_{1/2}$.

[b] Median treatment difference: 0.752 h; p = 0.2029; Wilcoxon signed-rank test.

In conclusion, coadministration of esomeprazole (40 mg QD for 6 days) with a single 400 mg dose of pralsetinib on Day 6 decreased pralsetinib C_{max} by 25% and $AUC_{0-\infty}$ by 15%, relative to a 400 mg dose of pralsetinib administered alone. These changes are modest and unlikely to be clinically relevant.

5.2.4.4 GP43162: Effect of Cyclosporine on Pharmacokinetics of Pralsetinib

GP43162 was a Phase I, single-center, open-label, fixed-sequence study to investigate the effect of co-administration of a single dose of cyclosporine, a P-gp inhibitor, on the single dose PK of pralsetinib in 15 healthy males and females of non-childbearing potential. The PK concentration-time profile for pralsetinib in plasma with or without cyclosporine are presented in Figure 7 and a summary of the PK parameters for pralsetinib in plasma with or without cyclosporine is presented in Table 17.

Figure 7 Arithmetic Mean (+SD) Pharmacokinetic Concentration-time Profile

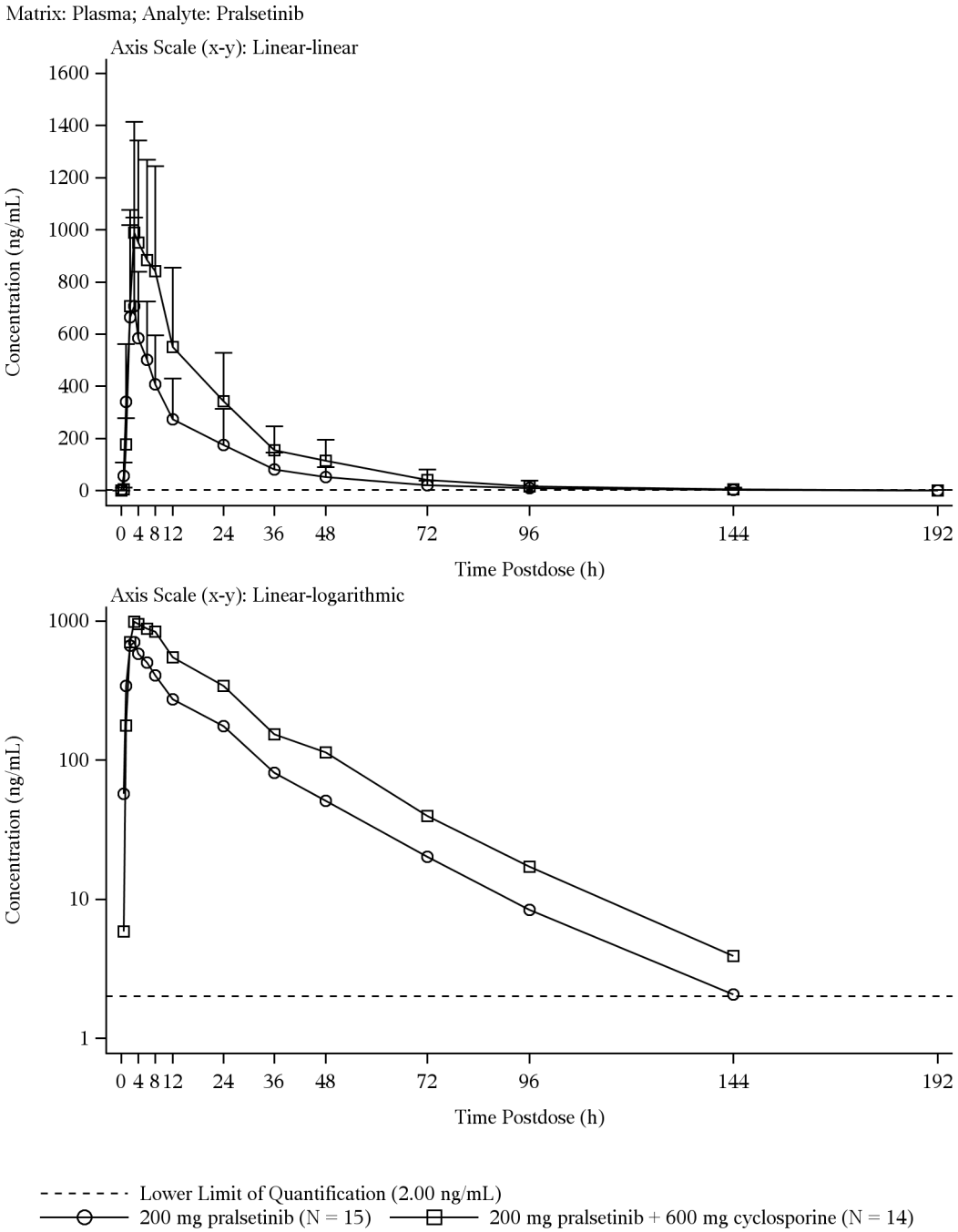

N = number of subjects; SD = standard deviation
Arithmetic mean pralsetinib concentrations were below the limit of quantification starting at 192 hours postdose for both treatments.

The time to maximum concentration (t_{max}) for pralsetinib was slightly delayed in the presence of cyclosporine. The median t_{max} for a single dose of pralsetinib (200 mg) administered alone was 3.00 hours and the median t_{max} for a single dose of pralsetinib (200 mg) coadministered with a single dose of cyclosporine (600 mg) was 4.00 hours.

The mean half-life ($t_{1/2}$) was similar regardless of cyclosporine administration (15.9 vs. 15.5 hours). In the presence of cyclosporine, the clearance of pralsetinib was approximately half of that observed when pralsetinib was administered alone.

Table 17 Summary of the Pharmacokinetic Parameters for Pralsetinib in Plasma

Parameter	200 mg pralsetinib (N = 15)	200 mg pralsetinib + 600 mg cyclosporine (N = 14)	GMR % (90% CI)
AUC_{0-t} (h*ng/mL)	9840 (65.1) [15]	16900 (71.6) [13]	179 (131, 245)
AUC0-192 (h*ng/mL)	9940 (64.2) [15]	17900 (71.5) [14]	181 (136, 241)
$AUC0-\infty$ (h*ng/mL)	9970 (64.4) [15]	18000 (71.6) [14]	181 (136, 241)
$\%AUC_{extrap}$ (%)	0.989 (70.5) [15]	0.819 (101.3) [14]	
C_{max} (ng/mL)	648 (53.6) [15]	955 (59.8) [14]	148 (109, 201)
t_{max} (h)	3.00 (2.00–3.23) [15]	4.00 (3.00–8.00) [14]	-
t_{last} (h)	96.0 (72.0–216) [15]	96.0 (72.0–192) [13]	-
λ_z (h^{-1})	0.0435 (44.1) [15]	0.0447 (29.7) [14]	-
$t_{1/2}$ (h)	15.9 (44.1) [15]	15.5 (29.7) [14]	-
CL/F (L/h)	20.1 (64.4) [15]	11.1 (71.6) [14]	-
V_z/F (L)	461 (61.5) [15]	249 (70.8) [14]	-

$AUC_{0-\infty}$ = area under the concentration–time curve from time 0 extrapolated to infinity;AUC_{0-t} = area under the concentration–time curve from Hour 0 to the time of the last quantifiable concentration; $AUC_{0-"t"}$ = area under the concentration–time curve from Hour 0 to "t", where "t" is a common nominal timepoint across subjects; CI = Confidence Interval; CL/F = apparent total clearance; C_{max} = maximum observed concentration; CV = coefficient of variation (%); GMR = Geometric Mean Ratio; n = number of subjects with valid observations; N = number of subjects; NC = not calculated; $t_{1/2}$ = apparent terminal elimination half–life; t_{last} = time of the last quantifiable concentration; t_{max} = time of the maximum observed concentration; V_z/F = apparent volume of distribution during the terminal phase after oral administration; $\%AUC_{extrap}$ = percentage of area under the concentration–time curve due to extrapolation from the last quantifiable concentration to infinity.Geometric mean (CV) [n] statistics presented; for t_{max} and t_{last}, median (minimum-maximum) [n] statistics presented.

The GMR corresponding to the AUC_{0-t} of pralsetinib coadministered with cyclosporine compared to pralsetinib alone was 179% (1.79-fold). The GMR corresponding to the $AUC_{0-\infty}$ of pralsetinib coadministered with cyclosporine compared to pralsetinib alone was 181% (1.81-fold). The GMR corresponding to the C_{max} of pralsetinib coadministered with cyclosporine compared to pralsetinib alone was 148% (1.48-fold). For each of AUC_{0-t}, AUC_{0-192}, AUC_{0-8}, and C_{max}, the 90% CI of the percentage GMR did not span unity.

The geometric mean C_{max} for cyclosporine was 2160 ng/mL and the geometric $AUC_{0-\infty}$ for cyclosporine was 13300 h*ng/mL. Exposure to cyclosporine was within the range of literature observations for the 600 mg dose level (Sam et al. 2011; Teng et al. 2014).

5.2.5 Hepatic Impairment (Study GP43163)

In the Phase I Study GP43163, the PK of pralsetinib following the administration of a single oral dose of 200 mg was evaluated in subjects with moderate or severe hepatic impairment, as defined by Child-Pugh classification (primary analysis) and NCI-ODWG (exploratory analysis), and demographically matched healthy subjects with normal hepatic function.

Results from this study suggested that moderate and severe hepatic impairment did not have a meaningful impact on the exposure of pralsetinib to warrant a dose adjustment in these patients.

In the primary analysis where impairment was defined by the Child-Pugh classification, the C_{max} and AUCs in subjects with moderate hepatic impairment were similar to subjects with normal hepatic function (GMRs: 98.6% for C_{max} and 112% for $AUC_{0-\infty}$) (Table 18). In subjects with severe hepatic impairment, the C_{max} was lower but the AUC was similar to subjects with normal hepatic function (GMRs: 67.9% for Cmax and 85.8% for $AUC_{0-\infty}$). Unbound C_{max} and AUCs in subjects with moderate or severe hepatic impairment compared to subjects with normal hepatic function, based on GMRs ranged from 114% to 131% for moderate hepatic impairment and from 129% to 164% for subjects with severe hepatic impairment (Table 18). Results from the exploratory analysis, where the hepatic impairment was categorized based on the NCI-ODWG classification criteria, were comparable to the results from the primary analysis (based Child-Pugh classification) presented above.

The unbound exposure in subjects with moderate and severe hepatic impairment was slightly higher compared to that in subjects with normal liver function, but it overlapped with the range of estimated unbound concentrations observed in other pralsetinib studies, after adjusting for dose and multiple dosing. The corresponding 90% CI for each GMR, albeit wide, spanned unity, so similarity in unbound systemic exposures between subjects with moderate or severe hepatic impairment and subjects with normal hepatic function could not be ruled out. However, between-subject variability was high across the three cohorts. In addition, no safety concerns were observed in this study. While this study was not powered to evaluate the safety and tolerability of pralsetinib in subjects with hepatic impairment and those with normal liver function, there was no obvious pattern of TEAEs within or across the cohorts. When interpreting these results, it needs to be considered that this was a small single-dose study conducted in subjects of generally good health except for their hepatic function. However, the TEAEs that were observed were in line with the known safety profile of pralsetinib or the underlying hepatic disease of the subjects. Overall, given the lack of meaningful change in the total exposure, high inter-subject variability, and consistent safety profile, the modest change

in the unbound pralsetinib exposure in subjects with severe hepatic impairment is determined to be not clinically relevant, thus not warranting a dose adjustment in these patients.

Table 18 Summary of Pharmacokinetic Parameters of Pralsetinib-Hepatic Impairment Classification based on Child-Pugh Score

Parameter	Cohort 1 Normal Hepatic Function (N = 14)	Cohort 2 Moderate Hepatic Impairment (N = 9)	Cohort 3 Severe Hepatic Impairment (N = 6)	GMR (90% CI) [Moderate (test) vs Normal (reference)]	GMR (90% CI) [Severe (test) vs Normal (reference)]
AUC_{0-t} (h*ng/mL)	12300 (61.8) [13]	11300 (72.3) [8]	13600 (62.5) [6]	113 (65.4, 194) [8]	86.4 (51.3, 146) [8]
AUC_{0-192} (h*ng/mL)	12400 (61.5) [13]	11400 (71.8) [8]	13700 (62.0) [6]	112 (65.3, 192) [8]	85.6 (51.0, 144) [6]
$AUC_{0-\infty}$ (h*ng/mL)	12400 (61.6) [13]	11400 (72.0) [8]	13700 (62.1) [6]	112 (65.4, 193) [8]	85.8 (51.1, 144) [6]
%AUC_{extrap} (%)	1.21 (71.2) [13]	0.936 (74.2) [8]	0.630 (76.3) [6]		
C_{max} (ng/mL)	619 (67.3) [13]	476 (56.5) [8]	508 (70.1) [6]	98.6 (59.7, 163) [8]	67.9 (35.3, 131) [6]
t_{max} (h)	3.00 (1.00-6.07) [13]	3.00 (1.00-6.00) [8]	3.50 (3.00-4.00) [6]		
t_{last} (h)	96.0 (71.9-144) [13]	120 (71.0-192) [8]	144 (71.9-192) [6]		
λz (h^{-1})	0.0449 (25.1) [13]	0.0395 (41.1) [8]	0.0368 (26.6) [6]		
$t_{1/2}$ (h)	15.4 (25.1) [13]	17.5 (41.1) [8]	18.9 (26.6) [6]		
f_u	0.0253 (27.5) [13]	0.0331 (23.1) [8]	0.0404 (27.3) [6]		
$C_{max,u}$ (ng/mL)	15.6 (52.7) [13]	15.7 (63.3) [8]	20.5 (69.2) [6]	114 (69.0, 190)	129 (70.4, 236)
$AUC_{0-t,u}$ (h*ng/mL)	310 (54.0) [13]	374 (77.9) [8]	548 (55.7) [6]	131 (75.8, 226)	164 (99.2, 271)
$AUC_{0-192,u}$ (h*ng/mL)	314 (53.8) [13]	377 (77.3) [8]	551 (55.3) [6]	130 (75.5, 224)	162 (98.6, 268)
$AUC_{0-\infty,u}$ (h*ng/mL)	314 (53.8) [13]	379 (77.6) [8]	552 (55.4) [6]	130 (75.6, 225)	163 (98.7, 268) [6]
CL/F (L/h)	16.1 (61.6) [13]	17.5 (72.0) [8]	14.6 (62.1) [6]		
V_z/F (L)	358 (55.6) [13]	443 (65.1) [8]	398 (51.8) [6]		

AUC_{0-192} = area under the concentration-time curve from Hour 0 to 192; $AUC_{0-192,u}$ = area under the concentration-time curve from Hour 0 to 192 of free drug; AUC_{0-t} = area under the concentration-time curve from Hour 0 to the time of the last measurable concentration; $AUC_{0-t,u}$ = area under the concentration-time curve from Hour 0 to the time of the last measurable concentration of free drug; $AUC_{0-\infty}$ = area under the concentration-time curve from time 0 extrapolated to infinity; $AUC_{0-\infty,u}$ = area under the concentration-time curve from time 0 extrapolated to infinity of free drug; CL/F = apparent systemic clearance; C_{max} = maximum observed concentration;

$C_{max,u}$ = maximum observed concentration of free drug; CV = coefficient of variation (%); f_u = fraction of unbound drug; n = number of subjects with valid observations; N = number of subjects; GMR = Geometric Mean Ratio; CI = Confidence Interval; t1/2 = apparent terminal elimination half-life; tlast = time of the last measurable concentration; tmax = time to maximum observed concentration; V_z/F = apparent volume of distribution during the terminal elimination phase; λ_z = apparent terminal elimination rate constant; $\%AUC_{extrap}$ = percentage of area under the concentration-time curve that is due to extrapolation from the last measurable concentration to infinity Geometric mean (CV) [n] statistics presented; for t_{max} and t_{last}, median (minimum-maximum) [n] statistics presented. Hepatic impairment severity: moderate = Class B (Child-Pugh total score 7 to 9, inclusive); severe = Class C (Child- Pugh total score 10 to 15, inclusive).

5.3 CLINICAL PHARMACODYNAMICS

5.3.1 Integrated Pharmacokinetic/Pharmacodynamic Analysis

5.3.1.1 Population PK Analysis

A population PK one-compartment model for pralsetinib following oral administration was developed using data from four Phase I studies in healthy volunteers (BP42858, BP42859, BP42861, and BP42862) and one Phase I/II study (BO42863) in patients with NSCLC and patients with RET-altered thyroid cancer. The previously developed population PK model was updated with additional data from patients with NSCLC and patients with RET-altered thyroid cancer (CCOD: 12 April 2021). A full covariate analysis was then undertaken in a pooled population PK analysis of healthy volunteers and patients with NSCLC and patients with RET-altered thyroid cancer. The original population PK model for pralsetinib exposure in patients with NSCLC and patients with RET-altered thyroid cancer was used to perform dose-exposure simulations for pralsetinib to guide dose selection in adolescent patients with thyroid cancer (12 to <18 years of age).

5.3.1.1.1 Pooled Population PK Analysis in Patients with NSCLC and RET-altered Thyroid Cancer

Patients with NSCLC had a higher exposure compared to healthy volunteers or patients with RET-altered thyroid cancer administered the same dose and patients with RET-altered thyroid cancer had a faster absorption compared to patients with NSCLC or healthy subjects administered the same dose.

The covariate effects of sex, race, renal function (creatinine clearance, estimated glomerular filtration rate [eGFR]), hepatic function (ALT, AST, bilirubin, albumin), and concomitant use of CYP3A4 inhibitors, proton pump inhibitors, H_2-receptor antagonists, or antacids were found to have no significant impact on the PK of pralsetinib. Consistent with the lack of correlation, no relevant difference in CL/F was observed among patients with mild (eGFR: 60 to 89 mL/min/1.73m^2; $n=242$) or moderate (eGFR: 30 to 59 mL/min/1.73m^2; $n=27$) renal impairment, or among patients with mild (total bilirubin within upper limit of normal (ULN) and AST $>$ ULN or total bilirubin 1 to 1.5 $\times$ ULN and any AST; $n=42$) or moderate (total bilirubin 1.5 to 3.0 × ULN and any AST; $n=2$) hepatic impairment, as compared with patients with normal renal ($n=336$) or hepatic ($n=624$) function. Hence, no dose adjustment is required for patients with mild hepatic impairment or mild or moderate renal impairment.

The statistically significant covariates identified in the model were as follows:

- increasing body weight increased CL/F and V/F
- patients over 37.5 years had a decrease in CL/F
- patients with RET-altered thyroid cancer had a 27% increase in absorption transit rate constant (KTR) on C1D1 (relative to patients with NSCLC or healthy subjects)

- patients with NSCLC had a 38% increase in F (relative to patients with RET-altered thyroid cancers or healthy subjects)
- patients with NSCLC administered Process I capsules had a 26% decrease in F (relative to patients with RET-altered thyroid cancers or healthy subjects)
- concomitant CYP3A4 inducer use increased CL/F by 13%
- capsule process had an effect on KTR.

Simulations indicate that adolescents (age 12 to $<$18 years, weight $\geq$29 kg) are expected to achieve similar PK exposures to adults when pralsetinib is administered at 400 mg QD.

5.3.1.2 Physiologically–Based Pharmacokinetic (PBPK) Analysis

Based on *in vitro* data, pralsetinib is a substrate of the enzyme CYP3A4 and a substrate of the efflux transporter P-gp, and therefore, its PK may be affected by co-administration of potent CYP3A4 inhibitors and inducers, P-gp inhibitors, and combined CYP3A4 and P-gp inhibitors.

A physiologically-based pharmacokinetic (PBPK) model for pralsetinib was developed using the Simcyp Population-Based ADME Simulator (version 21, release 1; Sheffield, UK) to assess the victim DDI risk for pralsetinib. The PBPK model for pralsetinib was developed and verified using *in vitro* data and clinical PK data obtained from oral administration of pralsetinib. The PBPK model was then further verified by simulating the clinically observed DDIs between pralsetinib and cyclosporine (CsA, strong P-gp inhibitor; Study GP43162), pralsetinib and itraconazole (ITZ, strong CYP3A4 inhibitor with P-gp inhibition; Study BP42861), and pralsetinib and rifampin (RIF, strong CYP3A4 inducer; Study BP42861). The verified PBPK model was then applied to predict the effects of moderate CYP3A4 inhibitors (with and without P-gp inhibition), moderate CYP3A4 inducers, and a strong CYP3A4 inhibitor without P-gp inhibition on pralsetinib PK.

PBPK predictions suggested that

- Coadministration of a strong CYP3A4 inhibitor (without any P–gp inhibition) with pralsetinib would increase the pralsetinib AUC by 122% and C_{max} by 20% compared to pralsetinib alone.
- Coadministration of a moderate CYP3A4 inhibitor (without any P–gp inhibition) with pralsetinib would the pralsetinib AUC by 71% and C_{max} by 15% compared to pralsetinib alone. Coadministration of a combined P–gp and moderate CYP3A4 inhibitor with pralsetinib would increase the pralsetinib AUC by 84-108% and C_{max} by 60-68% compared to pralsetinib alone.
- Coadministration of a moderate CYP3A4 inducer with pralsetinib would decrease the pralsetinib AUC by 32-45% and C_{max} by 14-18% compared to pralsetinib alone.

As noted in Section 5.2.4.2 and Section 5.2.4.4, DDI assessments in clinical studies have shown that

- Coadministration of a combined P−gp and strong CYP3A4 inhibitor, itraconazole, with pralsetinib increased pralsetinib $AUC_{0\text{-}inf}$ by 251% and C_{max} by 8 compared to pralsetinib alone (Study BP42861).
- Coadministration of a P−gp inhibitor cyclosporine with pralsetinib increased pralsetinib $AUC_{0\text{-}inf}$ by 81% and C_{max} by 48% compared to pralsetinib alone (Study GP43162).
- Coadministration of a strong CYP3A4 inducer, rifampin, with pralsetinib decreased pralsetinib $AUC_{0\text{-}inf}$ by 68% and C_{max} by 30% compared to pralsetinib alone (Study BP42861).

5.4 CLINICAL EFFICACY

5.4.1 Study BO42863: ARROW Study

Pralsetinib has demonstrated broad and durable antitumor activity in patients with RET fusion-positive NSCLC, RET-mutant MTC, RET fusion-positive thyroid cancer, and other RET fusion-positive solid tumors regardless of treatment history, RET-fusion partner or mutation, or central nervous system involvement.

Efficacy data (LPLV: 21 March 2024) are reported for patients with RET-fusion positive NSCLC, RET-mutant MTC, and RET fusion-positive thyroid cancer (treated with pralsetinib at the proposed indicated dose of 400 mg QD in Study BO42863 Efficacy data was also reported for patients with various other RET fusion-positive tumor types who received pralsetinib across all doses. Results obtained for Groups 6 and 7 (RET alteration-positive solid tumors previously treated with RET inhibitors and RET mutation-positive tumors [other than MTC]) did not demonstrate significant clinical efficacy. Due to the small sample size (n = 22 in Group 6 and n = 14 in Group 7), these results should be interpreted with caution.

5.4.1.1 Efficacy in Patients with RET fusion-positive NSCLC

In the 259 evaluable patients in the RET fusion-positive NSCLC RET-altered measurable disease population that received pralsetinib at the starting dose of 400 mg QD, an ORR of 70.3% (95% CI: 64.3, 75.8) was observed. Eighteen patients (6.9%) had a CR and 164 patients (63.3%) a PR. This ORR was consistent with that observed among patients regardless of prior therapy (78.3%, 64.7%, 63.1% for patients without any prior systemic treatment, patients who received any prior systemic treatment, and patients who received prior platinum treatment, respectively). Additionally, these responses were rapid, with a median time to first response of 1.84 months for responders who were treatment-naïve and 1.84 months for those who had previously received prior systemic treatment. Responses were also durable where median DOR was 19.1 months (95% CI: 14.5, 27.9) and DOR rate at 12 months was 59.5% (95% CI: 52.2, 66.8).

For all NSCLC patients, the median PFS is 13.1 months (95% CI: 11.4, 16.8) with 86 patients (30.6%) censored. KM estimates of PFS rates are 74.4% (95% CI: 69.1,

79.6) at 6 months, 54.7% (95% CI: 48.7, 60.8) at 12 months, 43.1% (95% CI: 37.0, 49.2) at 18 months, and 37.7% (95% CI: 31.7, 43.7) at 24 months. Median overall survival was 44.3 months (95% CI: 30.9, 53.1) and the OS rate was 77.8% at 12 months and 63.1% at 24 months.

A summary of efficacy data is provided in Table 19.

Table 19 Summary of Efficacy Data for NSCLC Patients –Study BO42863

	Treatment naïve	Prior systemic therapy	All NSCLC
ORR (RET-Altered Measurable Disease Population),	**(n = 106)**	**(n = 153)**	**(n = 259)**
No. of responders (%)	83 (78.3)	99 (64.7)	182 (70.3)
95% CI	(69.2, 85.7)	(56.6, 72.3)	(64.3, 75.8)
DOR (RET-Altered Measurable Disease Population)	**(n = 83)**	**(n = 99)**	**(n = 182)**
Patients with event (%)	57 (68.7)	66 (66.7)	123 (67.6)
Median (95% CI)	13.4 (9.4, 21.7)	31.4 (15.1, 38.8)	19.1 (14.5, 27.9)
DOR at 12 months	50.7 (39.5, 61.8)	66.6 (57.2, 76.1)	59.5 (52.2, 66.8)
DOR at 24 months	37.0 (26.0, 47.9)	51.5 (41.4, 61.6)	45.1 (37.6, 52.5)
DOR at 48 months	18.1 (5.3, 31.0)	28.8 (18.8, 38.8)	24.6 (17.2, 32.0)
PFS (Efficacy Population)	**(n = 116)**	**(n = 165)**	**(n = 281)**
Patients with event (%)	81 (69.8)	114 (69.1)	195 (69.4)
Median PFS (95% CI), month	12.1 (9.2, 16.6)	16.2 (11.7, 22.1)	13.1 (11.4, 16.8)
PFS rate at 12 months	50.6 (41.1, 60.1)	57.6 (49.7, 65.4)	54.7 (48.7, 60.8)
PFS rate at 24 months	33.5 (24.4, 42.7)	40.5 (32.6, 48.4)	37.7 (31.7, 43.7)
PFS rate at 48 months	20.8 (12.1, 29.4)	26.0 (18.6, 33.4)	23.9 (18.3, 29.6)
OS (Efficacy Population)	**(n = 116)**	**(n = 165)**	**(n = 281)**
Patients with event (%)	49 (42.2)	82 (49.7)	131 (46.6)
Median OS (95% CI), month	50.1 (28.3, NR)	39.7 (29.1, 53.1)	44.3 (30.9, 53.1)
OS rate at 12 months	82.6 (75.4, 89.7)	74.2 (67.1, 81.3)	77.8 (72.7, 82.9)
OS rate at 24 months	65.1 (55.8, 74.4)	61.6 (53.6, 69.7)	63.1 (57.1, 69.2)
OS rate at 48 months	52.0 (42.0, 62.0)	44.2 (35.6, 52.8)	47.1 (40.4, 53.7)

DOR = duration of response; NR = not reached; ORR = overall response rate; OS = overall survival PFS = progression-free survival.

5.4.1.2 Efficacy in Patients with RET-altered Thyroid Cancer

RET Mutation-positive MTC Patients Treated at 400 mg QD (Efficacy Population)

ORR in patients with RET mutation-positive MTC treated at 400 mg QD (RET-altered measurable disease population) overall was 68.2% (95% CI: 59.5, 76.0): 12 patients (9.1%) had a CR and 78 patients (59.1%) had a PR. ORR results were lower among RET mutation-positive MTC patients with prior treatments: ORR was 56.7% (95% CI: 43.2, 69.4) in MTC patients with prior cabozantinib and/or vandetanib treatment, 58.3% (95% CI: 36.6, 77.9) in MTC patients with prior cabozantinib and vandetanib treatment. ORR in MTC patients with no prior systemic treatment was 79.0% (95% CI: 66.8, 88.3). Additionally, median time to first response in the 90 RET mutation-positive MTC patients overall with a confirmed response was 4.75 months (range: 1.7–27.3). Median DOR was 39.6 months (95% CI: 29.4, NR) and DOR rate at 24 months was 64.6% (95% CI: 54.4, 74.8) and at 48 months was 45.7 (95% CI: 34.5, 56.8). The median PFS (efficacy population) was 37.2 months (95% CI: 27.5, 55.5). KM estimates of PFS rates were 89.4% (95% CI: 84.3, 94.5) at 6 months, 84.9% (95% CI: 79.0, 90.9) at 9 months, 80.4% (95% CI: 73.7, 87.0) at 12 months, 74.2% (95% CI: 66.8, 81.6) at 18 months, 65.5 (95% CI: 57.3, 73.6) at 24 months and 43.4 (95% CI: 34.5, 52.2) at 48 months. The median OS was not reached and the estimated OS rate was 90.7% (95% CI: 85.9, 95.5) at 12 months, 86.9% (95% CI: 81.3, 92.6) at 18 months and 83.9% (95% CI: 77.7, 90.1) at 24 months.

RET Fusion-positive Thyroid Cancer Patients Treated at 400 mg QD (Efficacy Population)

In the 27 evaluable patients in the RET-altered measurable disease population that received pralsetinib at the starting dose of 400 mg QD, an ORR of 85.2% (95% CI: 66.3, 95.8) was observed. Four patients (14.8%) had a CR and 19 patients (70.4%) had a PR. Additionally, median time to first response in the 23 RET fusion-positive thyroid cancer patients overall with a confirmed response was 1.84 months (range: 1.7–7.9). The median DOR was not reached and DOR rate at 24 months was 53.8% (95% CI: 32.5, 75.1). The median PFS (efficacy population) was not reached. KM estimates of PFS rates were 80.6% (95% CI: 66.7, 94.6) at 6 months and 9 months, 70.8% (95% CI: 54.8, 86.9) at 12 months, 60.5% (95% CI: 43.1, 78.0) at 18 months, 56.7% (95% CI: 38.9, 74.6) at 24 months, and 52.7% (95% CI: 34.4, 71.0) at 30 months and 36 months.. The median OS was not reached and the estimated OS rate was 87.1% (95% CI: 75.3, 98.9) at 6 months and 9 months, 80.4% (95% CI: 66.3, 94.5) at 12 months, 69.9% (95% CI: 53.4, 86.4) at 18 months, 66.4% (95% CI: 49.4, 83.5) at 24 months and 62.5% (95% CI: 44.8, 80.2) at 30 months and 36 months.

A summary of the efficacy data for patients with RET-altered thyroid cancer is provided in Table 20.

Table 20 Summary of Efficacy Data for RET-altered Thyroid Cancer Patients Treated at 400 mg QD (Efficacy Populations) –Study BO42863

	RET mutation-positive MTC	RET fusion-positive
ORR (RET-Altered Measurable Disease Population)	**(n = 132)**	**(n = 27)**
No. of responders (%)	90 (68.2%)	23 (85.2%)
95% CI	(59.5, 76.0)	(66.3, 95.8)
DOR (RET-Altered Measurable Disease Population)	**(n = 90)**	**(n = 23)**
Patients with event (%)	45 (50.0%)	10 (43.5%)
Median (95% CI)[a]	39.6 (29.4, NR)	NR (12.9,NR)
DOR rate at 24 months (95% CI)	64.6% (54.4, 74.8)	53.8% (32.5, 75.1)
PFS (Efficacy Population)	**(n = 145)**	**(n = 31)**
Patients with event (%)	74 (51.0%)	14 (45.2%)
Median PFS (95% CI), month	37.2 months (95% CI: 27.5, 55.5)	NR (95% CI: 14.7, NR)
PFS rate at 18 months	74.2% (95% CI: 66.8, 81.6)	60.5% (95% CI: 43.1, 78.0)
OS (Efficacy Population)	**(n = 145)**	**(n = 31)**
Patients with event (%)	53 (36.6%)	11 (35.5%)
Median OS (95% CI), month	NR	NR
OS rate at 12 months	90.7% (95% CI: 85.9, 95.5)	80.4 % (95% CI: 66.3, 94.5)
OS rate at 18 months	86.9% (95% CI: 81.3, 92.6)	69.9% (95% CI: 53.4, 86.4)

DOR = duration of response; MTC = medullary thyroid cancer NR = not reached; ORR = overall response rate; OS = overall survival PFS = progression-free survival.

[a] The 95% CI is based on Greenwood formula.

5.4.1.3 Efficacy in Patients with other RET fusion-positive tumors

Pralsetinib activity has been demonstrated in 9 patients with various other RET fusion-positive solid tumor types in the RET-altered measurable disease population who received pralsetinib at a 400 mg QD starting dose (n = 28), with an ORR of 46.4% (95% CI: 27.5, 66.1). Complete responses to pralsetinib treatment were observed in 3 patients and partial responses were observed in 10 patients. Anti-tumor activity was demonstrated in the following tumor types: pancreatic cancer (5 out of 5 patients), neuroendocrine tumor (2 out of 3 patients), sarcoma (2 out of 3 patients), cancer of unknown primary (1 out of 1 patient), head and neck cancer (1 out of 2 patients), SCLC (1 out of 2 patients) and hepatobiliary cancer (1 out of 4 patients).

5.4.2 Study ML42439: MyTACTIC Study (Arm O)

Overall, 3 patients with advanced unresectable or metastatic RET-fusion positive solid tumors were enrolled in Arm O of Study ML42439.

5.4.2.1 Efficacy Summary

Overall, 1 out of 3 patients (33.3%) achieved a confirmed objective response (95% CI: 0.8, 90.6; 70% CI: 5.3, 75.6). This patient (33.3%) achieved a partial response (PR). One patient (33.3%) had stable disease (SD) as their confirmed best overall response Overall, 2 out of 3 patients achieved disease control (disease control rate [DCR] of 66.7%, 95% CI: 9.4, 99.2)..The median duration of objective response (DOR) was not estimable. The median progression-free survival (PFS) was 7.10 months (95% CI: 1.84, not estimable). The PFS rate at 3 months was 66.67% (95% CI: 13.32, 100.00). For more details, please refer Table 21.

Table 21 Efficacy Summary: MyTACTIC Study (Arm O)

Parameter	Arm O
Primary Endpoint: cORR	
Number of patients (N)	3
cORR (n [%])	1 (33.3%)
(95% CI) [a]	(0.8, 90.6)
Secondary Endpoint: DOR [b]	
Responders (n)	1
Median DOR (months) [c]	NE
(95% CI) [d]	NE
Secondary Endpoint: DCR [e]	
Number of patients (N)	3
DCR (n [%])	2 (66.7%)
(95% CI) [a]	(9.4, 99.2)
Secondary Endpoint: PFS [f]	
Number of patients (N)	3
Patients with events (n [%])	2 (66.7%)
Median PFS (months)	7.10
(95% CI) [g]	(1.84, NE)
Secondary Endpoint: PFS rate	
Number of patients (N)	3
3 months	
Patients remaining at risk (n)	2
Event-free rate (%)	66.67%
(95% CI) [h]	(13.32, 100.00)

Table 21 Efficacy Summary: MyTACTIC Study (Arm O)

Parameter	Arm O
6 months	
Patients remaining at risk (n)	1
Event-free rate (%)	66.67%
(95% CI) [h]	(13.32, 100.00)

CI = confidence interval; cORR = confirmed objective response rate; CR = complete response; DCR = disease control rate; DOR = duration of response; NE = not estimable; PD = progressive disease; PFS = progression-free survival; PR = partial response; SD = stable disease.

Note: Percentages are based on number of patients (N).

[a] 95% CI and 70% CI for response rate was computed using the Clopper-Pearson method.

[b] DOR was defined as the date of the first confirmed CR/PR to the date of PD/Death or the date of last evaluable assessment.

[c] The median DOR is a Kaplan-Meier estimate.

[d] 95% CI for median DOR was computed by the method of Brookmeyer and Crowley.

[e] DCR was defined as the proportion of patients whose best response was confirmed CR, confirmed PR, or a response of CR, PR, SD, or NON-CR/NON-PD for a minimum of 98 days (for Arm O, a 28-day cycle arm) after first treatment date.

[f] PFS was defined as the time from the start of study treatment to the first occurrence of disease progression, or death, whichever occurs first. Patients who did not experience death or disease progression were censored on the day of the last available assessment. Disease Progression includes RECIST 1.1 or RANO progression and clinical progression.

[g] 95% CI for median PFS was computed by the method of Brookmeyer and Crowley.

[h] 95% CI for event-free rate was computed by the method of Greenwood.

5.5 CLINICAL SAFETY

5.5.1 Study BO42863: ARROW Study

5.5.1.1 Phase I Dose Escalation Safety Results

A total of 53 patients (51 with RET-altered tumors) were enrolled into the QD dose escalation of pralsetinib at doses ranging from 30 mg to 600 mg as outlined in Table 22. The dose escalation part (Phase I) of the study employed a Bayesian optimal interval (BOIN) design to determine MTD.

Pralsetinib demonstrated a dose dependent increase in exposure and pathway inhibition. Four patients were treated at 600 mg QD and 2 of the 4 patients experienced DLTs (Grade 3 hyponatremia and Grade 3 hypertension). While both DLTs were reversible, in accordance with the protocol guidelines, 600 mg QD was determined to have exceeded the MTD and the MTD for pralsetinib was determined to be 400 mg QD.

Table 22 Phase I Dose Escalation Summary (QD Dosing Schedule)

Cohort - Dose	No. of Patients Treated (n = 53)	No. of Evaluable Patients (n = 51[a])	Dose-Limiting Toxicity (DLT)
1 - 30 mg QD	2	1	0
2 - 60 mg QD	6	6	0
3 - 100 mg QD	5	5	1 ALT increased
4 - 200 mg QD	5	5	0
5 - 300 mg QD	5	5	1 tumor lysis syndrome; 1 hypertension
6 - 200 mg QD	8	7	0
7 - 300 mg QD	6	6	0
8 – 400 mg QD	12	12	1 myositis[b]; 1 hypertension
9 – 600 mg QD	4	4	1 hyponatremia; 1 hypertension

ALT = alanine aminotransferase; DLTdose-limiting toxicity; No. = number; QD = once daily.

[a]Two patients were not evaluable for DLT (at least 75% of Cycle 1 doses not completed and did not experience a DLT).

[b]This event was formerly reported by the site as asthenia.

A BID dosing schedule was also explored in Phase I. The BID dosing schedule started at a 300 mg total daily dose. Based on overall safety, exposure, and tolerability, QD was the preferred dosing schedule and chosen for the dose expansion, Phase II. An MTD for BID dosing was not defined and further exploration is not planned.

The overall safety in patients of Phase I of the study receiving pralsetinib across doses 60–400 mg QD was favorable. Most AEs were Grade 1; the most commonly reported AEs in Phase I of the study were: constipation (24%), ALT increased (22%), AST increased (20%), and hypertension (16%).

Rationale for the RP2D

Exposure at the 400 mg MTD provided sustained coverage above the predicted tumor and close to the brain RET inhibitory concentration (IC_{90}). Based on this, 400 mg was selected as the recommended dose for the expansion phase.

5.5.1.2 Safety Results for patients treated at 400 mg QD (including Phase I and Phase II)

Safety for patients treated with pralsetinib in this study was generally consistent across safety populations, regardless of indication and dose. The safety population consisted of 590 consecutively enrolled patients who received ≥1 pralsetinib dose (i.e., patients treated at all doses/schedules). Of this population, 540 patients received pralsetinib at a starting dose of 400 mg QD in either Phase 1 or Phase 2, regardless of tumor type or mutation status. Safety results (LPLV: 21 March 2024) for the 540 patients treated at

400 mg QD regardless of indication are presented in this section. The median treatment duration for these patients was 16.53 months (range: < 1–71.8).

5.5.1.2.1 Overview of Adverse Events

All 540 patients experienced an AE. The most frequently reported AEs (by PT) are presented in Table 23.

Table 23 Adverse Events Occurring in ≥20% of Patients by Preferred Term (Safety Population, Treated at 400 mg QD)

Preferred Term	All Patients N=540
Patients with AE	540 (100%)
Anaemia	286 (53%)
AST increased	274 (50.7%)
Constipation	238 (44.1%)
ALT increased	212 (39.3%)
Hypertension	192 (35.6%)
Diarrhoea	191 (35.4%)
Pyrexia	167 (30.9%)
White blood cell count decreased	157 (29.1)
Fatigue	154 (28.5%)
Cough	150 (27.8%)
Neutrophil count decreased	147 (27.2%)
Blood creatinine increased	143 (26.5%)
Hypocalcaemia	130 (24.1%)
Neutropenia	128 (23.7%)
Pneumonia	123 (22.8%)
Dyspnoea	118 (21.9%)
Nausea	115 (21.3%)
Decreased appetite	114 (21.1%)

ALT = alanine aminotransferase; AST = aspartate aminotransferase.

Notes: Adverse Events (AEs) are coded using MedDRA 26.1. AEs refer to treatment-emergent adverse events (TEAEs). All TEAEs including treatment-emergent SAEs are included in summary statistics. If a patient has multiple occurrences of an AE, the patient is presented only once in the respective patient count. Adjacent AEs for the same preferred term are linked per patient.

5.5.1.2.2 Adverse Events by Relatedness (Investigator-Assessed)

Overall, 94.4% of all patients treated at 400 mg QD in the safety population experienced an AE related to pralsetinib. The most frequently reported related AEs by PT are presented in Table 24.

Table 24 Treatment Related Adverse Events Occurring in ≥20% of Patients by Preferred Term (Safety Population, Treated at 400 mg QD)

Preferred Term	All Patients N=540
Patients with treatment related AE	510 (94.4%)
AST increased	229 (42.4%)
Anaemia	212 (39.3%)
ALT increased	179 (33.1%)
Constipation	146 (27%)
Hypertension	145 (26.9%)
White blood cell count decreased	145 (26.9%)
Neutrophil count decreased	135 (25%)
Neutropenia	119 (22%)

ALT = alanine aminotransferase; AST = aspartate aminotransferase.

Notes: Adverse Events (AEs) are coded using MedDRA 26.1. AEs refer to treatment-emergent adverse events (TEAEs). All TEAEs including treatment-emergent SAEs are included in summary statistics. If a patient has multiple occurrences of an AE, the patient is presented only once in the respective patient count. Adjacent AEs for the same preferred term are linked per patient.

5.5.1.2.3 Adverse Events by Intensity

Overall, 86.1% of all patients treated at 400 mg QD experienced a Grade ≥ 3 AE. The most frequently reported Grade ≥ 3 AEs by PT are presented in Table 25.

Overall, 64.4% of all patients treated at 400 mg QD experienced a Grade ≥ 3 AE related to pralsetinib. The most frequently (≥ 10%) reported Grade ≥ 3 related AEs by PT were anaemia (18.5%), hypertension (14.3%), neutropenia (10.76%) and neutrophil count decreased (10.2%).

Table 25 Grade≥3 Adverse Events Occurring in≥10% of Patients by Preferred Term (Safety Population, Treated at 400 mg QD)

Preferred Term	All Patients n=540
Patients with Grade≥3 AE	465 (86.1%)
Anaemia	132 (24.4%)
Hypertension	106 (19.6%)
Pneumonia	82 (15.2%)
Neutropenia	63 (11.7%)
Neutrophil count decreased	61 (11.3%)
Lymphocyte count decreased	60 (11.1%)

Notes: Adverse Events (AEs) are coded using MedDRA 26.1. AEs refer to treatment-emergent adverse events (TEAEs). All TEAEs including treatment-emergent SAEs are included in summary statistics. If a patient has multiple occurrences of an AE, the patient is presented only once in the respective patient count. Adjacent AEs for the same preferred term are linked per patient.

5.5.1.2.4 Deaths

Overall, 105 patients (19.4%) died during the study due to AEs of which 8 patients (1.5%) died due to a related AE. Related Grade 5 AEs included pneumonia (2 patients), death not otherwise specified (2 patients), and interstitial lung disease, pneumonitis, pneumocystic jirovecii pneumonia, liver injury, and rhabdomyolysis (1 patient each). Overall, 21 patients (3.9%) died due to lung neoplasm malignant, 12 patients (2.2%) died due to pneumonia, 6 patients (1.1%) experienced death (not otherwise specified), 5 patients (<1%) died due to disease progression, 4 patients each (<1%) died due to malignant neoplasm progression, sepsis and COVID-19, 3 patients each (<1%) died due to lung cancer metastatic, medullary thyroid cancer and metastatic neoplasm, and 2 patients each (<1%) died due to asphyxia, COVID-19 pneumonia, dyspnea, thyroid cancer, thyroid cancer metastatic,respiratory failure, and pneumonia aspiration. All other fatal AEs were reported in 1 patient each.

5.5.1.2.5 Serious Adverse Events

Overall, 70.6% of patients treated at 400 mg QD experienced a SAE. The most frequently reported SAEs are presented in Table 26.

Overall, 34.6% of patients experienced a Grade 3 SAE, 9.4% of patients experienced a Grade 4 SAE and 18.9% experienced a Grade 5 SAE.

Overall, 24.6% of patients experienced a SAE related to pralsetinib. The most frequently reported related SAEs (occurring in≥2%) were pneumonitis (4.4%), pneumonia (3.7%) and anemia (3.5%).

Table 26 Serious Adverse Events Occurring in≥2% of Patients, by Preferred Terms (Safety Population, Treated at 400 mg QD)

Preferred Term	All Patients N=540
Patients with SAE	381 (70.6%)
Pneumonia	87 (16.1%)
Anaemia	32 (5.9%)
Pneumonitis	27 (5.0%)
Lung neoplasm malignant	26 (4.8%)
Urinary tract infection	23 (4.3%)
Sepsis	20 (3.7%)
COVID-19	16 (3.0%)
Pyrexia	15 (2.8%)
COVID-19 pneumonia	13 (2.4%)
Pleural effusion	11 (2.0%)

Notes: Adverse Events (AEs) are coded using MedDRA 26.1. AEs refer to treatment-emergent adverse events (TEAEs). All TEAEs including treatment-emergent SAEs are included in summary statistics. If a patient has multiple occurrences of an AE, the patient is presented only once in the respective patient count. Adjacent AEs for the same preferred term are linked per patient.

5.5.1.2.6 Adverse Events That Led to Withdrawal of Study Treatment

A total of 130 patients (24.1%) experienced AEs leading to discontinuation of study treatment. The most frequently reported AEs leading to treatment discontinuation (occurring in>1%) were pneumonia (2.8%), pneumonitis (2.4%), anemia (1.3%) and lung neoplasm malignant (1.1%).

A total of 52 patients (9.6%) experienced treatment related AEs leading to discontinuation of study treatment.

5.5.1.2.7 Adverse Events that Led to Dose Modification

Overall, 407 patients (75.4%) experienced AEs leading to dose interruptions. The most frequently reported AEs leading to dose interruptions (occurring in ≥5%) were anemia (15.4%), pneumonia (11.7%), neutropenia (10.2%), pneumonitis and neutrophil count decreased (8.5% each), hypertension (8.1%), blood creatine phosphokinase increased (7.8%), COVID-19 (6.1%), pyrexia (5.7%), and aspartate aminotransferase increased (5.4%).

Overall, 283 patients (52.4%) experienced AEs leading to dose reductions. The most frequently reported AEs leading to dose reductions (occurring in ≥5%) were anemia (11.3%), neutropenia (8.5%), neutrophil count decreased (7.8%), pneumonitis (6.1%) and blood creatine phosphokinase increased (5.6%) and hypertension (5.0%).

5.5.1.2.8 Selected Adverse Events

Anemia

Overall 294/540 (54.4%) patients treated at 400 mg QD, experienced events of anemia (referred to as grouped anemia events). A total of 286 patients (53.0%) experienced PT anaemia, 12 patients (2.2%) experienced PT hemoglobin decreased, and 2 patients each (<1%) experienced PTs hematocrit decreased and red blood cell count decreased. No other PTs were reported in more than a single patient. A total of 220 patients (40.7%) experienced grouped anemia events that were assessed as related to pralsetinib. Serious grouped anemia events were reported in 32 patients (5.9%), and 19 (3.5%) such events (all PT anemia) were assessed as related to pralsetinib. Study treatment discontinuations due to grouped anemia events took place for 7 patients (1.3%) (PT anaemia). Overall, there were no clinically meaningful differences between cancer patients treated at 400 mg QD (N=540) and patients in the overall safety population (N=590).

Neutropenia

Overall, 258/540 patients (47.8%) experienced events of grouped neutropenia. A total of 147 patients (27.2%) experienced PT neutrophil count decreased, and 128 (23.7%) experienced PT neutropenia. A total of 242 patients (44.8%) experienced grouped neutropenia events that were assessed as related to pralsetinib. Serious grouped neutropenia events were reported in 9 patients (1.7%), of whom 8/540 patients (1.5%) had neutropenia SAEs that were assessed as related to pralsetinib. Study treatment discontinuations due to grouped neutropenia events took place in 2 patients (<1%) for neutropenia and 2 patients (<1%) for neutrophil count decreased.

An additional 8 patients (1.5%) experienced febrile neutropenia, of which 7 patients experienced febrile neutropenia events that were assessed as related to pralsetinib. Of the 8 patients with febrile neutropenia, 5 patients (<1%) experienced Grade 3 febrile neutropenia events, 2 (<1%) experienced Grade 4 febrile neutropenia events, and no patients experienced Grade 5 febrile neutropenia events. Five patients (<1%) experienced serious febrile neutropenia.One patient (<1%) experienced an event of febrile neutropenia that led to permanent discontinuation of pralsetinib.

Overall, there were no clinically meaningful differences between cancer patients treated at 400 mg QD (n=540) and patients in the overall safety population (n=590).

Lymphopenia

Overall, 150/540 patients (27.8%) experienced grouped lymphopenia AEs. A total of 90 patients (16.7%) experienced lymphocyte count decreased, and 68 patients (12.6%) experienced lymphopenia. A total of 116 patients (21.5%) experienced grouped lymphopenia events that were assessed as related to pralsetinib. Serious grouped lymphopenia events were reported in 3 patients (<1%), and 1 patient experienced an SAE of lymphopenia that was assessed as related to pralsetinib. Study treatment

discontinuations due to grouped lymphopenia (PTs: lymphopenia and lymphocyte count decreased) events tookplace in 1patient (<1%).

Overall, there were no clinically meaningful differences between cancer patients treated at 400 mg QD (N=540) and patients in the overall safety population (N=590).

Thrombocytopenia

Overall, 107/540 patients (19.8%) experienced grouped thrombocytopenia events. A total of 67 patients (12.4%) experienced PT platelet count decreased and 44 patients (8.1%) experienced PT thrombocytopenia. A total of 88 patients (16.3%) experienced grouped thrombocytopenia events that were assessed as related to pralsetinib. Serious grouped thrombocytopenia events were reported in 6 patients (1.1%), and all events were assessed as related to pralsetinib. Study treatment discontinuations due to grouped thrombocytopenia events took place for 3 patients (<1%) (PT thrombocytopenia in 2 patients, PT Platelet count decreased in 1 patient).

Overall, there were no clinically meaningful differences between cancer patients treated at 400 mg QD (N=540) and patients in the overall safety population (N=590).

5.5.1.2.9 Effects on Cardiac Depolarization/ Repolarization

Evaluation of Pralsetinib on QTc

The potential for pralsetinib to prolong the QT interval corrected for heart rate (QTc) was evaluated as a secondary objective of Study BO42863, and was analyzed for a subset of patients from all indications (i.e., patients with advanced, unresectable, RET-fusion NSCLC, MTC, and other RET-altered solid tumors). Patients were excluded from the study, according to predefined exclusion criteria, if they had a QTc corrected for heart rate by the Fridericia method (QTcF) value of>470 ms, uncontrolled cardiovascular disease, or poorly controlled hypertension. Cardiodynamic ECG assessments were analyzed in a subset of 34 patients treated with pralsetinib 400 mg QD in Phase 2 of Study BO42863 (expansion phase) to evaluate the effect of pralsetinib on QTcF and other ECG parameters (i.e., heart rate, PR interval, and QRS duration). Continuous 12-lead Holter ECG recordings and plasma samples were taken in triplicate at predefined time points in Cycle 1, relative to administration of pralsetinib.

Overall, 34/540 patients (6.3%) treated at 400 mg QD in the safety population experienced grouped events of QT prolongation. The most frequently reported PT was Electrocardiogram QT prolonged (33 patients [6.1%]) and 1 patient (<1%) experienced PT long QT syndrome. A total of 23 patients (4.3%) experienced grouped QT prolongation events that were assessed as related to pralsetinib. Two patients (<1%) experienced Grade 3 events and no patients experienced Grade 4 or Grade 5 events. A total of 2 patients (<1%) experienced serious QT prolongation events, of which both patients experienced events that were assessed as related to pralsetinib. No patients discontinued from study treatment due to grouped QT prolongation events.

Within the BLU-667-1101 Phase 1/2 study, there was a separate ECG sub-study on 34 patients to characterize the PK profile of BLU-667 and to assess the relationship between drug exposure and QT interval. The primary outcome measure for cardiac safety was an analysis of the regression relationship between ΔQTcF and the plasma concentration of pralsetinib at matching times postdose.

The endpoint outcome was defined by a comparison to 20 ms of the upper bounds of the 2-sided 90% confidence intervals (CIs; equivalent to 1-sided 95% upper confidence bounds) at the geometric mean C_{max} for pralsetinib with the 400 mg QD dose.

Pralsetinib did not result in clinically relevant prolongation of the QTcF interval at steady-state plasma concentrations after administration at a dose of 400 mg QD. The mean baseline QTcF (on Day 1) was 416.0 ms. On Day 15 (steady-state), the mean change from baseline in QTcF (ΔQTcF) was 5.6 ms at the predose time point, and above 5 ms at all postdose time points except 4 hours (1.0 ms), 8 hours (4.9 ms), and 24 hours (predose) (1.5 ms). The largest mean ΔQTcF was observed at 1 hour (7.7 ms) postdose.

No clinically relevant QTcF outlier values were found, further supporting the primary conclusion of no QT prolongation.

A linear model provided the best fit for the data, with a linear slope of -0.0003 ms/ng/mL and a p-value of 0.841, which was not significantly different from a slope of 0 and had no clinical relevance.

The validity of the model was not affected by hysteresis, HR effects, or effects due to QTcF correction. Linear criteria were superior to higher order fits. Goodness-of-fit plots supported the linear model fit as appropriate. Thus, the primary outcome measure indicated that pralsetinib had no clinically meaningful QTc interval prolongation.

5.5.2 Study BO42864: AcceleRET-Lung Study

BO42864 (AcceleRET-Lung) is a Phase III, randomized, open-label study designed to assess whether pralsetinib improves progression-free survival (PFS) as compared to Investigator's choice platinum-containing chemotherapy regimen with or without pembrolizumab for patients with RET fusion-positive metastatic NSCLC. A total of 226 patients are planned to be randomized (1:1) to receive either 400 mg PO QD pralsetinib (Arm A) or Investigator's choice platinum-containing chemotherapy regimen (chosen from a list of standard of care treatments, per protocol; Arm B) either with or without pembrolizumab.

The first patient was dosed on 29 July 2020 in Study BO42864.

The Sponsor decided to prematurely terminate Study BO42864 (AcceleRET-Lung) as a result of Blueprint Medicines' decision to discontinue global marketing and development

of Gavreto in all territories (excluding the United States and Greater China), as announced by Blueprint Medicines' during the JP Morgan 42nd Annual Healthcare conference. Blueprint Medicines' decision follows Roche's earlier decision to terminate its global collaboration with Blueprint Medicines to commercialize Gavreto worldwide, effective February 2024, after which Roche would no longer have rights to Gavreto. The decision to terminate Study BO42864 was not taken for any efficacy, safety, or quality reasons.

Patients who are still receiving treatment as decided by the investigator will be transitioned into a Post-Trial Access Program or Continued Access Solution.

In the course of signal management, a comparative analysis of severe infections between the pralsetinib and the SOC treatment arms resulted in the re-categorization of severe infection from a potential risk to an important identified risk. This signal assessment outcome occurred on 9 October 2024 and further details are included in Section 6.3 and Section 6.4.

5.5.3 Study BO41932: TAPISTRY Study

BO41932 (TAPISTRY) is a non-randomized, open-label, multi-cohort, non-controlled, Tumor-Agnostic Precision Immuno-oncology and Somatic Targeting Rational for You (TAPISTRY) Phase II platform trial. The first patient was dosed on 4 November 2021. As of the data cut-off date of this IB, no new risks have been identified.

The Sponsor decided to end enrollment in Cohort K (pralsetinib) of the BO41932 study for the reasons outlined in Section 5.5.2. This decision was not taken for any efficacy, safety, or quality reasons.

Patients currently still receieivng treatment as decided by the investigator will be transitioned into a Post-Trial Access Program or Continued Access Solution.

5.5.4 Study ML42439: MyTACTIC Study (Arm O)

5.5.4.1 Overview of Adverse Events

No new safety signals were identified for pralsetinib in patients with *RET* fusion –positive tumors. All patients (3/3, 100%) in Arm O experienced at least one AE. All 3 patients (100%) experienced at least one AE that was considered by the investigator as related to study treatment. An AE with fatal outcome was reported in 1 patient (33.3%); this event was not considered by the investigator as related to study treatment. In total, serious adverse events (SAEs) were reported in 2 patients (66.7%). A total of 2 patients (66.7%) experienced AEs leading to withdrawal from study treatment. An overview of the key safety results for patients in Arm O is provided in Table 27.

Table 27 Overall Safety Summary (MyTACTIC Study Arm O)

Overview of Key Adverse Events
Safety-Evaluable Patients, ARM O: Pralsetinib
Protocol: ML42439

	ARM O: PRALS (N=3)
Total number of patients with at least one AE	3 (100%)
Total number of AEs	51
Total number of deaths [1]	1 (33.3%)
Total number of patients withdrawn from study due to an AE [2]	0
Total number of patients with at least one	
AE with fatal outcome	1 (33.3%)
AE leading to withdrawal from treatment	2 (66.7%)
AE leading to dose modification/interruption	3 (100%)
Serious AE	2 (66.7%)
Related AE	3 (100%)
Related Serious AE	0
Serious AE leading to withdrawal from treatment	1 (33.3%)
Serious AE leading to dose modification/interruption	1 (33.3%)
Related AE leading to withdrawal from treatment	1 (33.3%)
Related AE leading to dose modification/interruption	3 (100%)
Grade 3/4 AE	3 (100%)
Related Grade 3/4 AE	3 (100%)
Grade 5 AE	1 (33.3%)
Related Grade 5 AE	0

Investigator text for AEs is coded using MedDRA version 26.1. Percentages are based on N in the column headings. Multiple occurrences of the same AE in one individual are counted only once except for "Total number of AEs" row in which multiple occurrences of the same AE are counted separately.
[1] Data from AE records, Long-Term Survival Follow-up, Death Attributed to Progressive Disease and Public Records.
[2] Data as collected in the "Disposition" page of the eCRF. This does not include patients who discontinued from the study with the reason given as death.
DBL Date: 12Mar2024

Program:
root/clinical_studies/RO4368451/CDT90032/ML42439/data_analysis/csr/prod/program/t_ae_summ.sas
Output:
root/clinical_studies/RO4368451/CDT90032/ML42439/data_analysis/csr/prod/output/t_ae_summ_ARMO_SE_12Mar2024_42439.out
22MAR2024 23:17 Page 1 of 1

5.5.4.2 Adverse Events Related to Treatment

All 3 patients (100%) in Arm O experienced at least one AE that was considered by the investigator as related to study treatment. The most frequently reported AEs related to treatment by SOC (≥2 patients) were gastrointestinal disorders (2 patients, 66.7%), investigations (2 patients, 66.7%), and nervous system disorders (2 patients, 66.7%). The most frequent related AE by PT was diarrhoea (2 patients, 66.7%).

5.5.4.3 Adverse Events by Intensity

All patients (3/3, 100%) in Arm O experienced AEs of Grade 3–5 as highest severity, according to the NCI CTCAE v5.0, including 1 patient (33.3%) who experienced a Grade 5 AE. There were no patients with Grade 4 AEs in Arm O of the study.

5.5.4.4 Deaths

One out of 3 patients (33.3%) in Arm O died due to an AE. This death was reported at study discontinuation. The patient experienced a Grade 5 AE of brain oedema that was not considered by the investigator as related to study treatment.

5.5.4.5 Serious Adverse Events

Overall, 2 patients (66.7%) in Arm O experienced at least one SAE during the study. The reported SAEs by SOC were blood and lymphatic system disorders (1 patient, 33.3%), gastrointestinal disorders (1 patient, 33.3%), infections and infestations (1 patient, 33.3%), and nervous system disorders (1 patient, 33.3%). All reported SAEs by PTs (anaemia, brain oedema, clostridium difficile infection, colonic abscess, diarrhoea and seizure) occurred in single patients. There were no SAEs that were considered by the investigator as related to study treatment reported in Arm O of the study. One patient (33.3%) experienced at least one SAE that led to withdrawal from treatment and one patient (33.3%) experienced at least one SAE that led to dose modification or interruption of the study treatment.

5.5.4.6 Adverse Events That Led to Withdrawal of Treatment

There were 2 patients (66.7%) in Arm O who experienced at least one AE leading to withdrawal of treatment during the study. The reported AEs leading to withdrawal of treatment by SOC were blood and lymphatic system disorders (1 patient, 33.3%) and nervous system disorders (1 patient, 33.3%). The reported AEs leading to withdrawal of treatment by PT were anaemia, brain oedema, and cognitive disorder (1 patient, 33.3% each).

5.5.4.7 Adverse Events That Led to Dose Modification or Interruption

All patients (3/3, 100%) in Arm O experienced at least one AE leading to dose modification or interruption of the study treatment during the study. The most frequently reported AEs leading to dose modification or interruption of the study treatment by SOC ($\geq$2 patients) were gastrointestinal disorders (2 patients, 66.7%) and nervous system disorders (2 patients, 66.7%). The most frequently reported AE leading to dose modification or interruption of the study treatment by PT ($\geq$2 patients) was diarrhoea (2 patients, 66.7%).

5.5.4.8 Other Safety Evaluation

The majority of patients in Arm O had no shifts from baseline in hematology and chemistry parameters. Of the patients with shifts in grade, most results remained $\leq$Grade 2. Vital sign parameters with values outside of normal limits were observed in some patients. The parameters with the most frequently reported values outside of normal limits ($>$1 patient) were high diastolic blood pressure (3/3 patients, 100%), low temperature (3/3 patients, 100%), and high systolic blood pressure (2/3 patients, 66.7%).

5.5.5 Pre-approval Access Program and Individual INDs

A total of 393 patients who have RET fusion-positive or RET-altered cancers and are either ineligible or are otherwise unable to access an ongoing pralsetinib clinical trial have been treated with pralsetinib as part of a PAAP and individual INDs under the CUP, of whom 2 patients received pralsetinib in combination with osimertinib and 1 patient received pralsetinib in combination with gefitinib as of 18 December 2021.

5.6 MARKETING EXPERIENCE

GAVRETO (pralsetinib) was first granted marketing approval in the U.S. on 4 September 2020, which marks its international birth date (IBD). GAVRETO was then further approved in over 60 countries worldwide, most of which are now discontinuing the commercialization of the product for commercial reasons. Since the marketing authorization, overall reported AEs have been consistent with the known safety profile of pralsetinib; no new risks have been identified in the post-marketing setting.

Since the IBD (4 September 2020), an estimated cumulative total of 2,322 patients have received GAVRETO from marketing experience.

6. GUIDANCE FOR THE INVESTIGATOR (INCLUDING REFERENCE SAFETY INFORMATION)

Investigators should also consult the local prescribing information if the IMP is approved in your country.

6.1 APPROVED INDICATIONS

The following indications are approved:

- Gavreto is indicated for the treatment of adult patients with RET fusion-positive, locally advanced or metastatic NSCLC.
- Gavreto is indicated for the treatment of adult and pediatric patients 12 years of age and older with locally advanced or metastatic RET-mutant MTC who require systemic therapy.
- Gavreto is indicated for the treatment of adult and pediatric patients 12 years of age and older with locally advanced or metastatic RET fusion-positive thyroid cancer who require systemic therapy and who are radioactive iodine-refractory (if radioactive iodine is appropriate).

The indication wording is based on the Core Data Sheet (CDS). Exact wording may vary from country to country.

6.2 CONTRAINDICATIONS

Pralsetinib is contraindicated in patients with a known hypersensitivity to pralsetinib or any of the excipients.

6.3 WARNINGS AND PRECAUTIONS

The warnings and precautions for pralsetinib are listed below. When pralsetinib is used with other drug(s), the Warnings and Precautions of the other drug(s) must also be consulted.

Pneumonitis/Interstitial Lung Disease

Cases of severe, life-threatening, and fatal pneumonitis/interstitial lung disease (ILD) have been reported in clinical trials with pralsetinib. Refer to Section 6.4 for information on this risk. Patients should be monitored for acute or worsening of pulmonary symptoms indicative of pneumonitis/ILD (e.g., dyspnea, cough, and fever). Dose modification and withdrawal criteria are included in the study protocols for confirmed pneumonitis/ILD.

Severe Infections

Pralsetinib can cause severe infections, including fatal and opportunistic infections. Refer to Section 6.4 for information on this risk. Patients should be monitored for signs and symptoms of infection and treated appropriately. Based on the severity of infection, pralsetinib should be withheld, dose reduced, or permanently discontinued. Guidance for

AE management (including dose modification guidelines for infections) is provided in the study protocols.

Hypertension

Hypertension has been reported in clinical trials with pralsetinib. Refer to Section 6.4 for information on this risk. Pralsetinib should not be initiated in patients with uncontrolled hypertension. Blood pressure should be monitored as specified in the study protocols. Standard of care (SOC) anti-hypertensive therapy should be initiated or adjusted as appropriate. Guidance for AE management (dose modification guidelines for non-hematologic toxicity) is provided in the study protocols.

Hepatic Transminase Elevations

Severe hepatic laboratory abnormalities including increased AST and increased ALT have been reported in clinical trials with pralsetinib. Refer to Section 6.4 for information on this risk. AST and ALT should be monitored as specified in the study protocols. Guidance for AE management (dose modification guidelines for non-hematologic toxicity) is provided in the study protocols.

Hemorrhagic events

Severe, including fatal, hemorrhagic events have been reported in clinical trials with pralsetinib. Refer to Section 6.4 for information on this risk. Guidance for AE management (dose modification guidelines for non-hematologic toxicity) is provided in the study protocols.

Embryo-Fetal Toxicity

Based on findings from animal studies and its mechanism of action, pralsetinib has the potential to cause fetal harm when administered to pregnant females. There are no available data on the use of pralsetinib in pregnant women. Oral administration of pralsetinib to pregnant rats during the period of organogenesis resulted in malformations and embryolethality at maternal exposures below the human exposure at the recommended clinical dose of 400 mg once daily.

Female patients of reproductive potential must use effective non-hormonal contraception during treatment with pralsetinib and for 2 weeks after the final dose. Pralsetinib may render hormonal contraceptives ineffective.

Male patients with female partners of reproductive potential must either abstain from sexual intercourse or use effective contraception, including a barrier method, during treatment with pralsetinib and for at least 1 week after the final dose.

6.4 IDENTIFIED RISKS AND ADVERSE DRUG REACTIONS

Identified Risks

The classification of an AE as an adverse drug reaction (ADR; identified risk) is based on the data available at the time of assessment. Data obtained at later dates (e.g., following unblinding of a Phase III trial) may refute the connection between an AE and pralsetinib, and lead to an ADR being subsequently reclassified as an AE, or confirm the association between an AE and pralsetinib, and cause the AE to be reclassified as an ADR. Descriptions of the important identified risks are summarized in Table 28, including population exposed to pralsetinib, and intensity and frequency of the risk.

Table 28 Summary of Important Identified Risks

Risk	Description of Risk
Pneumonitis	Pneumonitis is considered a class effect of TKIs (Abdel-Rahman and Fouad 2016; Nishino et.al. 2017). In the pivotal pralsetinib study BO42863, in the overall safety population treated with 400 mg QD pralsetinib (N=540) at a median treatment duration of 15.8 months, events of pneumonitis (including interstitial lung disease) occurred in 12.2% of patients, with a median time to onset of 16.1 weeks. Across indications the reporting rate was 14.2%, 9.7%, and 19.4% of patients with RET fusion-positive advanced NSCLC, RET mutation-positive MTC, and RET fusion positive thyroid cancer, respectively (who received treatment with pralsetinib 400 mg QD). A total of 60 patients (11.1%) experienced grouped pneumonitis events that were assessed as related to pralsetinib (investigator assessed). In 31/540 (5.7%) patients, a pneumonitis event was reported as serious. The majority of patients had mild (Grade 1 or 2) pneumonitis. For 19/540 (3.5%) patients, the pneumonitis event was of Grade ≥3 severity, mainly Grade 3 (15/540 [2.8%]). The majority of patients (45/66, 68.2%) had at least one pneumonitis event that resolved and 17/66 (25.8%) patients had at least one pneumonitis event that remained unresolved at time of data cut-off (4 March 2022). For 1 patient the pneumonitis event had a fatal outcome. Patients at risk for development of pneumonitis, are those who have medical history of pneumonitis, or prior therapy with external beam radiation to the chest/back/spine area. Early diagnosis and proper management could decrease mortality and morbidity. The diagnosis of pneumonitis and determination of causal relationship to the drug is often confounded by the underlying disease (especially lymphangitic carcinomatosis) and other factors such as lung infection and radiation effect due to non-specific signs and symptoms as well as similar radiological appearance.
Hypertension	Hypertension is attributed to be an off-target pharmacologic effect of pralsetinib on VEGFR. The nonclinical studies showed that pralsetinib doses ≥ 25 mg/kg resulted in increased blood pressure in rats. These findings were confirmed in the clinical setting, where patients within the overall 400 mg QD safety population had very commonly events of hypertension (grouped events including events of hypertension and blood pressure increased); hypertension was commonly reported across indications. In the pivotal study BO42863, 189/540 (35.0%) patients experienced hypertension events. Median time to onset of hypertension was 2.1 weeks. A total of 26.7% of patients experienced grouped events of hypertension that were assessed as related to pralsetinib. Of all patients, 95/540 (17.6%) had Grade ≥3 AEs. No Grade 4 or Grade 5 hypertension events were reported. The majority of patients (117/189, 61.9%) had at least one hypertension event that resolved, and 89/189 (47.1%) patients had at least one hypertension event that remained unresolved at the time of data cut-off (4 March 2022). Hypertension seen in the pralsetinib clinical programme was routinely managed by SOC anti-hypertensive treatments and did not lead to any significant clinical outcomes.

Risk	Description of Risk
Hemorrhage	The exact mechanism of action is unknown. Gastrointestinal epithelial erosion and ulceration has been observed in animal studies and described as secondary to VEGFR inhibition. In clinical trial data from BO42863 hemorrhage, including severe (Grade 3-5) hemorrhagic events have been observed. In the pivotal study BO42863, 111/540 patients (20.6%) experienced at least one haemorrhagic event. Median time to onset was 11.6 weeks. A total of 4.4% of patients experienced grouped haemorrhagic events that were assessed as related to pralsetinib. The haemorrhagic events were of Grade 1 intensity in the majority of these patients (14.3%). Severe (Grade ≥3) haemorrhagic events were experienced by 22 patients (4.1%), most commonly reported was gastrointestinal haemorrhage (4 patients), and haematoma (3 patients). One of the severe haemorrhagic events was a Grade 5 event. A total of 19 of the 22 patients (86.4%) who experienced severe (Grade ≥3) hemorrhagic events, had at least one severe hemorrhagic event which resolved and 3/22 patients (13.6%) had a severe hemorrhagic event that remained unresolved at time of data cut-off (4 March 2022).
Severe Infections	The finding in nonclinical studies of hematological abnormalities due to JAK2 inhibition indicates that pralsetinib is likely to be associated with an increased risk of infections, which may be severe. Additionally, patients may be immunocompromised due to prior treatment or the underlying malignancy. A significantly higher risk of severe infection with pralsetinib versus standard of care (SOC) chemotherapy was observed in the randomized clinical trial, Study BO42864. At the time of an ad-hoc review of severe infections in Study BO42864, 212 patients had received any amount of any study treatment, 108 patients in the pralsetinib arm, and 104 patients in the SOC arm. Fatal infection events occurred in 5 patients (4.6%) in the pralsetinib arm, and none in the SOC chemotherapy arm.

Risk	Description of Risk
	Severe (Grade 3-5) infection events occurred in 28 (25.9%) pralsetinib treated patients versus 8 (7.7%) patients receiving SOC. Statistical analysis on severe infection adverse events demonstrated a significant imbalance between treatment arms, with Fisher's exact two-tailed p-value of 0.0004. The risk ratio of severe infection with pralsetinib versus SOC was 3.33 (95% CI: [1.57, 7.06], Aalen-Johansen estimator, [Stegherr et al. 2021]), indicating a significantly higher risk of severe infection with pralsetinib. COVID-19 events and any adverse events that happened after SOC patients crossed over to pralsetinib were excluded from these analyses. An analysis of neutropenia and lymphopenia in Study BO42864 suggested that these events do not appear to account for the higher risk of severe infection in pralsetinib-treated patients. The majority (22/28) of pralsetinib-treated patients with severe infections did not present with any neutropenia/neutrophil count decreased or lymphopenia/lymphocyte count decreased adverse events prior to the onset of severe infections. The median time to first onset of severe infection in the pralsetinib arm was 66.5 days. Approximately half of the severe infections were lung infections. Within severe infections, opportunistic infections, including pneumocystis jirovecii pneumonia, cytomegalovirus pneumonia, legionella pneumonia, bronchopulmonary aspergillosis, and esophageal candidiasis occurred in 7 (6.5%) patients in the pralsetinib arm, and in 0 patients in the SOC arm. Of the 7 patients who developed opportunistic infections, 2/7 patients had been taking systemic corticosteroids prior to the onset of the infection. From this analysis, prior corticosteroid use does not appear to be a significant risk factor for the development of severe opportunistic infections in pralsetinib-treated patients in AcceleRET-Lung study (Study BO42864). The ARROW study (BO48263, without comparator) showed an incidence of 3.2% for patients with fatal infection AEs while 24.4% for patients with Grade 3-4 infection events.

AEs = adverse events; COVID-19 = Coronavirus disease 2019; QD = once daily; SOC = standard of care; TKI = tyrosine kinase inhibitor; JAK = Janus kinase; VEGFR = vascular endothelial growth factor receptor.

MedDRA versions: 19.1 (Study BO42863) and 27.0 (Study BO42864)

Note: Severe infections were re-categorized from important potential risk to important identified risk on 09 Oct 2024, mainly based on data from the AcceleRET-Lung study (BO42864).

A summary of ADRs occurring in patients treated with pralsetinib in clinical trials is shown in Table 29 and Table 30. These tables are based on 540 patients enrolled into study BO42863 and treated with pralsetinib 400 mg QD.

Table 29 Summary of Adverse Drug Reactions Occurring in Patients Treated with Pralsetinib (400 mg QD) in the ARROW Study (safety population)

System Organ Class Adverse reaction	Frequency category (All Grades)	Pralsetinib (N=540) All Grades (%)	 Grades 3–4 (%)
Blood and Lymphatic System Disorders			
Anemia[1]	very common	53.0	22.4
Neutropenia[2]	very common	46.7	21.1
Leukopenia[3]	very common	37.0	8.9
Lymphopenia[4]	very common	26.9	17.4
Thrombocytopenia[5]	very common	19.6	4.8
Gastrointestinal disorders			
Constipation	very common	43.9	0.6
Diarrhea	very common	33.1	3.1
Nausea	very common	19.6	0.2
Abdominal pain[6]	very common	17.8	1.5
Dry mouth	very common	16.5	0
Vomiting	very common	14.8	1.1
Stomatitis[7]	common	6.9	1.3
General Disorders and Administration Site Conditions			
Fatigue[8]	very common	42.2	4.1°
Edema[9]	very common	31.5	0.2
Pyrexia	very common	27.8	1.5
Hepatobiliary Disorders			
Aspartate aminotransferase increased	very common	49.1	6.9
Alanine aminotransferase increased	very common	37.0	4.8
Infection and Infestations			
Pneumonia[10]	very common	22.4	13.1#
Urinary tract infection	very common	14.8	4.4°
Musculoskeletal and Connective Tissue Disorders			
Musculoskeletal pain[11]	very common	44.4	2.6
Blood creatine phosphokinase increased	very common	16.7	7.6
Nervous system disorders			
Headache[12]	very common	18.0	0.6
Taste disorder[13]	very common	16.7	0

System Organ Class Adverse reaction	Frequency category (All Grades)	Pralsetinib (N=540) All Grades (%)	 Grades 3–4 (%)
Renal and Urinary Disorders			
Blood creatinine increased	very common	25.4	0.6
Respiratory, thoracic and mediastinal disorders			
Cough[14]	very common	28.1	0.6
Dyspnea	very common	20.4	2.0#°
Pneumonitis[15]	very common	12.2	3.3°
Skin and subcutaneous tissue disorders			
Rash[16]	very common	19.1	0
Vascular Disorders			
Hypertension[17]	very common	35.0	17.6
Hemorrhage[18]	very common	20.6	3.9°

Data cutoff 04 March 2022:

[1] Includes the preferred terms: Anaemia, Red blood cell count decreased, Aplastic anaemia, Haematocrit decreased, Haemoglobin decreased

[2] Includes the preferred terms: Neutropenia, Neutrophil count decreased

[3] Includes the preferred terms: Leukopenia, White blood cell count decreased

[4] Includes the preferred terms: Lymphopenia, Lymphocyte count decreased

[5] Includes the preferred terms: Thrombocytopenia, Platelet count decreased

[6] Includes the preferred terms: Abdominal pain, Abdominal pain upper

[7] Includes the preferred terms: Stomatitis, Aphthous ulcer

[8] Includes the preferred terms: Fatigue, Asthenia

[9] Includes the preferred terms: Oedema, Swelling face, Peripheral swelling, Generalised oedema, Oedema peripheral, Face oedema, Periorbital oedema, Eyelid oedema, Swelling, Localised oedema

[10] Includes the preferred terms: Pneumonia, Pneumocystis jirovecii pneumonia, Pneumonia cytomegaloviral, Atypical pneumonia, Lung infection, Pneumonia bacterial, Pneumonia haemophilus, Pneumonia influenzal, Pneumonia streptococcal, Pneumonia moraxella, Pneumonia staphylococcal, Pneumonia viral, Pneumonia Escherichia, Pneumonia pseudomonal

[11] Includes the preferred terms: Myalgia, Arthralgia, Pain in extremity, Neck pain, Musculoskeletal pain, Back pain, Musculoskeletal chest pain, Bone pain, Spinal pain, Musculoskeletal stiffness

[12] Includes the preferred terms: Dysgeusia, Ageusia

[13] Includes the preferred terms: Headache, Tension Headache

[14] Includes the preferred terms: Cough, Productive Cough

[15] Includes the preferred terms: Pneumonitis, Interstitial lung disease

[16] Includes the preferred terms: Rash, Rash maculo-papular, Dermatitis acneiform, Erythema, Rash generalised, Rash papular, Rash pustular, Rash macular, Rash erythematous

[17] Includes the preferred terms: Hypertension, Blood pressure increased

[18] Includes the preferred terms identified using the MedDRA 19.1 SMQ Haemorrhage (excl laboratory terms) narrow, with the exclusion of terms related to invasive drug administration, terms related to rupture, disseminated intravascular coagulopathy, term related to traumatic haemorrhages, and haemorrhagic terms related to pregnancy, birth or neonatal

° Additionally, 1 (0.2%) Grade 5 event was reported.

Additionally, 12 (2.2%) Grade 5 events were reported.

Note: Additionally, 2 (0.4%) Grade 5 events were reported.

Table 30 Pralsetinib Treatment-Emergent Shifts of Key Laboratory Abnormalities Worsening from Baseline in ≥20% Patients who Received Pralsetinib 400 mg QD in the ARROW Study (Safety Population)

	Pralsetinib 400 mg QD N=540	
Laboratory Test Abnormality	**Worsen to Grade 1–4 (%)**	**Worsen to Grade 3–4 (%)**
Hematology		
Decreased Leukocytes	76.3	12.6
Decreased Hemoglobin	75.9	18.0
Decreased Lymphocytes	72.2	32.8
Decreased Neutrophils	66.3	20.2
Decreased Platelets	32.6	4.6
Chemistry		
Increased Aspartate Aminotransferase (AST)	79.8	7.0
Increased Alanine Aminotransferase (ALT)	59.4	5.7
Increased Creatinine	44.1	1.3
Increased Alkaline Phosphatase	37.0	2.4
Increased Bilirubin	22.6	2.4
Decreased Calcium Corrected	56.9	5.0
Decreased Albumin	49.6	1.7
Decreased Phosphate	44.3	13.3
Decreased Sodium	39.4	7.2

Data cutoff: 04 March 2022:

Clinically relevant laboratory abnormalities in < 20% of patients who received pralsetinib included increased phosphate (17.4%).

6.4.1 Reference Safety Information (Expected Serious Adverse Reactions)

When this Investigator's Brochure is used as the Reference Safety Information, it serves as basis for the expectedness assessment of serious adverse reactions (SARs) for pralsetinib. The Reference Safety Information is not a comprehensive description of the safety profile of the product but rather the subset of SARs of the product.

Since development in the more vulnerable pediatric population is starting, a separate RSI section is provided in Section 6.4.1.1 and Section 6.4.1.2 for adults and pediatrics, respectively.

Table 31 and Table 32 provide a list of the SARs considered “expected” for adult and pediatric patients, respectively, in regard to regulatory reporting purposes by the Sponsor. Fatal or life-threatening SARs are not considered expected for regulatory reporting purposes.

6.4.1.1 Adult Population

Table 31 lists all expected SARs for pralsetinib in adult patients. These SARs were selected based on individual and aggregate assessment, medical review, and prior reports of the adverse reactions (as MedDRA preferred terms) in clinical trials. Frequencies are based on pooled clinical trial data using only related serious adverse events as noted.

Table 31 Serious Adverse Reactions to Pralsetinib in Adult Patients Considered Expected for Safety Reporting Purposes

		Cumulative Clinical Trial Exposure (N = 765)		
		All SARs	**Fatal SARs**	**Life-threatening SARs**
System Organ Class	**SARs (MedDRA PT)**	**n*(%)**	**n*(%)**	**n*(%)**
Infections and infestations	Pneumonia	26 (3.4)	n/a	n/a
	Pneumocystis jirovecii pneumonia	7 (0.9)	n/a	n/a
	Urinary tract infection	4 (0.5)	n/a	n/a
	Sepsis	4 (0.5)	n/a	n/a
	Septic shock	2 (0.3)	n/a	n/a
	Urosepsis	2 (0.3)	n/a	n/a
Blood and lymphatic system disorders	Anaemia	20 (2.6)	n/a	n/a
	Neutropenia	9 (1.2)	n/a	n/a
	Thrombocytopenia	6 (0.8)	n/a	n/a
Vascular disorders	Hypertension	6 (0.8)	n/a	n/a
Respiratory, thoracic and mediastinal disorders	Pneumonitis	37 (4.8)	n/a	n/a
	Interstitial lung disease	7 (0.9)	n/a	n/a
Gastrointestinal disorders	Diarrhoea	8 (1.0)	n/a	n/a
	Constipation	3 (0.4)	n/a	n/a
	Stomatitis	3 (0.4)	n/a	n/a
	Aphthous ulcer	2 (0.3)	n/a	n/a
	Vomiting	2 (0.3)	n/a	n/a
General disorders and administration site conditions	Pyrexia	5 (0.7)	n/a	n/a
	Fatigue	2 (0.3)	n/a	n/a
Investigations	Blood creatine phosphokinase increased	4 (0.5)	n/a	n/a
	Platelet count decreased	4 (0.5)	n/a	n/a

		Cumulative Clinical Trial Exposure (N = 765)		
		All SARs	Fatal SARs	Life-threatening SARs
System Organ Class	SARs (MedDRA PT)	n*(%)	n*(%)	n*(%)
Metabolism and Nutrition Disorders	Hyponatraemia	3 (0.4)	n/a	n/a
	Hypophosphatemia	3 (0.4)	n/a	n/a

n* = number of patients who experienced the SAR; PT = preferred term; SAR = serious adverse reaction; MedDRA = Medical Dictionary for Regulatory Activities

n/a: fatal or life-threatening SAR are considered unexpected for regulatory reporting purposes

All fatal or life-threatening SARs are considered unexpected for regulatory reporting purposes

MedDRA version: 27.1

Cut-off date for data extraction: 03-Sep-2024

Exposure data dated 03-Sep-2024 from DSUR trial summary output (combined exposure from studies BO42863, BO42864, ML41591, ML42439, BO41932, JO43701 and JO43175).

Expected SARs added to this table since the last IB update are indicated in bold. Sepsis, Septic Shock and Urosepsis have been added because of the new important identified risk of severe infections

Dyspnoea has been removed as it no longer fulfilled the criteria for inclusion in this table.

6.4.1.2 Pediatric Population

At the time of completion of the Investigator's Brochure, no SARs have been identified (Table 32). Therefore, there are no serious expected adverse drug reactions for this molecule. Any treatment-emergent serious adverse event deemed related to the investigational medicinal product (IMP) will be reported as a suspected unexpected Serious Adverse Reaction (SUSAR).

Table 32 Serious Adverse Reactions to Pralsetinib Considered Expected for Safety Reporting Purposes in Pediatrics

System Organ Class	SARs (Preferred Term)	Cumulative Clinical Trial Exposure (N = 2)		
		All SARs n* (%)	Fatal SARs n* (%)	Life-threatening SARs n* (%)
No serious adverse reactions have been identified for pralsetinib in pediatric patients.				

n* = number of patients who experienced the SAR

All fatal or life-threatening SARs are considered unexpected for regulatory reporting purposes

Cut-off date for data extraction: 03-Sep-2024

SAR = serious adverse reaction; SOC = system organ class

6.5 POTENTIAL RISKS

Potential risks are provided in Table 33.

Table 33 Summary of Potential Risks

Risk	Description of Risk
Hepatotoxicity	The clinical studies with pralsetinib showed mainly mild or moderate, asymptomatic and transient hepatic laboratory abnormalities (Increased AST and ALT are considered ADRs for pralsetinib (see Table 29). No reported events met the criteria for Hy's law and no clinical evidence of drug induced liver injury occurred. Reported cases were often confounded by relevant medical history, concomitant use of hepatotoxic medication, concurrent bacteremia or disease progression with multifocal liver metastases. The potential risk of hepatotoxicity is based on high incidence of increased AST/increased ALT and on the Grade 3 and Grade 4 events observed in the clinical development program for pralsetinib.
Physeal Dysplasia	Physeal dysplasa originates from pralsetinib's mode of action and are attributed to off-target VEGFR inhibition (Patyna et. al. 2008; Chen and Cleck 2009; Fletcher et.al. 2010). In animal toxicology studies, effects on bone including physeal dysplasia in both rodents and non-human primate were observed at exposures (AUC_{0-24}) similar to clinical exposures at 400mg QD dose. As physeal injuries affect the growth plates of children and adolescents, physeal dysplasia is an important potential risk of pralsetinib in pediatrics and adolescent patients with open growth plates. Pediatric patients have not been studied to date. No events of physeal dysplasia occurred during the pralsetinib clinical trials. Growth plates in adolescent patients with open growth plates should be monitored by performing serial X-rays as indicated in the protocols. If an effect on growth plates is observed and causality is at least possibly related to pralsetinib, consider interrupting, dose reduction, and/or discontinuation of therapy based on the severity of any growth plate abnormalities.
Tumor Lysis Syndrome	TLS results from the rapid destruction of malignant cells and the abrupt release of intracellular ions, nucleic acids, proteins, and metabolites into the extracellular space. These can overwhelm the body's normal homeostatic mechanisms, causing life threatening metabolic derangments, and renal failure. Clinical trial data from study BO42863 revealed very few cases of TLS. TLS was experienced by two patients (both MTC, both Grade 3) during the dose escalation portion of Study BO42863. These patients received 300 mg QD and 100 mg BID pralsetinib, respectively. Patients were hospitalized and received TLS specific treatment. Pralsetinib dosing was interrupted and resumed at a reduced dose after resolution of the events. These cases were confounded, as a decrease of the tumor marker calcitonin prior to starting pralsetinib to a point of already potential ongoing tumor regression in one patient occurred, and increased creatine and phosphate levels, hyperuricaemia and intermittent diarrhea at baseline were present in the other patient. Within the safety population of Study BO42863, one patient (MTC), who started treatment with 300 mg QD, was reported with a serious Grade 4 TLS event. However, this event occurred on study day 1057, 19 days after treatment with pralsetinib was discontinued due to patient's disease progression.

Risk	Description of Risk
	Further, two patients treated with 400 mg pralsetinib QD were identified who met the criteria for laboratory TLS with two or more coinciding metabolic abnormalities at study Day 7. However, no clinical consequences were reported for these two patients as a result of the metabolic abnormalities. As pralsetinib through its inhibitory effect on FGFR may lead to hyperphosphatemia and many patients with MTC have hypocalcaemia as concurrent condition, evaluation of these parameter in the context of TLS may be confounded. A clear association of pralsetinib and TLS has not yet been established. Note: Severe infections have been removed from this table for Potential Risks and has now been included in Table 28 of Section 6.4 Identified Risks and Adverse Drug Reactions

ADRs = adverse drug reactions; AEs = adverse events; AUC_{0-24} = area under the plasma concentration versus time curve from 0 to 24 hours; BID = twice daily; FGFR = fibroblast growth factor receptor; JAK = Janus kinase; MTC = medullary thyroid cancer; QD = once daily; TLS = tumor lysis syndrome; UTI = urinary tract infection; VEGFR = vascular endothelial growth factor receptor.

MedDRA version: 19.1

6.6 SPECIAL PATIENT POPULATIONS

6.6.1 Pregnancy

A reproductive toxicology study with pralsetinib in humans has not been performed. However, based on the preclinical embryofetal development study in rats that demonstrated severe embryofetal toxicity at all dosage levels, patients should be advised that pralsetinib may be toxic to a developing fetus. No information is available on the safety or efficacy of pralsetinib in pregnant females. Pralsetinib should not be administered to pregnant women.

Females of childbearing potential must either abstain from heterosexual intercourse or use a highly effective method of non-hormonal contraception (CTFG 2014) prior to initiating treatment with pralsetinib until at least 14 days after the last dose of pralsetinib.

Males with female partners of reproductive potential must either abstain from sexual intercourse or must use an effective method of contraception, to include barrier contraception, when engaging in sexual intercourse during treatment with pralsetinib and until at least 7 days after the last dose of pralsetinib. Additional guidance is provided in the clinical study protocols.

6.6.2 Nursing Mothers

It is not known whether pralsetinib is excreted in human milk. Because many drugs are excreted in human milk and because of the potential for serious adverse drug reactions in nursing infants, pralsetinib should not be administered to nursing mothers.

6.6.3 Children

The use of pralsetinib in pediatric patients 12 years of age and older is supported by extrapolation of evidence from clinical trials in adults to pediatric population, based on population pharmacokinetic data demonstrating similar drug exposure in adults and pediatric patients.

Safety and efficacy in pediatric patients below the age of 12 years have not been established.

In nonclinical repeat-dose toxicology studies physeal dysplasia in non-human primates and increased physeal thickness and incisor tooth degeneration in rats were observed at exposures (AUC_{0-24}) similar to clinical exposures at the 400 mg QD dose.

Monitor growth plates in adolescent patients with open growth plates. Consider interrupting or discontinuing therapy based on the severity of any growth plate abnormalities and based on an individual risk-benefit assessment.

6.6.4 Geriatric Patients

The safety of pralsetinib has not been specifically tested in a geriatric population. However, through clinical trial exposure, 196 patients > 65 years old have received pralsetinib.

6.6.5 Hepatic Impairment

Based on a population pharmacokinetic analysis, Gavreto exposures were similar between 68 subjects with mild hepatic impairtment (total bilirubin within upper limit of normal [ULN] and AST > ULN or total bilirubin > 1 to 1.5 times ULN and any AST) and 624 subjects with normal hepatic function (total bilirubin and AST within ULN). Following a single oral dose of 200 mg pralsetinib there was no significant impact of moderate or severe hepatic impairment on pralsetinib PK. No dose adjustment is required for patients with mild, moderate (total bilirubin >1.5 to 3.0 times ULN and any AST), or severe (total bilirubin >3.0 times ULN and any AST) hepatic impairment.

6.7 CONCOMITANT USE WITH OTHER MEDICATIONS

6.7.1 Potential Impact of Other Drugs on Pharmacokinetics of Pralsetinib

Coadministration of a combined P-gp and strong CYP3A4 inhibitor, itraconazole 200 mg once daily, with a single pralsetinib 200 mg dose increased pralsetinib Cmax by 84% and AUC0-inf by 251%. Hence, avoid coadministration of pralsetinib with strong CYP3A4 inhibitors or combined P-gp and strong CYP3A4 inhibitors.

Coadministration of a CYP3A4 inducer, rifampin 600 mg once daily, with a single pralsetinib 400 mg dose decreased pralsetinib Cmax by 30% and AUC0-INF by 68%. Therefore, avoid coadministration of pralsetinib with strong CYP3A4 inducers.

Coadministration of a P-gp inhibitor, cyclosporine 600 mg single dose, with a single pralsetinib 200 mg dose increased pralsetinib Cmax by 48% and AUC0-inf by 81%. Therefore, avoid coadministration of pralsetinib with P-gp inhibitors.

6.7.2 Potential Impact of Pralsetinib on Pharmacokinetics of Other Drugs

Pralsetinib is a moderate direct inhibitor of human CYP2C8, CYP2C9, and CYP3A4/5 at clinically relevant concentrations. Pralsetinib was also a time dependent inhibitor of CYP3A4/5. Pralsetinib is an inducer of CYP2C8, CYP2C9, and CYP3A4/5 at clinically relevant concentrations.

Coadministration of pralsetinib with sensitive CYP2C8, CYP2C9, and CYP3A substrates may alter their plasma concentrations, hence should be used with caution during treatment with pralsetinib.

Pralsetinib inhibited the transport activities of human efflux transporters P-gp, BCRP, BSEP as well as uptake transporters OATP1B1, OATP1B3, OAT1, OAT3, MATE1, and MATE2-K. Therefore, pralsetinib may have the potential for PK drug interactions with substrates of these transporters.

Based on these findings, lists of specific medications and foods that are prohibited or to be used with caution during treatment with pralsetinib are included in the clinical protocols.

6.8 OVERDOSE

There is no experience with overdosage in human clinical trials with pralsetinib. Patients who experience overdose should be closely supervised and supportive care instituted. There is no specific antidote for overdose with pralsetinib.

7. REFERENCES

7.1 SPONSOR REPORTS

Clinical Study Report, BLU-667-0101 (BP42858): An Open-Label, Randomized, Single-Dose, 2-Way Crossover Study to Evaluate the Effect of Food on the Pharmacokinetics of Pralsetinib in Healthy Adult Subjects. January 2019.

Clinical Study Report, BLU-667-0102 (BP42859): An Open-Label, Randomized, Single-Dose, 2-Period Crossover, Bioequivalence Study Comparing Four 100 mg Tablets with Four 100 mg Capsules of Pralsetinib in Healthy Adult Subjects. June 2019.

Clinical Study Report, BLU-667-0103 (BP42860): A Phase 1, Open-Label Study to Assess the Absorption, Metabolism, Excretion, and Mass Balance of [14C]Pralsetinib Following a Single Oral Dose in Healthy Adult Male Subjects. December 2019.

Clinical Study Report, BLU-667-0104 (BP42861): A Two-Part, Open-Label, Fixed-Sequence Study to Evaluate the Effect of Multiple Doses of Itraconazole and Rifampin on the Single-Dose Pharmacokinetics of Pralsetinib in Healthy Adult Subjects. January 2020.

Clinical Study Report, BLU-667-0105 (BP42862): An Open-Label, Fixed-Sequence Study to Evaluate the Effect of Esomeprazole and Gastric pH-Altering on the Pharmacokinetics of Pralsetinib in Healthy Adult Subjects. January 2020.

Clinical Study Report 1 BLU-667-1101 (BO42863) - A Phase 1/2 Study Of The Highly-Selective Ret Inhibitor, Blu-667, In Patients With Thyroid Cancer, Non-Small Cell Lung Cancer (NSCLC) And Other Advanced Solid Tumors. February 2020. (Cutoff date: 18 Nov 2019).

Clinical Study Report 2 BLU-667-1101 (BO42863) - A Phase 1/2 Study Of The Highly-Selective Ret Inhibitor, Blu-667, In Patients With Thyroid Cancer, Non-Small Cell Lung Cancer (NSCLC) And Other Advanced Solid Tumors. June 2020 (Cutoff date: 13 Feb 2020).

Update Clincal Study Report – BO42863 – A Phase I/II Study of the Highly-selective RET Inhibitor, BLU-667, in Patients with Thyroid Cancer, Non-Small Cell Lung Cancer (NSCLC) and Other Advanced Solid Tumors. Report No. 1109798. October 2021 (Cutoff date: 12 April 2021).

Update Clincal Study Report – Study BO42863, formerly known as BLU-667-1101, A phase 1/2 study of the highly selective RET inhibitor, BLU-667, in patients with thyroid cancer, non-small cell lung cancer (NSCLC) and other advanced solid tumors. Report No. 1113097. August 2022 (Cutoff date: 4 March 2022).

7.2 LITERATURE REFERENCES

Abdel-Rahman O, Fouad M. Risk of cardiovascular toxicities in patients with solid tumors treated with sunitinib, axitinib, cediranib or regorafenib: An updated systematic review and comparative meta-analysis. Crit. Rev. Oncol Hematol 2014; 92:194–207.

American Thyroid Association (ATA) Guidelines Taskforce on Thyroid Nodules and Differentiated Thyroid Cancer, Cooper DS, Doherty GM, Haugen BR, Kloos RT, Lee SL, et al. Revised American Thyroid Association management guidelines for patients with thyroid nodules and differentiated thyroid cancer. Thyroid 2009;19(11):1167–214.

Antonescu CR, Suurmeijer AJH, Zhang L, Sung YS, Jungbluth AA, Travis WD, et al. Molecular characterization of inflammatory myofibroblastic tumors with frequent ALK and ROS1 gene fusions and rare novel RET rearrangement. Am J Surg Pathol 2015;39(7):957–67.

Ballerini P, Struski S, Cresson C, Prade N, Toujani S, Deswarte C, et al. RET fusion genes are associated with chronic myelomonocytic leukemia and enhance monocytic differentiation. Leukemia 2012;26(11):2384–9.

Bentzien F, Zuzow M, Heald N, Gibson A, Shi Y, Goon L, Yu P, Engst S, Zhang W, Huang D, et al. In vitro and in vivo activity of Cabozantinib cabozantinib (XL184), an inhibitor of RET, MET, and VEGFR2, in a model of medullary thyroid cancer. Thyroid 2013; 23, 1569–77.

Brown AP, Courtney CL, King LM, Groom SC, Graziano MJ. Cartilage dysplasia and tissue mineralization in the rat following administration of a FGF receptor tyrosine kinase inhibitor. Toxicol Pathol 2005;33(4):449–55.

Broxmeyer HE. Erythropoietin: multiple targets, actions, and modifying influences for biological and clinical consideration. J Exp Med 2013;210(2):205–8.

Carlomagno F, Salvatore D, Santoro M, de Franciscis V, Quadro L, Panariello L, Colantuoni V, and Fusco A. Point mutation of the RET proto-oncogene in the TT human medullary thyroid carcinoma cell line. Biochem Biophys Res Commun 1995;207, 1022–1028.

Carlomagno F, Guida T, Anaganti, S, Vecchio G, Fusco A, Ryan AJ, Billaud M, and Santoro M. Disease associated mutations at valine 804 in the RET receptor tyrosine kinase confer resistance to selective kinase inhibitors. Oncogene 2004;23, 6056–6063.

Chen HX, Cleck JN. Adverse effects of anticancer agents that target the VEGF pathway. Nat Rev Clin Oncol 2009;6(8):465–77.

Clinical Trial Facilitation Group. (2014) Recommendations related to contraception and pregnancy testing in clinical trials http://www.hma.eu/fileadmin/dateien/Human_Medicines/01-About_HMA/Working_Groups/CTFG/2014_09_HMA_CTFG_Contraception.pdf.

Cooley LD, Elder FF, Knuth A, and Gagel RF. Cytogenetic characterization of three human and three rat medullary thyroid carcinoma cell lines. Cancer Genet. Cytogenet. 1995;80, 138–149.

Costantini F and Shakya R. GDNF/RET Signaling and the Development of the Kidney. Bioessays 2006;28 (2): 117–127.

Donis-Keller H, Dou S, Chi D, Carlson KM, Toshima K, Lairmore TC, et al. Mutations in the RET proto-oncogene are associated with MEN 2A and FMTC. Hum Mol Genet 1993;2(7):851–6.

Drilon AE, Subbiah V, Oxnard GR, et al. A phase 1 study of LOXO-292, a potent and highly selective RET inhibitor, in patients with RET-altered cancers. J Clin Oncol 2018;36(15_suppl):102–102.

Everds NE, Snyder PW, Bailey KL, Bolon B, Creasy DM, Foley GL, et al. Interpreting stress responses during routine toxicity studies: a review of the biology, impact, and assessment. Toxicol Pathol 2013;41(4):560–614.

Fletcher AM, Bregman CL, Woicke J, Salcedo TW, Zidell RH, Janke HE, et al. Incisor degeneration in rats induced by vascular endothelial growth factor/fibroblast growth factor receptor tyrosine kinase inhibition. Toxicol Pathol 2010;38(2):267–79.

Frazier KS. Drug-induced Physeal Abnormalities in Preclinical Toxicity Studies. Toxicologic Pathology 2017;45(7):869-875.

Hall, AP, Mitchard T, Rolf MG, et al. Femoral head growth plate dysplasia and fracture in juvenile rabbits induced by off-target antiangiogenic treatment. Toxicol Pathol 2016;44:866–73.

Hofstra RM, Landsvater RM, Ceccherini I, Stulp RP, Stelwagen T, Luo Y, et al. A mutation in the RET proto-oncogene associated with multiple endocrine neoplasia type 2B and sporadic medullary thyroid carcinoma. Nature 1994;367(6461):375–6.

ICH (2010). Guidance for Industry: S9 Nonclinical Evaluation for Anticancer Pharmaceuticals.

ICH. Clinical Safety Data Management: Definitions and Standards for Expedited Reporting. 1994: International Conference on Harmonisation of Technical Requirements for Registration of Pharmaceuticals for Human Use [Online]. Accessed at: https://www.ich.org/fileadmin/Public_Web_Site/ICH_Products/Guidelines/Efficacy/E2A/Step4/E2A_Guideline.pdf.

Kang H, Tan M, Bishop JA, Jones S, Sausen M, Ha PK, et al. Whole-exome sequencing of salivary gland mucoepidermoid carcinoma. Clin Cancer Res 2017;23(1):283–8.

Kato S, Subbiah V, Marchlik E, Elkin SK, Carter JL, Kurzrock R. RET aberrations in diverse cancers: next-generation sequencing of 4,871 patients. Clin Cancer Res 2017;23(8):1988–97.

Kohno T, Ichikawa H, Totoki Y, Yasuda K, Hiramoto M, Nammo T, et al. KIF5B-RET fusions in lung adenocarcinoma. Nat Med 2012;18:375–7.

Lipson D, Capelletti M, Yelensky R, Otto G, Parker A, Jarosz M, et al. Identification of new ALK and RET gene fusions from colorectal and lung cancer biopsies. Nat Med 2012;18(3):382–4.

Manié S., Santoro M., Fusco A., and Billaud M. (2001). The RET receptor: function in development and dysfunction in congenital malformation. Trends Genet TIG 17, 580–589.

Medico E, Russo M, Picco G, Cancelliere C, Valtorta E, Corti G, et al. The molecular landscape of colorectal cancer cell lines unveils clinically actionable kinase targets. Nat Commun 2015;6:1–10.

Morris DL, O'Neil SP, Devraj RV, Portanova JP, Gilles RW, Gross CJ, et al. Acute lymphoid and gastrointestinal toxicity induced by selective p38alpha MAP kinase and MAP kinase-activated protein kinase-2 (MK2) inhibitors in the dog. Toxicol Pathol 2010:38(4):606–18.

Mulligan LM, Kwok JB, Healey CS, Elsdon MJ, Eng C, Gardner E, et al. Germ-line mutations of the RET proto-oncogene in multiple endocrine neoplasia type 2A. Nature 1993;363(6428):458–60.

Mulligan LM. RET revisited: expanding the oncogenic portfolio. Nat Rev Cancer 2014;14(3):173–86.

Nishino M, Hatabu H, Hodi FS, et al. Drug-related pneumonitis in the era of precision cancer therapy. JCO Precis Oncol 2017;(1):1–12.

Parganas E, Wang D, Stravopodis D, Topham DJ, Marine JC, Teglund S, et al. Jak2 is essential for signaling through a variety of cytokine receptors. Cell 1998;93(3):385–95.

Patyna S, Arrigoni C, Terron A, et al. Nonclinical safety evaluation of sunitinib: a potent inhibitor of VEGF, PDGF, KIT, FLT3, and RET receptors. Toxicol Pathol 2008;36(7):905–16.

Romei C, Ciampi R, Elisei R. A comprehensive overview of the role of the RET proto-oncogene in thyroid carcinoma. Nat Rev Endocrinol 2016;12(4):192–202.

Romei C, Ciampi R, Casella F, Tacito A, Torregrossa L, Ugolini C, et al. RET mutation heterogeneity in primary advanced medullary thyroid cancers and their metastases. Oncotarget 2018;9(11):9875–84.

Sam R, Séverine C, Aimin F, et al. Effect of cyclosporine on the pharmacokinetics of aliskiren in healthy subjects. J Clin Pharmacol. 2011;51(11):1549-60.

Santoro M, Carlomagno F, Hay ID, Herrmann MA, Grieco M, Melillo R, et al. RET oncogene activation in human thyroid neoplasms is restricted to the papillary cancer subtype. J Clin Invest 1992;89(5):1517–22.

Schuchardt A, D'Agati V, Larsson-Blomberg L, Costantini F, Pachnis V. Defects in the Kidney and Enteric Nervous System of Mice Lacking the Tyrosine Kinase Receptor RET. Nature 1994;367 (6461): 380–3.

Springuel L, Renauld JC, Knoops L. JAK kinase targeting in hematologic malignancies: a sinuous pathway from identification of genetic alterations towards clinical indications. Haematologica 2015;100(10):1240–53.

Stegherr R, Schmoor C, Beyersmann J, Rufibach K, Jehl V, Brückner A, Eisele L, Künzel T, Kupas K, Langer F, Leverkus F. Survival analysis for AdVerse events with VarYing follow-up times (SAVVY)—estimation of adverse event risks. Trials. 2021, 29;22(1):420.

Stransky N, Cerami E, Schalm S, Kim JL, Lengauer C. The landscape of kinase fusions in cancer. Nat Commun 2014;5:4846.

Subbiah V, Hu M, Gainor JF, Mansfield AS, Alonso G, Taylor MH, Weijia Zhu V, Lopez PG, Amatu A, Doebele RC, Cassier PA, Keam B, Schuler MH, Zhang H, Clifford C, Palmer M, Green J, Turner CD, and Curigliano G. Clinical activity of the RET inhibitor pralsetinib (BLU-667) in patients with RET fusion+ solid tumors. J Clin Oncol 2020;38:15_suppl, 109–109.

Suzuki M, Makinoshima H, Matsumoto S, Suzuki A, Mimaki S, Matsushima K, Yoh K, Goto K, Suzuki Y, Ishii G, et al. Identification of a lung adenocarcinoma cell line with CCDC6-RET fusion gene and the effect of RET inhibitors in vitro and in vivo. Cancer Sci 2013;104, 896–903.

Takeuchi K, Soda M, Togashi Y, Suzuki R, Sakata S, Hatano S, et al. RET, ROS1 and ALK fusions in lung cancer. Nat Med 2012;18(3):378–81.

Teng, R., Kujacic, M. and Hsia, J. Pharmacokinetic interaction study of ticagrelor and cyclosporine in healthy volunteers. Clin Drug Investig 34, 529–536 (2014).

Wang K, Russell JS, McDermott JD, Elvin JA, Khaira D, Johnson A, et al. Profiling of 149 salivary duct carcinomas, carcinoma ex pleomorphic adenomas, and adenocarcinomas, not otherwise specified reveals actionable genomic alterations. Clin Cancer Res 2016;22(24):6061–68.

Yanochko GM, Vitsky A, Heyen JR, Hirakawa B, Lam JL, May J, et al. Pan-FGFR inhibition leads to blockade of FGF23 signaling, soft tissue mineralization, and cardiovascular dysfunction. Toxicol Sci 2013;135(2):451–64.

Appendix 1 Summary of Nonclinical Pharmacology Studies

Report number (Reference) Species (strain)	Pralsetinib Dose/route Formulation/vehicle	Study design (Laboratory, GLP status)	Results
Primary Pharmacodynamics			
BPM-0015 Enzymes	In vitro, 10-point concentration effect curve (0.004–1000 nM) DMSO	Biochemical activity of pralsetinib, cabozantinib, vandetanib, regorafenib and ponatinib vs RET, RET V804L, RET V804M, RET M918T, CCDC6-RET, KDR and FGFR1 enzymes (Blueprint Medicines, Non-GLP)	Pralsetinib is a potent sub-nM inhibitor of RET and activating oncogenic mutants of RET including the V804L, V804M, M918T point mutations and the CCDC6 RET oncogenic fusion. In biochemical assays, pralsetinib was 80 times more active on RET than KDR and 25 times more active on RET than FGFR1.
BPM-0016 Ba/F3 cells	In vitro; Immunoblot: 4-point concentration effect curve (1–1000 nM); AlphaLISA and Proliferation: 10-point concentration effect curve (0.0096–25000 nM) DMSO	Activity of pralsetinib on wild-type and mutant RET kinase in Ba/F3 cells (Blueprint Medicines, Non-GLP)	Pralsetinib demonstrated potent low nM inhibitory activity on wild-type KIF5B RET cellular activity and potently blocked proliferation of Ba/F3 cells driven by wild-type or gate-keeper mutant variants of KIF5B-RET.
BPM-0017 Thyroid and lung cancer cell lines	In vitro; Immunoblot: 4point concentration effect curve (1–1000 nM-); Proliferation: 10point concentration effect curve (0.05–1000 nM-) DMSO	Activity of pralsetinib on thyroid and lung cancer cell lines driven by oncogenic RET fusions and mutations (Blueprint Medicines, Non-GLP)	Pralsetinib suppressed RET kinase activity, RET pathway signaling, RET-dependent gene expression, and cellular proliferation in a number of cancer cell lines with oncogenic RET mutations or fusions.

Report number (Reference) Species (strain)	Pralsetinib Dose/route Formulation/vehicle	Study design (Laboratory, GLP status)	Results
BPM-0018 FGFR2, JAK2 and VEGFR2 expressing cell lines	In vitro; FGFR2: 7-point concentration effect curve (0.64−10000 nM); JAK2: 10-point concentration effect curve (0.1−25000 nM); VEGFR2: 8-point concentration effect curve (3−10000 nM) DMSO	Characterization of pralsetinib cellular activity against FGFR2, JAK2 and VEGFR2 kinases (Blueprint Medicines, Non-GLP)	Pralsetinib inhibited the cellular kinase activity of FGFR2, JAK2, and VEGFR2 with IC50 of 201 nM, 58 nM, and 70 nM, respectively.
BPM-0020 In vivo tumor models	In vitro and oral	PK, PD and efficacy relationship of pralsetinib in RETdriven- in vivo tumor models (integration of data from multiple studies) (Blueprint Medicines, Non-GLP)	Pralsetinib doses of 10 and 30 mg/kg BID correlated with approximately 90% inhibition of phospho(Y1062)-RET. The mouse plasma concentrations required for 50%, 75%, or 90% inhibition of in vivo RET activity were 117, 299, and 769 ng/mL pralsetinib, respectively.
BPM-0021 RET kinase domain sequences for 5 species were retrieved from the NCBI Proteins database and entered into the EBI ClustalW2 multiple sequence alignment program	N/A	Comparison of RET kinase domain sequences across species (Blueprint Medicines, Non-GLP)	The analysis reveals that the preclinical species, rat, mouse, dog, and monkey, contain identical or highly homologous amino acids surrounding the pralsetinib binding site in RET, making all of these species suitable for assessing RET-mediated pharmacology in preclinical safety studies.

Report number (Reference) Species (strain)	Pralsetinib Dose/route Formulation/vehicle	Study design (Laboratory, GLP status)	Results
1110-003 Nu/nu nude mice; tumor-bearing	0, 3, 10, 30 mg/kg BID; 60 mg/kg QD; 28 days Oral gavage 10% DMSO + 10% Solutol + 80% (20% HP-β-CD in water)	In vivo evaluation of pralsetinib in a low passage champions TumorGraft™ model of human non-small cell lung carcinoma in immunocompromised mice (Champions Oncology, Non-GLP)	Pralsetinib was well-tolerated and showed significant antitumor activity against a KIF5B-RET expressing NSCLC PDX on a PO/QDx28 days or PO/BID × 28 days schedule.
CPB-P18-21802	0, 3, 10, 30 mg/kg BID; 42 days Oral gavage 10% DMSO + 10% Solutol HS 15 + 80% (20% HP-β-CD in water)	In vivo efficacy study of pralsetinib on Ba/F3-KIF5B-RET brain orthotopic inoculation model in BALB/c nude mice (ChemPartner, Non-GLP)	Pralsetinib at 3 mg/kg, 10 mg/kg and 30 mg/kg BID demonstrated dose-dependent efficacy in the Ba/F3-KIF5B-RET-luc brain orthotopic model significantly prolonging survival relative to the vehicle control group.
E0400-U1523	0, 10, 30 mg/kg BID; 60 mg/kg QD; 30, 174, 33; 33 days Oral gavage 10% DMSO + 10% Solutol HS 15 + 80% (20% HP-β-CD in water)	In Vivo Efficacy Study of Pralsetinib in the Treatment of HuPrime® Colorectal Cancer Xenograft Model CR2545 in BALB/c Nude Mice (CrownBio, Non-GLP)	Pralsetinib at 10 mg/kg and 30 mg/kg BID dosing or 60 mg/kg QD demonstrated significant antitumor activity against the HuPrime® colorectal cancer patient-derived xenograft model CR2545, harboring a CCDC6-RET (V804M) fusion.
E0400-U1608 BALB/c nude mice; tumor-bearing	0, 3, 10, 30 mg/kg BID; 60 mg/kg QD; 21 days Oral gavage 10% DMSO + 10% Solutol HS 15 + 80% (20% HP-β-CD in water)	In vivo efficacy study of pralsetinib in the treatment of HuPrime® colorectal cancer xenograft Model CR2518 in BALB/c nude mice (CrownBio, Non-GLP)	Pralsetinib at 3 mg/kg, 10 mg/kg and 30 mg/kg BID or 60 mg/kg QD demonstrated significant antitumor activity against the HuPrime® colorectal cancer patient-derived xenograft model CR2518, harboring a CCDC6-RET fusion.

Report number (Reference) Species (strain)	Pralsetinib Dose/route Formulation/vehicle	Study design (Laboratory, GLP status)	Results
E0400-U1804	0, 10, 30 mg/kg BID; 58, 96, 96 days Oral gavage 10% DMSO + 10% Solutol HS 15 + 80% (20% HP-β-CD in water)	In Vivo Efficacy Study of Pralsetinib in the Treatment of Intracranial Inoculation HuPrime@ Colorectal Cancer Xenograft Model CR2518 in Female BALB/c Nude Mice (CrownBio, Non-GLP)	Pralsetinib at 10 mg/kg and 30 mg/kg BID demonstrated dose-related antitumor activity in the intracranial HuPrime® colorectal cancer patient-derived xenograft model CR2518, harboring a CCDC6-RET fusion, resulting in improved survival with 6/10 and 0/10 animals with intracranial tumors, respectively, at day end of study (day 96).
E0400-U1806 BALB/c nude mice; tumor-bearing	0, 3, 10, 30 mg/kg BID; 28 days Oral gavage 10% DMSO + 10% Solutol HS 15 + 80% (20% HP-β-CD in water)	In Vivo Efficacy Study of Pralsetinib in the Treatment of Subcutaneously HuPrime@ Colorectal Cancer Xenograft Model CR1520 in Female BALB/c Nude Mice (CrownBio, Non-GLP)	Pralsetinib at 3 mg/kg, 10 mg/kg and 30 mg/kg BID demonstrated significant antitumor activity against the HuPrime® colorectal cancer patient-derived xenograft model CR1520, harboring a NCOA4-RET fusion.
CPB-P15-5515 BALB/c nude mice; tumor bearing	0, 3, 10, 30 mg/kg BID; 20 mg/kg QD; 14 days Oral gavage 10% DMSO + 10% Solutol + 80% (20% HP-β-CD in water)	PK/PD and efficacy study of pralsetinib in a Ba/F3 KIF5B-RET VE subcutaneous xenograft model in BALB/c nude mice (ChemPartner, Non-GLP)	Pralsetinib at 3 mg/kg, 10 mg/kg, or 30 BID, or 20 mg/kg resulted in significant antitumor efficacy in the Ba/F3-KIF5B-RET VE subcutaneous xenograft tumor-bearing mice.
CPB-P16-5645 BALB/c nude mice; tumor-bearing	0, 3, 10, 30 mg/kg BID; 60 mg/kg QD; 28 days Oral gavage 10% DMSO + 10% Solutol + 80% (20% HP-β-CD in water)	PK/PD and efficacy study of pralsetinib in a TT subcutaneous xenograft model in BALB/c nude mice (ChemPartner, Non-GLP)	Pralsetinib at 3, 10, and 30 mg/kg BID or 60 mg/kg QD demonstrated significant dose-dependent antitumor activity against the TT subcutaneous xenografts.

Report number (Reference) Species (strain)	Pralsetinib Dose/route Formulation/vehicle	Study design (Laboratory, GLP status)	Results
CPB-P16-5665 BALB/c nude mice; tumor-bearing	0, 3, 10, 30 mg/kg BID; 20 mg/kg QD; 14 days Oral gavage 10% DMSO + 10% Solutol + 80% (20% HP-β-CD in water)	PK/PD and efficacy study of pralsetinib in a Ba/F3-KIF5B-RET subcutaneous xenograft model in BALB/c nude mice (ChemPartner, Non-GLP)	Pralsetinib at 3 mg/kg, 10 mg/kg BID, or 30 mg/kg BID, or 20 mg/kg QD resulted in significant dose-dependent antitumor activity in the Ba/F3-KIF5B-RET subcutaneous xenograft tumor-bearing mice.
Secondary Pharmacodynamics			
100023499/100023915 Inhibition of binding for a radioactively labeled ligand specific for each target	In vitro; Screening: 10 µM; IC_{50}: 5-HT2A: 8-point concentration effect curve (30 nM–1 mM); Na+ channel site 2: 8-point concentration effect curve (3 nM–1 mM); DMSO	Pralsetinib tested in binding assays (CEREP, Non-GLP)	Pralsetinib causes > 50% inhibition of binding against 2 receptors, the 5-HT2A (62.7%; IC_{50} = 3.6 µM) and Na+ channel site 2 (80.7%; IC_{50} = 3.4 µM) receptors.
100023499/100023915 Inhibition of binding for a radioactively labeled ligand specific for each target	In vitro; Screening: 10 µM; IC_{50}: 5-HT2A: 8-point concentration effect curve (30 nM–1 mM); Na+ channel site 2: 8-point concentration effect curve (3 nM–1 mM); DMSO	Pralsetinib tested in binding assays (CEREP, Non-GLP)	Pralsetinib causes > 50% inhibition of binding against 2 receptors, the 5-HT2A (62.7%; IC_{50} = 3.6 µM) and Na+ channel site 2 (80.7%; IC_{50} = 3.4 µM) receptors.

5-HT2A = 5-hydroxytryptamine 2A; BID = twice daily; CCDC6 = coiled-coil domain containing 6; CHO = Chinese hamster ovary; CMC = carboxymethylcellulose; DMSO = dimethylsulfoxide; EBI = European Bioinformatics Institute; FGFR1 = fibroblast growth factor receptor 1; GLP = Good Laboratory Practice; hERG = human ether-à-go-go related gene; HP-β-CD = hydroxypropyl-β-cyclodextrin; HR = heart rate; IC50 = half maximal inhibitory concentration; JAK2 = Janus activating kinase 2; Kd = dissociation constant; KDR = kinase insert domain receptor; KIF5B = kinesin family member 5b; N/A = not applicable; NCBI = National Center for Biotechnology Information; NOEL = no-observed-effect level; NSCLC = non-small cell lung cancer; PD = pharmacodynamic; PDX = patient-derived xenograft; PK = pharmacokinetic; PO = oral; QD = once daily; RET = rearranged during transfection; SD = standard deviation; VEGFR = vascular endothelial growth factor receptor.

Appendix 2 Summary of Nonclinical Pharmacokinetic and Metabolism Studies

Study Type [Reference]	Species/ Test System	Animals/ Group (M/F)	Route	Dose (mg/kg/day) OR Initial Concentration (µM)	Key Results
Absorption/PK[a]					
Single-dose study to determine PK parameters following IV bolus or PO dose of pralsetinib in male SD rats (ChemPartner, Non-GLP) **(CPB-P15-10033R02)**	Rat/Sprague Dawley		IV Oral gavage:	1 mg/kg 10% DMSO + 10% Solutol + 80% (20% HP-β-CD in water) 10 mg/kg 10% DMSO + 10% Solutol + 80% (20% HP-β-CD in water)	IV: concentrations declined with a $t_{1/2}$ of 3.50±0.262 hr. AUC_{last} and AUC_{INF} were 1137 ± 128 hr*ng/mL and 1149 ± 131 hr*ng/mL, respectively. CL and V_{dss} were 0.877±0.0947 L/hr/kg and 3.32±0.352 L/kg, respectively. PO: C_{max} was 2345 ± 341 ng/mL and T_{max} was 2.67 ± 1.15 hr. AUC_{last} and AUC_{INF} were 18797 ± 4483 hr*ng/mL and 19055 ± 4504 hr*ng/mL, respectively. Bioavailability of pralsetinib in SD rats was estimated to be 166 ± 39.2 %.
Single-dose study to determine PK parameters following PO dose of pralsetinib in male Beagle dogs (ChemPartner, Non-GLP) **(CPB-P15-10204D03)**	Dog/Beagle		Oral gavage	1 mg/kg 5% DMSO + 5% Solutol HS + 90% Saline	C_{max} was 1789 ± 784 ng/mL and T_{max} was 2.00 hr. AUC_{last} and AUC_{INF} were 16910 ± 8008 hr*ng/mL and 17355±8376 hr*ng/mL, respectively.
Single-dose study to determine PK parameters following IV bolus dose of pralsetinib in male Beagle dogs (ChemPartner, Non-GLP) (**CPB-P15-10082D01)**	Dog/Beagle		IV	0.5 mg/kg 5% DMSO + 5% Solutol HS + 90% Saline	Concentrations in dog plasma declined with a $t_{1/2}$ of 3.50 ± 0.200 hr. AUC_{last} and AUC_{INF} were 4184 ± 771 hr*ng/mL and 4218 ± 772 hr*ng/mL, respectively. CL and V_{dss} were 0.121 ± 0.0205 L/hr/kg and 0.492 ± 0.100 L/kg, respectively.

Study Type [Reference]	Species/ Test System	Animals/ Group (M/F)	Route	Dose (mg/kg/day) OR Initial Concentration (µM)	Key Results
Single-dose study in Beagle Dogs to determine the PK of pralsetinib dosed as Capsules or Tablets (Charles River Laboratories, Non-GLP) **(WIL-124750)**	Dog/Beagle		Oral	100 mg total dose Immediate Release HPMC hard Tablets (2 × 50 mg) or Aesthetically coated immediate release HPMC Capsules (1 × 100 mg). Both were spray dried dispersion formulations.	The tablet formulation of pralsetinib was absorbed more rapidly (peak concentrations at 3-4 h postdose) when compared to the capsule formulation (peak concentrations at 8 hours postdose). The exposure differences between pralsetinib in Tablets vs Capsule formulation were $<$ 2-fold.
Single-dose study to determine PK parameters following PO dose of pralsetinib in male Cynomolgus- monkeys (ChemPartner, Non-GLP) **(CPB-P15-10204K04)**	Monkey/Cynomolgus		Oral gavage	1 mg/kg 5% DMSO + 5% Solutol HS + 90% Saline	$t_{1/2}$ was 3.63 ± 0.544 hours. Mean C_{max} was 396 ± 51.2 ng/mL and T_{max} was 2.00 hr. AUC_{last} and AUC_{INF} were 2917 ± 638 hr*ng/mL and 2953 ± 660 hr*ng/mL, respectively.
Single-dose study to evaluate PK profile of pralsetinib following capsule or nasogastric (spray dried dispersion formulation) administration to male Cynomolgus monkeys. Additionally, this study investigated the PK profile of pralsetinib in combination with famotidine. (Charles River, Non-GLP) **(WIL-124618)**	Monkey/ Cynomolgus		IV	265 mg/animal ± 0.03 mL/kg famotidine Citric acid (capsule formulation) or spray dried dispersion (nasogastric intubation)	Exposure to pralsetinib was 1.3 to 1.4-fold higher for animals that received the spray dried dispersion formulation as compared to animals that received the citric acid formulation in capsule. Single administration of 2 different formulations of pralsetinib was not significantly altered with or without a pretreatment with famotidine.

Study Type [Reference]	Species/ Test System	Animals/ Group (M/F)	Route	Dose (mg/kg/day) OR Initial Concentration (µM)	Key Results
Single-dose study to determine PK parameters following IV bolus dose of pralsetinib in male Beagle dogs (ChemPartner, Non-GLP) **(CPB-P15-10082K01)**	Monkey/ Cynomolgus		IV	0.5 mg/kg 5% DMSO + 5% Solutol HS + 90% Saline	Plasma concentrations declined in a first order kinetics manner with a $T_{1/2}$ of 3.74 ± 1.23 hr. AUC_{last} and AUC_{INF} were 1389 ± 548 hr*ng/mL and 1437 ± 527 hr*ng/mL. CL and V_{dss} were 0.391 ± 0.178 L/hr/kg and 1.66 ± 0.192 L/kg, respectively.
Study to assess the intestinal permeability of pralsetinib across Caco-2 cell monolayers in both the A-B and B-A directions. (ChemPartner, Non-GLP) **(CPB-P15-10082-CACO2)**	In vitro, Caco-2 cell monolayers	NA	NA	In vitro; 10 µM DMSO	Pralsetinib showed high permeability (> 10×10^{-6} cm/sec). Efflux ratio was determined to be < 2, suggesting that pralsetinib is not an efflux transporter substrate in the Caco-2 assay system.
Study to assess the permeability of pralsetinib in MDR1-MDCK cell monolayers in both the A-B and B-A directions. (ChemPartner, Non-GLP) **(CPB-P15-10141)**	In vitro, MDCK cell monolayers	NA	NA	In vitro; 5 µM DMSO	Pralsetinib showed low permeability (< 5×10^{-6}cm/sec) in the A-B direction. Efflux ratio was determined to be 8.25, suggesting that pralsetinib is a human P-gp (MDR1) substrate.
Distribution					

Study Type [Reference]	Species/ Test System	Animals/ Group (M/F)	Route	Dose (mg/kg/day) OR Initial Concentration (µM)	Key Results
Study to assess protein binding of pralsetinib in human, rat, mouse, dog and monkey plasma using equilibrium dialysis. (ChemPartner, Non-GLP) **(CPB-P16-10980)**	In vitro, human, rat (Sprague Dawley), mouse (CD-1), dog (Beagle), and monkey (Cynomolgus) plasma	NA	NA	In vitro; 10 µM DMSO	Pralsetinib showed high protein binding (≥ 95.4%) in human, rat, mouse, dog, and monkey plasma. The unbound fraction was highest in monkey plasma (4.6%) and lowest in mouse plasma (0.5%).
Study to determine the pralsetinib partitioning between RBC and plasma in human, rat, mouse, dog and monkey blood. (ChemPartner, Non-GLP) **(CPB-P15-10118)**	In vitro, human, rat (Sprague Dawley), mouse (CD-1), dog (Beagle), and monkey (Cynomolgus) whole blood and plasma	NA	NA	In vitro; 5 µM DMSO	Pralsetinib did not exhibit preferential partitioning into RBCs in vitro in human, rat, mouse, dog, or monkey whole blood.
Study to assess the stability of pralsetinib in vitro in human plasma. (ChemPartner, Non-GLP) **(CPB-P15-10307)**	In vitro, human plasma	NA	NA	In vitro; 2 µM DMSO	Pralsetinib was stable in human plasma ($t_{1/2}$ > 120 min).
Metabolism					

Study Type [Reference]	Species/ Test System	Animals/ Group (M/F)	Route	Dose (mg/kg/day) OR Initial Concentration (μM)	Key Results
BLU-R5482 Study to investigate the metabolism, mass balance, and excretion routes of [^{14}C]-pralsetinib in intact and BDC male Sprague Dawley rats following a single PO or IV dose. (Frontage Laboratories, Non-GLP)	Rat/Sprague Dawley		Oral gavage IV	[^{14}C]-pralsetinib Oral gavage: 30 mg/kg IV (in BDC rats): 30 mg/kg 0.5% carboxymethylcellulose (CMC, medium viscosity)-Na (w/v):1% Tween® 80 (w/v) in deionized water (pH 2-3) for the PO administration while the IV dose was made up in 20% DMSO in 80% PEG200 (final pH 4- 5).	The metabolic pathways of [^{14}C]-pralsetinib in rats included hydroxylation/ oxidation (M549a,b, M563), N-glucuronidation (M709a,b,c), and GSH conjugation (M836, M838).
BLU-R4655 Study to assess metabolism of pralsetinib in the presence of liver microsomes and cryopreserved hepatocytes from CD-1 mice, Sprague Dawley rats, Beagle dogs, Cynomolgus monkeys, and humans (Frontage Laboratories, Non-GLP)	In vitro, human, rat (Sprague Dawley), mouse (CD-1), dog (Beagle), and monkey (Cynomolgus) liver microsomes and hepatocytes		NA	In vitro; 10 μM DMSO	Pralsetinib appears to be relatively stable in the presence of liver microsomes and hepatocytes from CD-1 mice, Sprague Dawley rats, Beagle dogs, Cynomolgus monkeys and humans. No unique metabolites were observed in human liver microsomes and hepatocytes. In mouse, rat, and dog liver microsomes, a single metabolite (M549b) was detected and it was proposed to be formed via hydroxylation/oxidation of the cyclohexyl ring. In addition, metabolites M549a and M549c were also detected in monkey and human liver microsomes. Two additional metabolites, M464 and M563 were found in monkey liver microsomal extracts.

Study Type [Reference]	Species/ Test System	Animals/ Group (M/F)	Route	Dose (mg/kg/day) OR Initial Concentration (µM)	Key Results
					Mouse hepatocytes converted pralsetinib to a single metabolite, M549b which was also found in the mouse liver microsomal extract. In rat hepatocytes, a glutathione conjugate, M838 was observed in addition to the hydroxylated analogs M549a and M549b. Dog hepatocytes produced M549b and the glutathione conjugate, M838. Pralsetinib was metabolized to a number of metabolites by monkey hepatocytes including the hydroxylated isomers, M549a and M549b, and the glutathione conjugate, M838. In addition to these, another glutathione conjugate, M836 and a glucuronide conjugate, M709, were also found in the monkey hepatocyte extracts. Human hepatocytes metabolized pralsetinib to mostly the glucuronide conjugate, M709 and to a lesser extent, the hydroxylated analogue, M549b. None of the glutathione conjugates were found in human hepatocytes.
150521/150604 Study to evaluate in vitro and in vivo hepatic clearance of pralsetinib in mouse, rat, dog, monkey, and human cryopreserved hepatocytes. (Alliance, Non-GLP)	In vitro, mouse (CD-1), rat (Sprague Dawley), dog (Beagle), and monkey (Cynomolgus) and human hepatocytes	NA	NA	In vitro; 0.5 µM DMSO	Low turnover of pralsetinib was observed in hepatocytes from mouse, rat, dog, monkey, and human. Metabolic stability ranking in hepatocytes (most to least stable) was as follows: rat, monkey, mouse, human ~ dog.

Study Type [Reference]	Species/ Test System	Animals/ Group (M/F)	Route	Dose (mg/kg/day) OR Initial Concentration (µM)	Key Results
CYP-P15-10033 Metabolic stability of pralsetinib was evaluated upon incubation in liver microsomes at 37ºC and analyzed by LC-MS/MS. (ChemPartner, Non-GLP)	In vitro, human, rat (Sprague Dawley), mouse (CD-1), dog (Beagle), and monkey (Cynomolgus) liver microsomes	NA	NA	In vitro; 1 µM DMSO	BLU-667 was metabolized in liver microsomes across species. Metabolic stability ranking (most to less stable) was as follows: human > dog ~ rat > mouse > monkey.
Excretion					
BLU-R5482 Study to investigate the metabolism, mass balance, and excretion routes of [^{14}C]-pralsetinib in intact and BDC male Sprague Dawley rats following a single PO or IV dose. (Frontage Laboratories, Non-GLP)	Rat/Sprague Dawley		Oral gavage IV	[^{14}C]-pralsetinib Oral gavage: 30 mg/kg IV (in BDC rats): 30 mg/kg 0.5% CMC (medium viscosity)-Na (w/v):1% Tween® 80 (w/v) in deionized water (pH 2-3)	PO: [^{14}C]-pralsetinib-related components were rapidly excreted in the first day post-dose and completely excreted mainly in feces within 168 hours postdose (mean total recovery was 93.30% ± 2.45% at 168 hours). IV: in BDC rats, total radioactivity was rapidly excreted in the first day postdose and almost completely excreted mainly in bile and feces within 72 hours postdose. The mean total recovery of radioactivity was 87.02% ± 4.12% within 0 to 72 hours).
Drug–Drug Interaction					

Study Type [Reference]	Species/ Test System	Animals/ Group (M/F)	Route	Dose (mg/kg/day) OR Initial Concentration (μM)	Key Results
OPT-2016-062 Study to determine whether pralsetinib is transported by human BCRP, P-gp, MATE1, OCT1, OCT2, OCT3, and MRP2. (Optiva Biotechnology, Non-GLP)	Human MDCK-II cell and MDCK-MDR1 cell monolayers	NA	NA	In vitro; 20 μM DMSO	For P-gp, the efflux ratio was determined to be 2.16, slightly above the threshold of 2.0, suggesting that pralsetinib may be a substrate for P-gp. Pralsetinib was not a substrate for OCT1, OCT2, OCT3, MATE1, MRP2, or BCRP.
BLU-R5843 Study to identify the human CYP enzymes involved in the metabolism of pralsetinib. (Frontage Laboratories, Non-GLP)	Human liver microsomes	NA	NA	In vitro; 10 μM DMSO	The pattern of metabolism in CYP enzymes was similar to that observed in human liver microsomes and resulted in the formation of the same main hydroxylated metabolite M549b. The formation of M549b and the other metabolites was catalyzed by CYP1A2, CYP2D6, and CYP3A4. Thus, multiple CYP enzymes have the potential to contribute to the oxidative metabolism of pralsetinib in humans.
BLU-R5500 Study to identify the UGT enzymes involved in the metabolism of pralsetinib. (Frontage Laboratories, Non-GLP)	Human liver microsomes	NA	NA	In vitro; 0.5 and 10 μM DMSO	Thus the in vitro data indicate that UGT1A4 is the primary UGT involved in the metabolism of pralsetinib. UGT1A1 and UGT1A3 also appear to play a minor role in the glucuronidation of pralsetinib.

Study Type [Reference]	Species/ Test System	Animals/ Group (M/F)	Route	Dose (mg/kg/day) OR Initial Concentration (μM)	Key Results
CPB-P15-10082-CYP Study to assess the inhibitive potential of pralsetinib on CYP1A2, 2C9, 2C19, 2D6, CYP3A4 (midazolam), CYP3A4 (testosterone) using human liver microsomes. (ChemPartner, Non-GLP)	Human liver microsomes	NA	NA	In vitro; 20 μM DMSO	Pralsetinib was a weak inhibitor of CYP2C9, and not an inhibitor of CYP1A2, CYP2C19, CYP2D6, or CYP3A4.
BLU-R4687 Study to assess the potential of pralsetinib to inhibit the major human liver microsomal CYP enzymes in a direct and metabolism-dependent manner in vitro in human liver microsomes. (Frontage Laboratories, Non-GLP)	Human liver microsomes	NA	NA	In vitro; 3 μM DMSO	Pralsetinib did not prove to be a direct or metabolism-dependent inhibitor of CYP1A2, 2B6, 2C8, 2C9, 2C19, 2D6, or 3A.
BLU-R5844 Study to assess the potential of pralsetinib to inhibit CYP2C9 in human liver microsomes. (Frontage Laboratories, Non-GLP)	Human liver microsomes	NA	NA	In vitro; 0.01, 0.05, 0.1, 0.5, 1, 5, 10, 25, 50, and 100 μM DMSO	Pralsetinib inhibited CYP2C9 in a concentration-dependent manner, with the highest inhibition of (86%) being achieved with the highest concentration tested (100 μM). Pralsetinib inhibited CYP2C9 with an IC_{50} of 12.6 μM.

Study Type [Reference]	Species/ Test System	Animals/ Group (M/F)	Route	Dose (mg/kg/day) OR Initial Concentration (µM)	Key Results
CYP0915-R10b Study to evaluate the potential for pralsetinib to activate the human PXR nuclear receptor (CYP induction screening assay). (Puracyp, Non-GLP)		NA	NA	In vitro; 0.3125, 0.625, 1.25, 2.5, 5, 10 µM DMSO	Pralsetinib (up to 10 µM) activated PXR < 30% of the positive control suggesting that it is not a CYP3A4 inducer.

[a] Multiple-dose pharmacokinetic data were obtained during toxicology studies, which are listed in the Toxicology & Safety Pharmacology Tabulated Summary Overview in Appendix 3.

A-B = apical to basolateral; ADME = absorption, distribution, metabolism, and excretion; AUC_{INF} = area under the plasma versus concentration time curve from time 0 to infinity; AUC_{last} = area under the plasma versus concentration-time curve from time 0 to the last measurable concentration; B-A = basolateral to apical; BCRP = breast cancer resistance protein; BDC = bile-duct cannulated; CL = total clearance; C_{max} = maximum plasma concentration; CMC = carboxymethylcellulose; CYP = cytochrome P450; DMSO = dimethylsulfoxide; GLP = Good Laboratory Practice; GSH = glutathione; HP-β-CD = hydroxypropyl-β-cyclodextrin; HPMC = hydroxypropyl methylcellulose; IV = intravenous; LC-MS/MS = liquid chromatography/tandem mass spectrometry; MATE = multidrug and toxin extrusion protein; MDR1-MDCK = Madin-Darby canine kidney type II cells overexpressing the human *MDR1* gene; MRP2=multidrug resistance protein; OCT = organic anion transporter; PK = pharmacokinetic; P-gp = P-glycoprotein; PO = oral; PXR = Pregnane X receptor; $t_{1/2}$ = apparent terminal elimination half-life; T_{max} = time of the maximum plasma concentration; UGT = uridine 5'-diphospho-glucuronosyltransferase; V_{dss} = apparent volume of distribution at steady-state.

Appendix 3 Summary of Toxicology Studies

Study Type (Reference)	Treatment Duration	Species/ Test system	Animals/ Group	Dose (mg/kg/day)	Mean C_{max} (ng/mL) M/F	Mean AUC_{0-24h} (h • ng/mL) M/F	Major Effects
General Toxicity							
Single-dose toxicity **(WIL-124550)**	1 day	Rat/SD	3M	10 [a]	2000	21400	**MTD ≥ 300 mg/kg/day**
				100 [a]	18100	4E+05	No noteworthy findings reported.
				300 [a]	34500	1.16E+06	
				300 [b]	32500	1.13E+06	
Single-dose toxicity **(WIL-124590)**	1 day	Rat/SD	6M	50 [b]	12900	149000	**MTD ≥ 50 mg/kg/day** No noteworthy findings reported.
Single-dose toxicity **(WIL-124557)**	1 day	Dog/Beagle	3M	5 [b]	4160	62600	**MTD = 25 mg/kg/day**
			3M	25 [b]	15000	347000	5 mg/kg/day: decreased defecation
			3M	75 [b]	26700	786000	≥ 25 mg/kg/day: Emesis, abnormal feces, salivation, and/or diarrhea.
			3M	25 [c]	5420	98900	75 mg/kg/day: Mortality: 3M;
			4M	25 [b,d]	10500	323000	AP: GALT necrosis and hemorrhage.
Single-dose toxicity **(WIL-124569)**	1 day	Monkey/ Cynomologus	3M	10	5430	38100	**MTD = 30 mg/kg/day**
				30	11400	126000	≥ 10 mg/kg/day: pale face/body.
				300	20500	524000	300 mg/kg/day: Mortality 1M; AP: intestinal erosion/ulceration and hemorrhage.
Single-dose toxicity (**WIL-124591)**	1 day	Monkey/ Cynomolgus	3M	30	12300	145000	**MTD not determined** No noteworthy findings

Study Type (Reference)	Treatment Duration	Species/ Test system	Animals/ Group	Dose (mg/kg/day)	Mean C_{max} (ng/mL) M/F	Mean AUC_{0-24h} (h • ng/mL) M/F	Major Effects
Repeat-dose toxicity **(WIL-124551)**	7 day (QD)	Rat/SD	6M (Tox) 3M (TK)	15* 50 200	1930 16400 33400	17100 186000 485000	**NOAEL = 15 mg/kg/day** ≥ 15 mg/kg/day: hematologic abnormalities (decreased WBCs, reticulocytes) and lymphoid effects (decreased cellularity in lymphoid organs). ≥ 50 mg/kg/day: decrease BW, BWG and FC. Hemorrhage/necrosis in multiple soft tissues; physeal dysplasia; decrease liver weight. 200 mg/kg/day: Mortality 9M; hypoactivity, hypothermia, hunched posture; decreased liver weight; increase ALP, BUN;
Repeat-dose toxicity **(WIL-124592)**	7 day (QD)	Rat/SD	6F	15 50*	5070 17700	49200 221000	**NOAEL = 50 mg/kg/day** Well tolerated at all dose levels; no additional noteworthy findings reported.
Repeat-dose toxicity **(WIL-124570)**	4-Week/QD (plus 2-week recovery)	Rat/SD	15M/15F (Tox) 9M/9F (TK)	10 20 30 75	1970 / 3690 5120 / 6680 7180 / 9120 22400 / 20600 [e]	22000 / 40600 64300 / 82100 125000 / 101000 NC/NC	**STD10 = 30 mg/kg/day (M/F)** ≥ 10 mg/kg/day: decreased BW. 20 and 30 mg/kg/day: increased physeal thickness, tooth degeneration, stomach mineralization; decreased RBCs. 75 mg/kg/day: Mortality 5M and 9F (Tox) and 4M and 1F (TK); Remaining animals were euthanized (study day 9) due to clinical signs. Hemorrhage/ mineralization/necrosis in multiple soft tissues (heart, kidney, ovaries, spinal cord); increased physeal thickness (AP).

Study Type (Reference)	Treatment Duration	Species/ Test system	Animals/ Group	Dose (mg/kg/day)	Mean C_{max} (ng/mL) M/F	Mean AUC_{0-24h} (h • ng/mL) M/F	Major Effects
Repeat-dose toxicity **(00124770)**	13-Week (QD)	Rat/ Cr:CD(SD)	10M/10F (Tox) 9M/9F (TK)	5	751 / 1280	9040 / 12800	**NOAEL = 10 mg/kg/day (M/F)**
				10*	2360 / 3580	33300 / 42300	20 mg/kg/day: (AP) incisor degeneration/ fracture, hematologic abnormalities (decreased RBC, reticulocytes) decreased lymphoid cellularity; testicular tubular degeneration/ atrophy (decreased testis and epidymis weight, M), CL degeneration (F).
				20	6570 / 8420	101000 / 108000	
Repeat-dose toxicity **(WIL-124558)**	7 day (QD)	Dog/Beagle	3M	3*	2600	24500	**NOAEL = 3 mg/kg/day**
				10	9770	169000	≥ 10 mg/kg/day: GALT necrosis (ileum, cecum and/or colon).
				30	NA	NA	30 mg/kg/day: Mortality 3M, euthanized in extremis on D3; decreased BW, decreased FC, abdominal pain, diarrhea; GALT necrosis and hemorrhage (lung, gallbladder).
Repeat-dose toxicity **(WIL-124572)**	7 day (QD)	Monkey/ Cynomolgus	3M	10*	4570	42700	**NOAEL = 10 mg/kg/day**
				30	13500	194000	30 mg/kg/day: Mortality 1M euthanized on D2; AP: GI erosion/ulceration with secondary bacterial sepsis; lymph node inflammation (n = 1).
				150/75	NA	NA	150/75 mg/kg/day: Mortality 3M (2M euthanized in extremis on D2 and remaining animal lowered to 75mg/kg/day found dead on D4). CS: diarrhea, pale gums, hypoactivity, ataxia, tremors, decreased respiratory rate. AP: GI erosion/ulceration with secondary bacterial sepsis and lymph node inflammation (n = 2).

Study Type (Reference)	Treatment Duration	Species/ Test system	Animals/ Group	Dose (mg/kg/day)	Mean C_{max} (ng/mL) M/F	Mean AUC_{0-24h} (h • ng/mL) M/F	Major Effects
Repeat-dose toxicity **(WIL-124571)**	4-week (QD)	Monkey/ Cynomolgus	5M/5F	5/2.5 [f]	703 / 866	4780 / 6190	**STD = 15 mg/kg/day (180 mg/m²/day).**
			7M/5F	15/7.5 [g]	3190 / 3320	28400 / 25800	**HNSTD = 7.5 mg/kg/day (90 mg/m²/day)**
			5M/5F	40 [h]	NA / NA	NA / NA	15 mg/kg/day: Mortality 1M (study day 5) CS: hunched, dermal atonia, emesis, salivation, pale, shallow respiration, hypoactivity. AP: GI erosion/ulceration with secondary bacterial sepsis; decreased cellularity in lymphoid organs and bone marrow, physeal dysplasia. 40 mg/kg/day: Mortality 3M & 4F (day 3). CS: diarrhea, hypothermia, pale, lethargic, decreased respiratory rate, ataxia, decreased BW. CP: increased PT, APTT, ALT, AST, decreased Ca, TP, Cl/Na. AP: GI toxicity (erosion/ ulceration) with secondary bacterial sepsis; decreased cellularity in lymphoid organs and bone marrow
Repeat-dose toxicity **(00124768)**	13-week (QD)	Monkey/ Cynomolgus	4M/4F	2	485 / 478	4370 / 5030	**NOAEL = 10 mg/kg/day (M/F)**
				5	1620 / 1120	15700 / 13400	Well tolerated. All animals survived to scheduled necropsy. CP and AP findings were considered to be nonadverse.
				10*	2790 / 2850	43200 / 31900	

Study Type (Reference)	Treatment Duration	Species/ Test system	Animals/ Group	Dose (mg/kg/day)	Mean C_{max} (ng/mL) M/F	Mean AUC_{0-24h} (h • ng/mL) M/F	Major Effects
Repeat-dose toxicity **(20-2057)**	28-day	Wild type CByB6F1/Tg(HRAS)2Jic mice	10M/10F (Tox) 36M/36F (TK)	10	7300	39100	Well tolerated up to 30 mg/kg/day (MTD).
				30	22900	154000	100 mg/kg: Mortality 2F (Tox) and 6M & 1F (TK). CS: hunced posture, hypothermia, dehydration, decreased activity, decreased BW and FC. CP: decreased WBC, lymphocytes, eosinophils, monocytes, neutrophils, RBC, and reticulocytes, glucose, triglyceride, albumin, phosphorus. increased RDW, platelet counts, AST, ALT, ALP, CK, total bilirubin, cholesterol, globulin, urea, K. AP: decreased hematopoietic cells in the bone marrow, increased thickness of the physis in sternum and femur, increased cellularity in lymphoid organs (spleen and thymus), atrophy of the ovary and uterus/cervix, mineralization in the stomach and mixed cell inflammation in the lungs.
				100	44800	380000	
Repeat-dose carcinogenicity **(21-1108)**	26-week (QD)	CByB6F1/TgrasH2 mice	25M/25F	3	1360	NC	Pralsetinib was not carcinogenic and had no impact on survival. Pralsetinib-related non-neoplastic findings included testicular degeneration/atrophy accompanied by decreased sperm in the epididymides, and decreased cellularity in the bone marrow, thymus and spleen.
				10	7890	42500	
				30	19,500	164,000	
Genotoxicity							

Study Type (Reference)	Treatment Duration	Species/ Test system	Animals/ Group	Dose (mg/kg/day)	Mean C_{max} (ng/mL) M/F	Mean AUC_{0-24h} (h • ng/mL) M/F	Major Effects
Salmonella-E-coli/Mammalian Microsome Reverse Mutation Assay **(WIL-124573)**	NA	TA1537 TA98 TA100 TA1535 WP2uvrA	NA	100 - 5000 μg/plate	NA	NA	Pralsetinib was negative for inducing mutagenicity.
In Vitro Micronucleus Assay **(00124797)**	27 hr -S9 4 hr ±S9	TK6 Cells	NA	≤40μg/mL	NA	NA	Pralsetinib was considered negative for inducing micronuclei in TK6 cells.
In Vivo Micronucleus Assay **(00124769)**	2 day (QD)	Rat/ Crl:CD(SD)	6M/6F	75 150 300	NA	NA	Oral administration of pralsetinib resulted in a negative response for induction of bone marrow micronuclei.
Carcinogenicity							
26-week transgenic mice carcinogenicity study **(21-1108)**	26 weeks (QD)	Mouse/CByB6 F1-Tg(HRAS)2Jic Hemizygous (transgenic)	25M/25F	3 10 30	1360 7890 19500	NC 42500 164000	Pralsetinib was not carcinogenic and had no impact on survival.
Reproductive and Developmental Toxicity							
Preliminary Embryo-Fetal Development **(00124766)**	GDs 6-17	Rat/SD	10F (Tox) 8F (TK)	5 10 20 30	967 2600 7130 10900	7910 20600 65700 128000	Based on the adverse effects on intrauterine survival and fetal malformation (kidney, ureter, skeletal) at all dosage levels, a NOAEL for embryo/fetal development could not be determined.

Study Type (Reference)	Treatment Duration	Species/ Test system	Animals/ Group	Dose (mg/kg/day)	Mean C_{max} (ng/mL) M/F	Mean AUC_{0-24h} (h • ng/mL) M/F	Major Effects
Fertility and early embryonic development **(00124841)**	Study Day -28 to 63 (M) Study Day -14 to GD 7 (F)	Rat/ Crl:CD(SD)	25M/25F	0 5 10[γ] 20[ϕ]	NA	NA	No effects on female estrous cyclicity, precoital intervals, male or female reproductive performance, or male sperm parameters at any dose level. 20 mg/kg/day: early postimplantation loss, decreased viable embryos.
Fertility and early embryonic development **(21-0310)**	9 weeks (males only)	Rat/Crl:CD(SD)	25M/25F	20	5720 (M)	61,000 (M)	No effects on male reproductive performance (mating, fertility, and pregnancy indices) and no effects on intrauterine survival.
Safety Pharmacology							
In Vitro Cardiovascular **(CPB-25-15-010A-0169)**	QPatch Electrophysio logy	CHO cells expressing hERG K^+ channels	Patch clamp recording of 2 cells at each concentration	0.1 μm 0.3 μm 1 μm 3 μm 10 μm 30 μm	NA	NA	Pralsetinib inhibited hERG current by (mean ± SD): 7.07 ± 1.41% 13.52 ± 2.02% 17.43 ± 2.00% 33.66 ± 1.20% 64.58 ± 1.80% 87.23 ± 1.54% The IC_{50} was calculated to be 5.18 μm. The IC_{50} for cisapride (positive control) was 0.073 μm.
Cardiovascular Safety Pharmacology **(WIL-124581)**	Single oral dose	Rat/Crl:CD (SD)	6M	50 200	NA	NA	NOEL could not be determined under study conditions. ≥ 50 mg/kg: decrease heart rate, body temperature; increase systolic, diastolic, and mean blood pressure

Study Type (Reference)	Treatment Duration	Species/ Test system	Animals/ Group	Dose (mg/kg/day)	Mean C_{max} (ng/mL) M/F	Mean AUC_{0-24h} (h • ng/mL) M/F	Major Effects
Cardiovascular Safety Pharmacology **(WIL-124606)**	Single oral dose	Rat/Crl:CD (SD)	6M	10* 25	NA	NA	25 mg/kg: decrease heart rate; increase systolic, diastolic, and mean blood. Cardiovascular function and body temperature were unremarkable at 10 mg/kg.
Receptor binding	Inhibition of binding for a radioactively labeled ligand		Pralsetinib (30 nM to 1mM) Na^+ channel (3 nM to 1 mM)	10 μM screening	NA	NA	Pralsetinib causes > 50% inhibition of binding against 2 receptors: - 5-HT_{2A} receptor: 62.7%, IC_{50} = 3.6 μM - Na^+ channel site 2 receptor: 80.7%; IC_{50} = 3.6 μM
Local Tolerance							
Local tolerance of pralsetinib in the gastrointestinal tract of rats and cynomolgus monkeys was characterised in the GLP-compliant 28-day toxicology studies (**WIL-124570 and WIL-124571)**							
Other Toxicity							
Neutral Red Uptake Phototoxicity Assay - GLP **(20143108)**	90 minutes	BALB/c 3T3 Mouse fibroblasts	NA	1.00 – 56.2 μg/mL	NA	NA	Pralsetinib was not phototoxic.
Study on Impurities **(WIL-124665)**	14-Day (QD)	Rat/SD	10M/10F (Tox) 9M/9F (TK)	10 mg/kg Pralsetinib + Impurities* 20 mg/kg Pralsetinib+ Impurities	1920 / 2510 3700 / 4260	21500 / 19500 52500 / 47200	Results consistent with previous toxicity studies. No impurity specific findings.

Study Type (Reference)	Treatment Duration	Species/ Test system	Animals/ Group	Dose (mg/kg/day)	Mean C_{max} (ng/mL) M/F	Mean AUC_{0-24h} (h • ng/mL) M/F	Major Effects
Study on Impurities **(WIL-124746)**	14-Day (QD)	Rat/SD	10M/10F (Tox) 9M/9F (TK)	20 mg/kg Pralsetinib + Impurity 1 20 mg/kg Pralsetinib + Impurity 2	5680 / 6550 4370 / 6320	58000 / 74000 58700 / 63100	Results consistent with previous toxicity studies. No impurity specific findings.

Abbreviations: ALP = alkaline phosphatase; AP = anatomic pathology; APTT = activated partial prothrombin time; ALT = alanine aminotransferase; AST = aspartate aminotransferase; $AUC_{(0-t)}$ = area under the plasma concentration versus time curve from 0 to the last measurable concentration; BUN = blood urea nitrogen; BW = body weight; BWG = body weight gain; CA = serum calcium; Cl/Na = chloride and sodium; C_{max} = maximum plasma concentration; CP = clinical pathology; CS = clinical signs; D = Day; DLT = dose-limiting toxicity; DMSO = dimethylsulfoxide; *E. coli* = *Escherichia coli*; F = female; FC = food consumption; GALT = gut-associated lymphoid tissue; GD = Gestation Day; GI = gastrointestinal; GLP = Good Laboratory Practice; HNSTD = highest nonseverely toxic dose; NA = not applicable; M = male; MTD = maximum tolerated dose; NC=not calculated; NOAEL = no-observed-adverse-effect level; QD = quaque die (once a day); PT = prothrombin time; RBC = red blood cell count; S9 = 9000*g* supernatant; SD = Sprague Dawley; STD = severely toxic dose; STD_{10} = severely toxic dose in 10% of animals; TK = toxicokinetics; TP = total protein; WBC = white blood cell count.

[a] Vehicle: 10% Solutol (HS15), in 20% cyclodextrin

[b] Vehcile: 0.5% carboxymethylcellulose (CMC; medium viscosity)-Na (w/v):1%Tween-80 in deionized H_2O (pH 2-3)

[c] Vehicle: 50% Labrasol in deionized water.

[d] Pretreated with a single intramuscular dose of 6 ug/kg Pentagastrin

[e] C_{max} calculated from samples collected on Study Day 9 due to early termination at this dose.

[f] 5 mg/kg/day on Days 0 to 4 (males) and 0 to 3 (females) and 2.5 mg/kg/day on Days 5 to 27 (males) and 4 to 27 (females).

[g] 15 mg/kg/day on Days 0 to 4 (males) and 0 to 3 (females) and 7.5 mg/kg/day on Days 7 to 27 (males) and 6 to 27 (females). Dosing holiday on Days 5-6 (males) and 4-5 (females).

[h] 40 mg/kg/day dose group terminated on Day 5 (males) and Day 4 (females)

∗The highest NOAEL.

γ The NOAEL for embryo-fetal toxicity.

ϕ The NOAEL for reproductive toxicity.

Appendix 4 Summary of Clinical Studies

Protocol No., No. of Center(s) (Reference)	Study Design	Study Population: Diagnosis, Inclusion Criteria	Objectives/ Criteria for Evaluation	Dosing Regimen, Duration, Formulation	No. of Subjects/ Patients Sex (M/F) Age (yrs)	Study Status Study Dates
Clinical Pharmacology Studies						
BP42858 1 center in 1 country	Open-label, randomized, single-dose, 2-way crossover	Healthy volunteers	To assess the effect of a high-fat meal compared to fasting on the relative bioavailability and PK of pralsetinib	Capsule: 2 × 100 mg administered in the fasting state or after the completion of a standardized high-fat meal	20 subjects	Study completed
BP42859 1 center in 1 country	Open label, single-dose, 2-period crossover	Healthy Volunteers	To assess the bioequivalence between four 100 mg tablets and four 100 mg capsules of pralsetinib under fasting conditions	Tablet: 4 × 100 mg tablets Capsule: 4 × 100 mg capsules	87 subjects	Study completed
BP42860 (Mass Balance Study) 1 center in 1 country	Open label, single-dose	Healthy Volunteers	Absorption, Metabolism, Excretion, and Mass Balance of [^{14}C]-pralsetinib	~310 mg pralsetinib (~100 μCi) administered orally as 3 × 100 mg capsules and 1 capsule containing ~100 μCi [^{14}C]-pralsetinib (~10 mg) after an overnight fast	6 adult male subjects	Study completed

Protocol No., No. of Center(s) (Reference)	Study Design	Study Population: Diagnosis, Inclusion Criteria	Objectives/ Criteria for Evaluation	Dosing Regimen, Duration, Formulation	No. of Subjects/ Patients Sex (M/F) Age (yrs)	Study Status Study Dates
BP42861 1 center in 1 country	Two-part, open-label, fixed-sequence, 2-period study	Healthy Volunteers	Part 1: To evaluate the PK of pralsetinib in the presence and absence of itraconazole (a strong CYP3A4 inhibitor) Part 2: To evaluate the PK of pralsetinib in the presence and absence of rifampin (a strong CYP3A4 inducer)	Part 1 (Itraconazole DDI Study): 2 × 100 mg pralsetinib capsules alone on Day 1 (Period 1) 200 mg (10 mg/mL oral solution) itraconazole BID on Day 1 followed by 200 mg itraconazole QD on Day 2 through Day 14 with 200 mg pralsetinib single oral dose coadministered on Day 4 (Period 2) Part 2 (Rifampin DDI Study): 4 × 100 mg pralsetinib capsules alone on Day 1 (Period 1) 2 × 300 mg rifampin capsules QD on Day 1 through Day 18 with 400 mg pralsetinib single oral dose coadministered on Day 9 (Period 2)	Part 1: 25 subjects Part 2: 25 subjects	Study completed

Protocol No., No. of Center(s) (Reference)	Study Design	Study Population: Diagnosis, Inclusion Criteria	Objectives/ Criteria for Evaluation	Dosing Regimen, Duration, Formulation	No. of Subjects/ Patients Sex (M/F) Age (yrs)	Study Status Study Dates
BP42862 1 center in 1 country	Open-label, fixed-sequence, 2-period study	Healthy Volunteers	To evaluate the effect of esomeprazole and gastric pH-altering on the PK of pralsetinib	Period 1: 4 × 100 mg pralsetinib capsules Period 2: 40 mg esomeprazole capsule orally QD on Day 1 to Day 6 with 400 mg pralsetinib single oral dose administered 1 hour after esomeprazole administration on Day 6	36 subjects	Study completed
GP43162 1 center in 1 country	Open-label, fixed-sequence	Healthy Volunteers	To evaluate the effect of single dose of cyclosporine on the single dose PK of pralsetinib	Day 1: 2 × 100 mg pralsetinib capsules Day 10: 2 × 100 mg pralsetinib after 6 × 100 mg cyclosporine capsules	15 patients	Study completed
JO43175 in Japan	Single-arm, open-label	Patients with RET altered solid tumors	To evaluate the PK of pralsetinib	Pralsetinib 400mg PO QD	Planned: 6 patients Actual: 4 patients	Study ongoing
JO43701 in Japan	Single-arm, open-label	Pre-treated RET positive NSCLC patients	To evaluate the PK of pralsetinib	Pralsetinib 400 mg PO QD	Planned: 24 patients Actual: 4 patients	Study ongoing

Protocol No., No. of Center(s) (Reference)	Study Design	Study Population: Diagnosis, Inclusion Criteria	Objectives/ Criteria for Evaluation	Dosing Regimen, Duration, Formulation	No. of Subjects/ Patients Sex (M/F) Age (yrs)	Study Status Study Dates
GP43163	Open-label, single-dose	Patients with moderate or severe hepatic impairment compared to healthy subjects	To evaluate the PK and safety of pralsetinib in subjects with moderate or severe hepatic impairment compared to healthy subjects	Single dose of pralsetinib 200mg	29 patients	Study completed
GP43164	Open-label, two-arm	Patients with advanced or metastatic solid tumors that are not responsive to standard therapies or for which there is no effective therapy	To evaluate the PK and safety of pralsetinib in subjects with advanced or metastatic solid tumors	Arm A: Day 1 & 10: A single oral dose of transporter-substrate cocktail: digoxin (0.25 mg), furosemide (1 mg), metformin (10 mg), and rosuvastatin (10 mg). Day 3 to 12: 400 mg QD of oral pralsetinib	Planned: 36 patients	Study ongoing

Protocol No., No. of Center(s) (Reference)	Study Design	Study Population: Diagnosis, Inclusion Criteria	Objectives/ Criteria for Evaluation	Dosing Regimen, Duration, Formulation	No. of Subjects/ Patients Sex (M/F) Age (yrs)	Study Status Study Dates
				Arm B: Day 1 & 14: a single oral dose CYP-substrate cocktail (midazolam [2 mg], warfarin [10 mg], and montelukast [10 mg]) and vitamin K (10 mg) Day 2, 3, 15 & 16: vitamin K (10 mg) Day 7 to 20: 400 mg QD of oral pralsetinib Day 5 & 18: single oral dose of COC (norethindrone [1 mg] /ethinyl estradiol [35 µg])		

Protocol No., No. of Center(s) (Reference)	Study Design	Study Population: Diagnosis, Inclusion Criteria	Objectives/ Criteria for Evaluation	Dosing Regimen, Duration, Formulation	No. of Subjects/ Patients Sex (M/F) Age (yrs)	Study Status Study Dates
Clinical Studies						
BO42863 (ARROW) 74 centers in13 countries	Nonrandomized, open label, single group, non-controlled	Patients with Thyroid Cancer, Non-Small Cell Lung Cancer (NSCLC) and Other Advanced Solid Tumors	Phase I: Identify MTD/RP2D and assess safety and tolerability Phase II: ORR and assess safety and tolerability	400 mg QD: pralsetinib 400 MG, Once Per Day, Oral Other doses: pralsetinib, Oral, from 30mg to 600mg, QD or BID	400 mg QD (N = 540) Other doses (N = 50)	Phase I: complete Phase II: complete (LPLV: 21 March 2024) Study dates: March 2017 (FPFV) December 2021 (LPI)
BO42864 140 centers (planned) in 26 countries	Randomized, open label, parallel, active controlled	Patients with RET fusion−positive, metastatic non−small cell lung cancer	Assess PFS compared to platinum-containing chemotherapy regimens in patients with RET fusion-positive metastatic NSCLC	Arm A: pralsetinib (at a starting dose of 400 mg PO QD) in continuous dosing Arm B: SOC (non-squamous histology: platinum/pemetrexed ± pembrolizumab; squamous histology: platinum/gemcitabine) or platinum/pembrolizumab + paclitaxel or nab-paclitaxel	Planned: Arm A: 113 patients Arm B: 113 patients	Study complete LPLV: 27 January 2025 (CSR is under preparation) Study dates: July 2020 (FPFV)

Protocol No., No. of Center(s) (Reference)	Study Design	Study Population: Diagnosis, Inclusion Criteria	Objectives/ Criteria for Evaluation	Dosing Regimen, Duration, Formulation	No. of Subjects/ Patients Sex (M/F) Age (yrs)	Study Status Study Dates
BO41932 (TAPISTRY; cohort K)	Nonrandomized, open label, single Group, non-Controlled	RET fusion-positive patients (excluding NSCLC) ≥12 years old, who have not received prior treatment with RET inhibitors	To evaluate the efficacy of pralsetinib in patients with RET fusion-positive advanced or metastatic solid tumors (excluding NSCLC)	A - Entrectinib: Rozlytrek 600 mg/day, Oral, (100-600 mg for paediatric patients) B - Entrectinib: Rozlytrek 600 mg/day, Oral, (100-600 mg for paediatric patients) C - Alectinib: Alectinib 600 mg, Oral, (4 × 150 mg caps BID) D - Atezolizumab: atezolizumab 1200 mg, Oral, IV (15 mg/kg for paediatric patients) E - Ipatasertib: Ipatasertib - GDC-0068 400 mg, Oral, QD (200 mg for paediatric patients) F - Kadcyla: Kadcyla 3.6 mg/kg, IV Q3W G - GDC-0077: INAVOLISIB 9 mg, Once Per Day, Oral I - Belvarafenib-BRAF Class II: belvarafenib 400 mg, Two Times Per Week, Oral	Cohort K: Planned: 70 patients Actual: 23 patients	Study complete (cohort K) Study dates: November 2021 (FPFV) LPLV: 6 February 2025

Protocol No., No. of Center(s) (Reference)	Study Design	Study Population: Diagnosis, Inclusion Criteria	Objectives/ Criteria for Evaluation	Dosing Regimen, Duration, Formulation	No. of Subjects/ Patients Sex (M/F) Age (yrs)	Study Status Study Dates
				J-Belvarafenib-BRAF Class III: belvarafenib 400 mg, Two Times Per Week, Oral K-Pralsetinib: Gavreto 400 mg, QD, Oral		
ML41591 (NAUTIKA1; RET cohort)	Non-randomized, open label, single group, non-controlled	RET cohort: Patients with RET altered NSCLC	RET cohort: To evaluate the efficacy and safety of pralsetinib	RET cohort: Gavreto 400 mg QD, Oral	RET cohort: Actual: 1 patient	Study complete (RET cohort) Study dates: November 2020 (FPFV)
ML42439 (MYTACTIC; Arm O)	Non-randomized, open label, parallel, non-controlled	Arm O: Patients with RET altered solid tumors	Arm O: To evaluate the efficacy and safety of pralsetinib	Arm O: Gavreto 400 mg QD, Oral	Arm O: Actual: 3 patients	Study complete Study dates: January 2021 (FPFV) 4 December 2023 (LPLV)

BID = twice daily; DDI = drug-drug interaction; FPFV = first patient first visit; IV = intravenous; LPI = last patient in; MTD = maximum tolerated dose; NSCLC = non-small cell lung cancer; ORR = overall response rate; PFS =progression free survival; PK = pharmacokinetics; PO = oral; Q3W = every 3 weeks; QD = once daily; RET = rearranged during transfection; RP2D = recommended Phase 2 dose; SOC = standard of care.

All studies were conducted in accordance with Good Clinical Practice guidelines.

Signature Page for Published Report - Investigator Brochure (IB) - RO7499790 (pr
System identifier: RIM-CLIN-1035797

Approval Task	Astrid Scalori (scaloria) Company Signatory 25-Apr-2025 13:23:02 GMT+0000